UNIVERSIDADE DE SÃO PAULO
Faculdade de Medicina de Ribeirão Preto
Departamento de Genética

Flávia Sacilotto Donaires Ramos

Dinâmica telomérica e diferenciação hematopoética de células-tronco pluripotentes induzidas humanas com mutação em *DKC1*

Telomere dynamics and hematopoietic differentiation of human *DKC1*-mutant induced pluripotent stem cells

Ribeirão Preto
2015

Flávia Sacilotto Donaires Ramos

Dinâmica telomérica e diferenciação hematopoética de células-tronco pluripotentes induzidas humanas com mutação em *DKC1*

Telomere dynamics and hematopoietic differentiation of human *DKC1*-mutant induced pluripotent stem cells

Tese apresentada à Faculdade de Medicina de Ribeirão Preto da Universidade de São Paulo para obtenção do título de Doutor em Ciências, área de concentração em Genética

Orientador: **Prof. Dr. Rodrigo do Tocantins Calado De Saloma Rodrigues**

Ribeirão Preto

2015

FICHA CATALOGRÁFICA

Donaires Ramos, Flávia Sacilotto
Dinâmica telomérica e diferenciação hematopoética de células-tronco pluripotentes induzidas humanas com mutação em *DKC1* – Ribeirão Preto, 2015.

165 p. : il. ; 30cm

Tese de Doutorado apresentada à Faculdade de Medicina de Ribeirão Preto/USP. Área de concentração: Genética.

Orientador: Rodrigo T. Calado.

1. Células-tronco pluripotentes induzidas (iPSCs).
2. Telômeros. 3. Telomerase. 4. *DKC1*.
5. Disceratose congênita ligada ao X.
6. Diferenciação hematopoética.

APOIO E SUPORTE FINANCEIRO

Este trabalho foi realizado com o apoio financeiro das seguintes entidades e instituições:

- Fundação de Amparo à Pesquisa do Estado de São Paulo – **FAPESP**
  - Bolsa de doutorado no país: **2012/08119-4**
    Período: 01/08/2012 a 31/03/2016
  - Bolsa Estágio de Pesquisa no Exterior (BEPE): **2012/18434-4**
    Período: 07/01/2013 a 06/01/2014
  - Centro de Terapia Celular – CTC (CEPID): **2013/08135-2**

- Faculdade de Medicina de Ribeirão Preto da Universidade de São Paulo (**FMRP** – USP)

- Fundação Hemocentro de Ribeirão Preto (**FUNDHERP** – HCFMRP – USP)

- Fundação de Apoio ao Ensino, Pesquisa e Assistência do Hospital das Clínicas da Faculdade de Medicina de Ribeirão Preto da Universidade de São Paulo (**FAEPA** – HCFMRP – USP)

- National Institutes of Health – **NIH** (Bethesda, MD, USA)

AGRADECIMENTOS / ACKNOWLEDGEMENTS

Ao meu orientador **Prof. Dr. Rodrigo T. Calado** pela condução deste trabalho, pela oportunidade única que me proporcionou, pela confiança em me aceitar em seu grupo de pesquisa e por todo o aprendizado imensurável que me proporcionou durante esses quatro anos. Muito obrigada!

I would like to thank **Dr. Cynthia E. Dunbar**, who provided me the opportunity to join her team at NIH in 2013. Her insightful comments have always incented me to go deeper in my research.

My sincere gratitude to **Dr. Thomas Winkler**, for his patience, motivation, and immense knowledge. His guidance was and still is indispensable for my research. Without his precious support it would not be possible to conduct this research. Also I thank his amazing family for receiving me in their house. Danke!

Aos membros da **banca examinadora** por terem aceitado participar da avaliação deste trabalho, contribuindo para sua melhoria.

À **Profa. Dra. Fabíola Traina** por ter sido parte de minha banca de qualificação, proporcionando uma ótima arguição. E pela imensa ajuda na execução e análise dos resultados do CytoScan.

Ao **Prof. Dr. Ademilson Espencer E. Soares** e à **Profa. Dra. Silvana Giuliatti**, pelo apoio constante como coordenadores do Programa de Pós-graduação em Genética.

Às secretárias do Departamento de Genética, especialmente à **Susie** e à **Sílvia**, por toda a ajuda prontamente prestada.

Ao pessoal do Hemocentro, especialmente à **Cleide**, **Dalvinha** e **Maristela**, pelo apoio constante na condução do trabalho.

À **Bárbara Amélia** (a especialista de verdade), por ser excelente quando o assunto é ensinar aquela técnica complicada que faz parte do projeto. Também pela amizade e pelos ótimos momentos de cappuccino!

À minha querida amiga **Raquel Paiva**, pela amizade de imensurável valor, pelo companheirismo, pela divisão dos estresses do dia-a-dia, e pelos ensinamentos valiosos que me proporcionou. A Raquel é uma das pessoas mais incríveis e generosas que já conheci. Aprendi muito não só na parte científica, mas também aprendi lições de vida. Muito obrigada!

A todas as minhas grandes amizades do laboratório, cultivadas cuidadosamente durante anos de convívio! Às vezes cultivar amizades é mais difícil do que cultivar células: células não têm dias bons ou ruins, não têm variações de humor ou problemas (se tiverem, a gente joga fora). Também não têm a capacidade de nos ajudar, de nos ouvir ou dar conselhos. Admito que nessa complicada tarefa de cultivar amizades, todos foram impecáveis. Em ordem alfabética, incluindo aqueles que já se foram do lab mas deixaram muita saudade: **Ana Paula Lange**, **Ana Paula Nunes** (a *minona*!), **André** (que mal chegou e já está aqui na lista), **Bruna**, **Fernanda Borges** (a pessoa mais fantástica pra se contar quando o assunto é cariotipagem), **Fernanda Guti** (que vai ser um sucesso nos NIH em 2016), **Florencia** (minha companheira de *colonhas*), **Gustavo Borges** (nem sei o porquê de acrescenta-lo aqui... hehehe), **Jaqueline**, **João Paulo** (o Jonny Prep), **Katarina**, **Larissa**, **Lilian** (minha *dupra* querida que me ajudou imensamente), **Natália Scatena**, **Mariana Benício**, **Renata**, **Sílvia**, e possivelmente alguém que tenha me esquecido de acrescentar mas que não deixa de ser importante.

I thank my fellow labmates at NIH for the stimulating discussions and for all the fun we have had in 2013. Special thanks to **William Hughes**, **So Gun Hong**, and **Moonjung Jung**.

Aos "ex-amigos de laboratório", porém não ex-amigos, **Ana Paula**, **Danilo** (Xitão), **Felipe** (Magal), **Léo**, **Paulo** (Cop) pela amizade, pelas dicas, pelos conselhos e pelos divertidos momentos de conversa! À **Gi** (minha *druguinha*) por sua grande amizade e companheirismo. Passamos momentos muito bons (e também muito ruins) juntas aqui ou lá na terra do tio Sam, mas sempre com muitas risadas.

À minha querida xará (**Flávia Freitas**), que apesar de ser uma abelhudinha (no bom sentido!) e estar em outro hemisfério, me ajudou muito com dicas, sugestões e também me ouvindo nos momentos em que nada dava certo. Além disso, me ajudou muito na correção deste trabalho, a qual me foi muito importante. Sua amizade também é parte dos meus "resultados", aliás, um dos melhores!

A todos os meus amigos fora dos muros da universidade, que direta ou indiretamente contribuíram para que eu pudesse completar esse trabalho.

A minha família: meus irmãos, cunhados, sobrinhos e agregados, que sempre me apoiaram e estiveram ao meu lado, mesmo que a distância. Agradeço especialmente à minha mãe **Maria**, sem a qual não teria conseguido chegar até aqui! Ela é meu maior exemplo de mulher dedicada e sábia. É minha maior inspiração como pessoa, uma grande amiga e

companheira. Em memória de meu pai, **Rubens**, que um pouco antes de nos deixar se referiu a mim como sendo uma pessoa vitoriosa por ter conseguido chegar até aqui.

Ao meu amado companheiro, marido, porém eterno namorado, **Felipe Ramos**. Talvez ele tenha sido a maior "vítima" dos meus maus momentos, mas sempre esteve pronto a me ouvir e me acalmar. Obrigada por toda paciência e compreensão, e por me apoiar em coisas que poucas pessoas apoiariam (por exemplo, se ausentar por um ano logo após o noivado para poder realizar o sonho de fazer parte do doutorado fora). Você não é só meu marido, mas é meu grande amigo. Meu sucesso é em grande parte devido ao seu apoio e amor constantes.

E por último, porém mais importante, Àquele que criou todas as coisas as quais tentamos, na nossa limitada concepção, compreender com o que chamamos de "ciência". A Deus, por ser minha fortaleza, meu alvo e meu maior mestre. Os anos que se sucederam ao longo desse trabalho foram muito bons e muitos ruins em alguns momentos. Foram muito intensos. E sei que todos esses momentos foram graças a Ele. Agradeço a Deus pelas grandes conquistas e também pelos momentos ruins, que foram os que moldaram meu caráter.

Soli Deo gloria

TABLE OF CONTENTS

Resumo

Dinâmica telomérica e diferenciação hematopoética de células-tronco pluripotentes induzidas humanas com mutação em *DKC1*

Telômeros são sequências repetitivas de nucleotídeos nas terminações dos cromossomos lineares que são protegidos por proteínas específicas. Assim, os telômeros conferem estabilidade e proteção do material genético nos cromossomos. Os telômeros são encurtados como resultado da divisão celular mitótica, mas são mantidos em células com alta capacidade proliferativa por meio da telomerase, que enzimaticamente adiciona repetições teloméricas na extremidade 3′ da molécula de DNA. O complexo da telomerase é composto pela transcriptase reversa (TERT), por um componente de RNA (TERC) e proteínas que estabilizam o complexo, como a discerina (codificada pelo gene *DKC1*). Mutações nesses genes podem resultar em doenças como a disceratose congênita (DC), uma síndrome de falência da medula óssea herdada. Células-tronco pluripotentes induzidas (iPSCs) podem ser utilizadas como modelo de doenças, já que as células reprogramadas de pacientes mantêm as características genotípicas. As iPSCs superam a senescência replicativa por meio da reativação da telomerase e, consequentemente, do alongamento telomérico. No presente estudo, iPSCs foram derivadas a partir de fibroblastos de um paciente com DC e mutação no *DKC1* (A353V). Os efeitos dessa mutação na dinâmica dos telômeros e na diferenciação hematopoética foram investigados. iPSCs foram derivadas com sucesso e mantidas em cultura por um longo período sem apresentar sinais de diferenciação espontânea (última passagem: 140). Os telômeros encurtaram durante as primeiras passagens após a reprogramação, mas se mantiveram estáveis após a passagem 20. Mecanismos alternativos de alongamento telomérico e variações no número de cópias no genoma foram descartados como responsáveis pelo comportamento observado nos telômeros, sugerindo que os mesmos foram mantidos pela ativação tardia da telomerase. Diferenciação hematopoética foi realizada em dois clones das iPSCs, os quais apresentaram capacidade aumentada de gerar linhagens hematopoéticas. Em contraste com estudos anteriores, esses resultados sugerem que as iPSCs com mutação em *DKC1* superam as limitações decorrentes da mutação por, eventualmente, alcançar estabilidade do comprimento telomérico e, assim, manter a proliferação celular e a capacidade de auto-renovação em passagens tardias. O modelo apresentado nesse estudo pode ser útil para futuros estudos moleculares da biologia dos telômeros, além de servir como uma plataforma para o teste de moléculas que possam potencialmente superar o fenótipo mutante.

Palavras-chave: células-tronco pluripotentes induzidas (iPSCs), telômeros, telomerase, disceratose congênita ligada ao X, *DKC1*, diferenciação hematopoética.

Abstract

Telomere dynamics and hematopoietic differentiation of human *DKC1*-mutant induced pluripotent stem cells

Telomeres are nucleotide repetitive sequences at linear chromosome endings coated by specific proteins (shelterin) and providing chromosomal protection and stability. Telomeres shorten due to cellular mitotic division, but are maintained in cells with high proliferative capacity by telomerase, which enzymatically adds telomere repeats to the 3′ ends of the DNA strand. The telomerase complex is composed of a reverse transcriptase (TERT), an RNA component (TERC), and proteins that provide stability, as dyskerin (encoded by the *DKC1* gene). Mutations in these genes may result in human diseases as dyskeratosis congenita (DC), an inherited bone marrow failure syndrome. Induced pluripotent stem cells (iPSCs) may serve to model disease, as patients' reprogrammed cells maintain genotypic characteristics. The iPSCs overcome replicative senescence by reactivating telomerase and restoring telomere lengths. In this study, iPSCs were derived from fibroblasts of a DC patient carrying a *DKC1* mutation (A353V). The effects of this mutation in telomere dynamics and hematopoietic differentiation were investigated. iPSCs were successfully derived and maintained in long-term culture without signs of spontaneous differentiation (last passage, 140). Telomeres shortened during the first passages after reprogramming, but were maintained in length after passage 20. Alternative lengthening of telomeres and genome copy number variations in the iPSCs were ruled out as responsible for this telomere behavior, suggesting that telomeres were maintained by late telomerase activation. Hematopoietic differentiation was carried out in two *DKC1*-mutant iPSCs clones, displaying increased capacity to generate hematopoietic lineages. In contrast to previous studies, these findings suggest that *DKC1*-mutant iPSCs overcome the limitations imposed by the *DKC1* gene defect by eventually achieving telomere length stability and maintaining cell proliferation and self-renewal at late passages. The model presented here may be useful for further molecular studies on telomere biology and so may serve as a platform for the screening of molecules that potentially overcome the mutant phenotype.

Keywords: induced pluripotent stem cells (iPSCs), telomeres, telomerase, X-linked dyskeratosis congenita, *DKC1*, hematopoietic differentiation.

1. INTRODUCTION

1. Introduction

1.1. Telomeres

The eukaryotic genomes are organized in chromosomes, which are formed by long and linear molecules of DNA condensed around nuclear proteins. The ends of chromosomes are called *telomeres* (from the Greek terms *telos* and *meros*, meaning "end" and "part", respectively). The main function of telomeres is to ensure chromosome stability through their unique properties, such as (1) prevent deoxyribonucleases from degrading the ends of the linear DNA molecules, (2) prevent fusion of the ends with other DNA molecules, and (3) facilitate replication of the ends of the linear DNA without loss of material, due to peculiarities of the replication mechanism (Snustad and Simmons, 2012).

Hermann J. Muller, who first introduced the term telomere in 1938, demonstrated that *Drosophila* chromosomes with radiation-induced breaks were not transmitted to progeny (Muller, 1938). In the early 1940s, Barbara McClintock demonstrated that new ends of broken maize chromosomes were sticky and tended to fuse with each other. In contrast, the natural ends of the chromosomes were stable and showed no tendency to fuse to other broken or unbroken ends (McClintock, 1941). These observations indicated that telomeres have special structures that differ from the ends produced by chromosome breakage.

Telomeres are specialized DNA-protein structures composed of short repetitive nucleotide sequences and capping proteins. The telomeric DNA sequences differ among species, but the basic repeat unit has the pattern 5′ $T_{1–4}A_{0–1}G_{1–8}$ 3′ in almost all the species. In humans and other vertebrates, sequences are highly conserved consisting of thousands TTAGGG tandem repeats (Moyzis *et al*., 1988). The telomere-capping proteins, also called shelterin complex, are important for the tertiary structure of telomeres and to protect the integrity of the complex (de Lange, 2005). Shelterin is composed of six different proteins: Telomeric Repeat Binding Factor 1 (TRF1 or TERF1), Telomeric Repeat Binding Factor 2 (TRF2 or TERF2), Protection of Telomeres 1 (POT1), TRF1-interacting Nuclear Factor 2 (TIN2 or TINF2), Adrenocortical Dysplasia Protein Homolog (ACD or TPP1), and Telomeric Repeat Binding Factor 2, Interacting Protein (TERF2IP or Rap1). Three proteins bind specifically to telomeric nucleotides: TRF1 and TRF2 bind to double-stranded repeats, and POT1 binds to single-stranded repeats. TIN2 and TPP1 tether POT1 to DNA-bound TRF1 and TRF2. The TRF2-associated protein Rap1 participates in the regulation of

telomere length (Snustad and Simmons, 2012). Shelterin complex is represented on Figure 1.1.

Telomeres are not just repetitive linear nucleotide sequences at the end of the chromosomes but they form complex structures called T loops, and the shelterin complex is crucial for their formation and integrity (Griffith *et al*. 1999; Stansel *et al*. 2001). The telomeric leading strand terminates as a G-rich single-stranded region of DNA with a 3′-hydroxyl (a so-called 3′ overhang). This protrusion forms due to the catalytic addition of telomeric repeats at this strand and the post-replicative processing of the lagging strand (Makarov *et al*. 1997). The resulting overhang (containing 50 to 500 bases in humans) folds back in the double-stranded telomere repeats, base pairing with part of the C-rich strand, forming the T loop structure, which tucks the end of the linear DNA molecule (de Lange, 2005). Thus T loops and shelterin proteins prevent the exposure of single stranded telomeric overhang that would trigger the DNA damage response machinery. Furthermore, it prevents end-to-end fusion or recombination of chromosomes (de Lange, 1992). A representation of the telomere structure is provided on Figure 1.1.

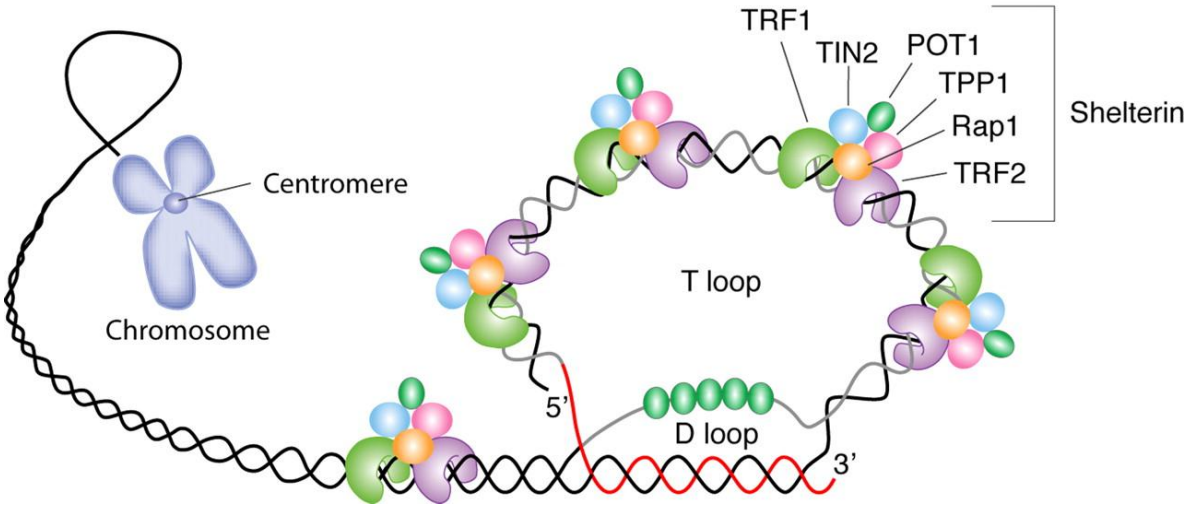

Figure 1.1 – The telomere structure. The telomeric leading strand ends in a G-rich 3′-hydrohyl overhang that invades the double-strand and base pairs with the C-rich strand, forming the T loop. The G-rich single-strand that remains inside the structure as a result of the T loop is denominated D loop. In human cells, telomeres are composed of hundreds to thousands of TTAGGG tandem repeats coated by complexes of six proteins (TRF1, TRF2, TPP1, POT1, TIN2, and RAP1), collectively termed shelterin, that are responsible for DNA protection (from Calado and Young, 2008; public domain material; reproduced under authors' consent).

1.2. Telomerase

DNA polymerase requires an RNA primer with a 3′-hydroxyl donor for replication of the lagging strand. Primer binding becomes impossible at the end of replication leaving a not replicated segment at chromosomal termini. Without a compensatory mechanism the linear DNA molecule would lose several bases with each mitotic division (Cong *et al*., 2002; Harley *et al*., 1990). This observation was termed the "end-replication problem" and was firstly described by Alexey Olovnikov (Olovnikov, 1971). Telomeres solve the problem of losing genetic information with cell division but eventually also all telomeric sequences would be lost particularly in highly proliferative tissues. When telomeres become critically short cellular signaling pathways to arrest of cell proliferation, senescence, and apoptosis become activated (Herbig *et al*., 2004). Leonard Hayflick postulated in 1965 that human cells in culture have a limited proliferative capacity (Hayflick, 1965), the so-called "Hayflick limit" (Shay and Wright, 2000), and telomere shortening below a critical limit has been later mechanistically associated. However, some cells like germ-line cells, embryonic and adult stem cells, and some immortalized and cancer cells exhibit a higher proliferation capacity than predicted by the Hayflick limit and they also maintain their telomere length to some degree.

In the early 1980s, Elizabeth Blackburn, Jack Szostak, and Carol Greider discovered and characterized the enzyme telomerase (Szostak and Blackburn, 1982; Greider and Blackburn, 1985). Telomerase is a ribonucleoprotein complex with reverse transcriptase activity that adds the telomere sequences in the 3′ ends of chromosomes using an RNA template (Cong *et al*., 2002). Thus telomerase overcomes the deficiency of DNA polymerase to completely synthesize a new DNA strand. The ribonucleoprotein complex telomerase comprises a reverse transcriptase (encoded by *TERT* gene) that uses the telomerase RNA component (encoded by *TERC*) as a template for synthesis of telomeric DNA. Additionally the functional telomerase complex requires other proteins, such as NHP2 ribonucleoprotein (NHP2), NOP10 ribonucleoprotein (NOP10), GAR1 ribonucleoprotein (GAR1), and dyskerin for efficient telomere synthesis (Calado and Young, 2009) – Figure 1.2.

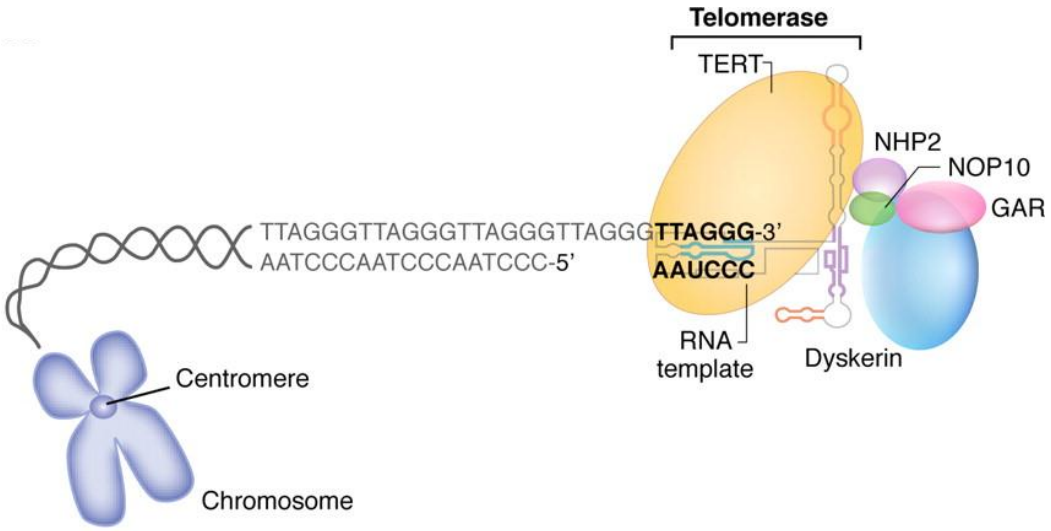

Figure 1.2 – The structure of telomerase complex. The reverse transcriptase TERT enzymatically adds TTAGGG repetitions to the 3′ termini of the leading strand using the RNA component (TERC) as a template. Other proteins, such as dyskerin, NHP2, NOP10, and GAR1, also binding to TERC to provides the stabilization of the complex (from Calado and Young, 2008; public domain material; reproduced under authors' consent).

Dyskerin, the nucleolar protein encoded by the Dyskeratosis Congenita 1 (*DKC1*) gene, plays multifunctional roles as nucleocytoplasmic trafficking (Meier and Blobel, 1992, 1994), rRNA transcription and ribosome biosynthesis (Cadwell *et al*., 1997), and RNA pseudouridylation. Moreover, this protein is responsible for the stabilization of small nucleolar RNAs (snoRNAs) that contain an H/ACA sequence motif, such as *TERC* (Lafontaine *et al*., 1998). Thus, dyskerin is important for the recognition of *TERC* and assembling of the telomerase complex in the Cajal bodies. Furthermore, dyskerin plays a role in the translocation of telomerase to the telomeres (Mitchell *et al*., 1999).

The telomerase genes are highly expressed in cells with high proliferative capacity, and usually absent in terminally differentiated somatic cells (Broccoli *et al*., 1995). The ectopic expression of *TERT* in somatic cells restores telomere length and consequently "immortalizes" cells (Bodnar *et al*., 1998; Vaziri *et al*., 1998; Hahn *et al*., 1999). Telomerase is not the only mechanism to maintain telomere length. Alternative lengthening of telomeres (ALT) has been described, mainly in cancer cells. This mechanism relies on homologous recombination-mediated DNA replication. Cells displaying ALT activity retain the canonical attributes of telomeres as wells as specific features, as the presence of abundant extrachromosomal telomeric DNA that may be linear double-stranded or form circular structures from double-stranded telomere DNA (t-circles), to partially single-stranded circles (C-circles or G-circles) (Cesare and Griffith, 2004; Wang *et al*., 2004; Henson *et al*., 2009;

Nabetani and Ishikawa, 2009). Other characteristics usually found are heterogeneity among telomere length of the chromosomes, elevated levels of recombination at telomeres, and association of telomeric DNA with promyelocytic leukemia (PML) nuclear bodies, the ALT-associated PML bodies (APBs) (Bryan *et al*., 1995; Yeager *et al*., 1999; Londono-Vallejo *et al*., 2004). However, ALT has been documented as an anomalous situation observed in cancer cells and genetically modified organisms (Cesare and Reddel, 2010).

1.3. Telomeropathies

Observations in the late 1990s and early 2000s associated very short telomeres with human diseases. Ball *et al*. (1998) and Brummendorf *et al*. (2001) reported progressive telomere attrition in aplastic anemia (AA) patients. AA is a heterogeneous bone marrow failure (BMF) disease that is characterized by pancytopenia due to a progressive loss of hematopoietic stem cells (HSC) (Young, Scheinberg, and Calado, 2008). Etiologically, T-cell mediated autoimmune processes against HSC have been described. The compensatory replicative stress within the HSC compartment may explain the progressive telomere attrition seen in patients' blood cells but also a primary telomerase defect could not be excluded.

With dyskeratosis congenita (DC) Mitchell *et al*. firstly described in 1999 a primary telomere dysfunction responsible for a human disease. DC is a rare multi-system disorder, which in its classical form is characterized by a triad of mucocutaneous abnormalities encompassing abnormal skin pigmentation, nail dystrophy, and oral leukoplakia (Dokal, 1999). Multiple organ involvement, commonly the bone marrow and the lung, accompany the mucocutaneous findings. Despite variation in the clinical presentation and organ involvement, bone marrow dysfunction is observed in more than 80% of cases (Kirwan and Dokal, 2009), which represents also the risk factor for mortality in these patients (Calado and Young, 2009). Historically, classical linkage analysis of large pedigrees has associated dysfunctional dyskerin with the X-linked DC. Subsequently, short telomeres were found to be a defining characteristic of the disease (Heiss *et al*., 1998). Then, Mitchell *et al*. (1999) observed that dyskerin was associated not only with H/ACA small nucleolar RNAs, but also with TERC, which contains an H/ACA RNA motif, finally associating dysfunctional telomeres with diseases.

After this hallmark, telomere attrition has been linked to dysfunctions with broad clinical spectrum, more generally termed telomeropathies. These diseases manifest from birth to late

adulthood and most often lead to hematopoietic dysfunctions that may range from no abnormalities or mild hematologic abnormalities to BMF (Calado and Young, 2009). Apart from the X-linked form of DC, mutations in other telomerase and shelterin genes have been associated with DC and telomeropathies in general. Among those are autosomal dominant (mutations in *TERT*, *TERC*, and *TIN2*), and autosomal recessive (mutations in *NOP10*, *NHP2*, and *TCAB1*) (Dokal, 2000). Mutations or deletions in *TERC* are present in about 10% of DC families and tend to be milder that the X-linked disease (Knight *et al*. 1999; Vulliamy *et al*. 2006; Calado and Young 2008; Dokal *et al*. 2011; Mason and Bessler 2011). DC caused by single amino acid substitutions in *TERT* is clinically more severe and presents the phenomenon of anticipation, in which later generations have shorter telomeres (Mason and Bessler 2011; Nelson and Bertuch, 2012). Moreover, novel mutations were identified in *RTEL1* gene in patients with Hoyeraal-Hreidarsson syndrome, a severe variant of DC. *RTEL1* is a DNA helicase, essential for genome stability, that has been implicated in the disruption of D loop formation during homologous recombination (Uringa *et al*. 2011; Le Guen *et al*. 2013; Lee *et al*. 2013; Walne *et al*. 2013), also essential for the disassembly of T loops during DNA replication (Vannier *et al*. 2012).

Mutations in *TERC* and *TERT* have also been described in cases of apparently acquired AA without the classical DC phenotypes (Fogarty *et al*., 2003; Yamaguchi *et al*., 2005), providing a molecular mechanism for short telomeres in about 10% of these patients (Calado and Young, 2009). Moreover, similar studies have found telomerase mutations in families with idiopathic pulmonary fibrosis, a restrictive lung disease usually associated with aging, but whose etiology and pathogenesis were still unclear. It was observed that short telomeres account for about 15% of the termed 'idiopathic' cases (Armanios *et al*., 2007; Tsakiri *et al*., 2007). Finally, mutations in telomerase were associated with familial liver disorders, which cause a pattern of fibrosis with inflammation and nodular regenerative hyperplasia. The mutations were found to confer genetic risk factors for the development of cirrhosis (Calado *et al*., 2009; Calado *et al*., 2011; Hartmann *et al*., 2011). Interestingly, the penetrance and phenotype in these cases is very variable.

Traditional disease models utilize either immortalized cell lines or short-term culture of some primary cell types *in vitro*. In telomeropathies, the isolation and propagation of affected cells (mainly the primary stem cells) from patients is difficult, since the stem cells from tissues of interest are likely reduced in number (e.g. aplastic marrow, fibrotic liver and lung). Moreover, animal models, such as mice, fail in completely recapitulate the pathophysiology of these diseases. Since laboratory mice have very long telomeres, the telomerase deficient

animals need extensive breeding to reach critically short telomeres (Calado and Dumitriu, 2013). Recent advances in pluripotent stem cells (PSCs)-based models may provide useful alternatives for the investigation of disease mechanisms as well as for drug screening (Jung *et al*., 2015).

1.4. Induced pluripotent stem cells for disease modeling

Embryonic stem cells (ESCs) are pluripotent cells derived from early mammalian embryo (blastocyst). Unlimited self-renewal and the capacity to differentiate into cells of all germ layers define their phenotype (Evans and Kaufman, 1981; Martin, 1981). The first derivations of ESCs were reported in mouse from the inner cell mass of blastocysts (Evans and Kaufman, 1981; Martin, 1981). These first studies have established the culture conditions for growing pluripotent ESCs *in vitro*, as well as the specific markers that define these cells. The derived ESCs displayed normal karyotypes, generated derivatives of the three primary germ layers, and formed teratomas (tumors harboring cell types from all three primary germ layers) when injected into immunodeficient mice.

Human ESCs (hESCs) were first isolated from blastocysts by Bongso *et al*. in 1994. Cells retained a stem cell-like morphology, but some inner cell mass clumps differentiated into fibroblasts and the cells were no longer maintained in culture (Bongso *et al*., 1994; Bongso *et al*., 1994). Four years later, Thomson *et al*. derived hESCs from the inner cell mass of blastocysts produced by *in vitro* fertilization. The generated cell lines (H1, H7, H9, H13, and H14) were cultured through many passages and maintained normal karyotypes, high levels of telomerase activity, and expression of cell surface markers typical of hESCs as alkaline phosphatase, SSEA-4, TRA-1-60, and TRA-1-81. Moreover, these cell lines were able to generate teratomas when injected into mice, demonstrating their pluripotent capacity (Thomson *et al*., 1998). Thomson's work represents a milestone for pluripotent stem cells-based disease models and also a source for potential cell-based therapies. However, ethical implications regarding the source of hESCs, whose isolation involves the destruction of human embryos, have generated controversies that hindered the development of hESC-based applications. Moreover, the use of hESCs for therapy might be impaired due to problems of tissue rejection following patients' transplantation. An alternative to overcome these issues might be the induction of a pluripotent status in human somatic cells (Yamanaka, 2007).

Gurdon (1962) performed nuclear transfer from amphibian differentiated intestinal cells

into oocytes, which led to cloned frogs. This demonstration showed that all genes necessary to make an organism are present into the differentiated cells. Later, Blau and Chiu (1983) demonstrated that mammalian cell differentiation is reversible. In 1997, the first mammalian was cloned (Dolly the sheep) through nuclear transfer (Wilmut *et al*., 1997). In 2006, Kazutoshi Takahashi and Shinya Yamanaka demonstrated that the overexpression of four transcription factors in murine fibroblasts was sufficient to revert their phenotype into cells that resemble ESCs. The four transcription factors (*Oct3/4*, *Sox2*, *Klf4*, and *c-Myc*) are highly expressed in ESCs. The researchers designated these cells as *induced pluripotent stem cells* (iPSCs) (Takahashi and Yamanaka, 2006). Using a similar approach, several groups successfully reprogrammed adult human dermal fibroblasts into iPSCs after expressing the transcription factors. Human iPSCs are indistinguishable from hESCs in morphology, proliferation, surface antigens, gene expression, and epigenetic status of pluripotent cell-specific genes, also presenting high telomerase activity and the ability of differentiation into cell types of the three germ layers both *in vitro* (formation of embryoid bodies) and *in vivo* (formation of teratomas in mice) (Takahashi *et al*., 2007).

Since then, the generation of iPSCs from human somatic cells has expanded the frontiers in stem cell research. Patient-derived iPSCs may serve to study the molecular basis of a broad range of human diseases that are otherwise difficult to model. Moreover, these cells can be differentiated into virtually any cell type, maintaining the genotypic characteristics of the patient. The differentiated cells are useful for screening the efficacy and safety of drug candidates for treating diseases, as well as for autologous transplant (Nishikawa *et al*., 2008; Yamanaka and Blau, 2010).

The latter events of reprogramming process encompass the upregulation of telomerase, telomeres elongation and maintenance, and then acquisition of unlimited self-renewal (Marion *et al*., 2009; Stadtfeld *et al*., 2008; Takahashi *et al*., 2007). Therefore, iPSCs could be very useful to study telomere dynamics in cells derived from normal individuals and from patients with telomeropathies. Two groups have generated iPSCs from dermal fibroblasts of classical DC patients carrying mutations in *DKC1*, *TERT*, *TERC*, or *TCAB1*. Agarwal *et al*. (2010) first demonstrated that reprogramming restored telomere elongation in DC cells despite genetic lesions affecting telomerase. The mean terminal restriction fragment (TRF) length and total telomeric DNA was increased in DC iPSCs relative to the parental fibroblasts. Although formally fulfilling criteria of pluripotency, *DKC1* (del37L) fibroblast line presented poor reprogramming efficiency (2-5 colonies from 10^5 input cells), but exhibited all the hallmarks of pluripotency. The iPSCs displayed induction of endogenous

TERT and telomerase activity. Telomeres remained shorter than the parental fibroblasts immediately after derivation, but increased over time achieving lengths comparable to the fibroblasts (around passage 20). iPSCs showed normal self-renewal capacity during prolonged culture. Another fibroblast cell line was reprogrammed from autosomal dominant DC patient carrying a heterozygous 821-base-pair (bp) deletion in the 3′ region of the *TERC* locus. Several independent iPSCs lines were obtained, all fulfilling the pluripotency criteria, also accompanied by up-regulation of endogenous *TERC* levels (three-fold higher than parental fibroblasts). In analogy to *DKC1*[del37L] iPSCs, these iPSCs displayed continuous self-renewal and restoration of telomere maintenance. These observations were considered as the consequence of the up-regulation of several telomerase components as *TERT*, *TERC*, and *DKC1* after reprogramming. The authors suggested that *TERC* was up-regulated to a degree sufficient to overcome limitations in telomere maintenance due to dyskerin dysfunction.

Conversely, Batista *et al*. (2011) described progressive telomere attrition and senescense during culture of *DKC1*-mutant iPSCs. The researchers reprogrammed *DKC1*[L54V] and *DKC1*[del37L] fibroblasts. The later mutated fibroblasts were derived from the same individual as the ones used by Agarwal *et al*. (2010). Reprogramming efficiency was higher (40 colonies from 10^5 input cells) but the authors used several rounds of transduction of the retroviruses containing the "Yamanaka" reprogramming factors. Additionally, they derived the cells under low oxygen conditions (5% O_2). These iPSCs expressed both *TERT* and *TERC* at levels higher than fibroblasts, though *TERC* expression was much lower than control iPSCs (wild-type). Telomerase activity ranged from 5-15% of controls. Around passage 36, the *DKC1*[del37L] iPSCs could no longer be maintained in an undifferentiated state, indicating loss of self-renewal, which was suggested by the authors as a reflection of premature exhaustion of stem cells observed in patients. Additional iPSCs were derived from *TERT*-mutant fibroblasts (P704S and R979W). These iPSCs elongated telomeres relative to the parental fibroblasts, but this elongation was blunted compared to elongation in control iPSCs. Unlike *DKC1*-mutant iPSCs, *TERT* and *TERC* expression levels were similar to levels in control iPSCs. However, telomerase activity was 50% of the activity in the control iPSCs, compatible with a mechanism of telomerase haploinsufficiency as observed in patients. *TCAB1*-mutant iPSCs were also generated from fibroblasts of DC patients carrying H376Y and G435R mutations. *TCAB1*-mutant iPSCs displayed up-regulation of *TERT*, *TERC*, and *DKC1*, but reduced levels of TCAB1 protein. Despite normal telomerase activity, pronounced mislocalization of TCAB1, dyskerin, and TERC was observed in Cajal bodies, the nuclear sites of telomerase assembling. The authors suggested that the mislocalization of

the telomerase complex without affecting telomerase activity might be responsible for very short telomeres in DC patients carrying *TCAB1* mutations.

Winkler *et al*. (2013) derived iPSCs from four patients with AA or hypocellular bone marrow carrying heterozygous mutations in either *TERT* or *TERC*. The patients did not show features of classical DC. The mutant-iPSCs elongated telomeres but at lower rates compared with iPSCs from healthy subjects reprogrammed in parallel. Telomere elongation varied among different clones derived from the same patient, supporting the use of multiple clones from the same individual. Two out of the four iPSCs were generated from siblings harboring the same *TERT* mutation, *TERT*[R889X], but presenting distinct clinical manifestations: one with progressive AA, and her brother, with hypocellular bone marrow and normal blood counts. After differentiating the iPSCs towards hematopoietic progenitors, it was observed that iPSCs mirrored the clinical phenotypes observed in the four patients. The differentiation in the mutant-iPSCs was impaired in comparison to the healthy iPSCs, especially in the iPSCs derived from the sibling with AA.

Together, the data from Batista *et al*. (2011) and Winkler *et al*. (2013) are a proof of principle that telomeropathies are accurately recapitulated in patient-derived iPSCs. However, the telomere dynamics in *DKC1*-mutant iPSCs remains unclear. Agarwal and Daley (2011) argued that apparently conflicting results in Batista and Agarwal's works might have been due to significant clonal variability among iPSCs and inefficiency of the reprogramming process, that also involves genetic variation and subsequent selection.

1.5. *In vitro* hematopoiesis

In high proliferative tissues in which telomerase is active, the effects of telomerase dysfunction are likely to be the most severe, since critically short telomeres are reached much earlier than normal. Only a few cell types including male germ-line cells, activated lymphocytes, and stem cells are dependent on telomerase activity after embryonic development (Cong *et al*., 2002). Deregulation of stem cells are likely to give rise to defects in multiple organs, thus representing the critical cell type in telomeropathies such as DC. Since BMF is a hallmark of these diseases, the hematopoietic stem cell (HSC) has received the most research attention, and BMF has been considered a result of qualitative impairment of differentiation and development, as well as a quantitative reduction of the HSC pool (Kirwan and Dokal, 2009). A representation of the defects in HSC proliferation and

differentiation that give rise to DC is provided on Figure 1.3.

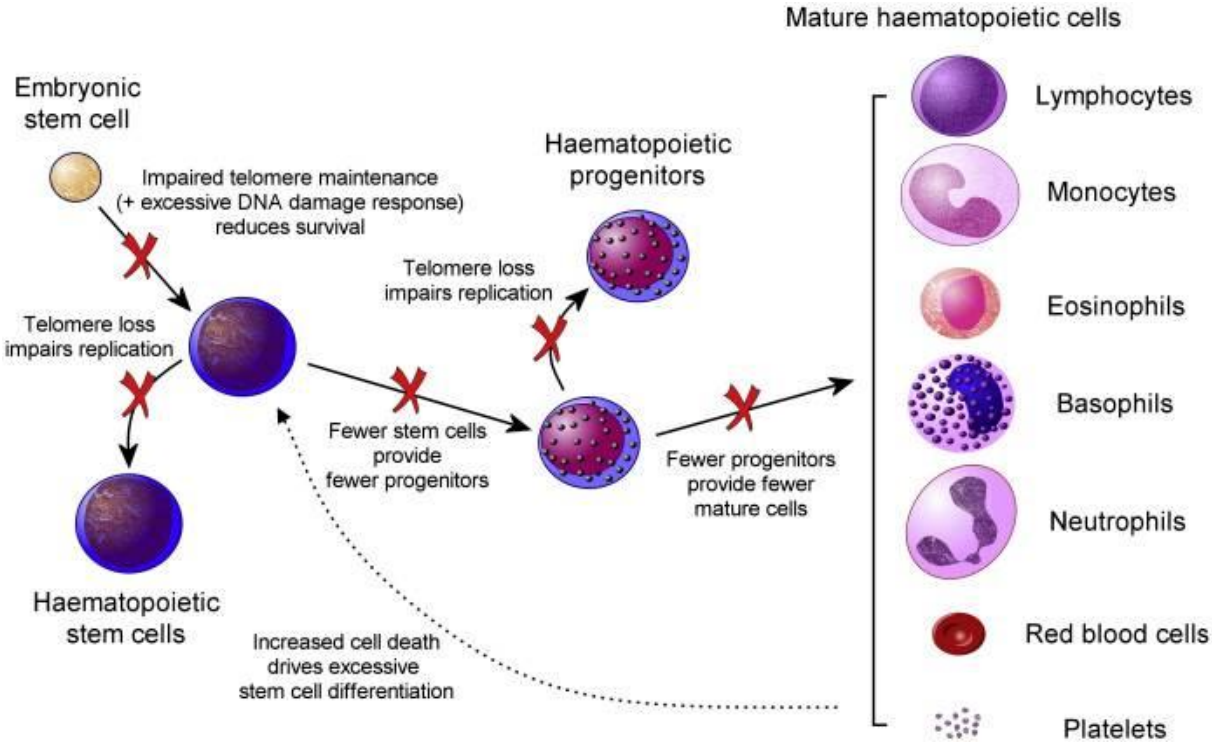

Figure 1.3 – The defects in hematopoietic stem cell proliferation and differentiation in DC. Due to impaired telomere maintenance, telomere attrition is reached much earlier than normal. The short telomeres impair stem cell replication starting with the embryonic stem cells, continuing through adult stem cells. In the hematopoietic tissue, the limitation of HSC proliferation and differentiation lead to reduced numbers of HSC, hematopoietic progenitors, and mature cells (from Kirwan and Dokal, 2009; reproduced under authors' consent).

Understanding human hemogenesis is fundamental for the elucidation and development of therapeutic strategies in telomeropathies. Much has been understood by analogy with the mouse system, as well as by inducing pluripotent stem cells (ESCs and iPSCs) through hematopoietic differentiation (Kardel and Eaves, 2012). The first methods of hematopoietic differentiation were refined in mouse ESCs using two distinct approaches then applied to human pluripotent cells: (1) co-culture with stromal cells, usually OP9 cell line (Nakano *et al*., 1996), (2) formation of three-dimensional aggregates with pluripotent cells, called embryoid bodies (EBs), then cultured in medium containing several hematopoietic cytokines, as bone morphogenetic protein-4 (BMP-4), FMS-like tyrosine kinase-3 ligand (Flt-3L), interleukin-3 (IL-3), interleukin-6 (IL-6), and granulocyte colony–stimulating factor (G-CSF) (Keller *et al*., 1993; Dang *et al*., 2002). These methods attempt to mimic the *in vivo* process

of mesodermal specification followed by embryonic blood lineage development (Orkin and Zon, 2008). Regardless of the differentiation strategy, kinetic studies have demonstrated that the first hematopoietic progenitor cells to appear are colony-forming cells (CFCs) of primitive erythroid cells, then CFCs of definitive erythroid cells and macrophages, and finally multipotent CFCs and cells with lymphoid potential (Keller *et al*., 1993; Keller, 1995; Nakano *et al*., 1996; reviewed in Kardel and Eaves, 2012; and Jung *et al*., 2015).

1.6. Motivation

The importance of normal telomere function in human health is demonstrated by the severe implications seen in DC and non-DC telomeropathies. This makes DC an ideal model to study both the normal and abnormal behavior of telomere biology in humans. Pluripotent stem cells and in particular iPSCs provide an innovative model: (1) to study basic questions on telomere maintenance and biology; (2) to dissect aberrant pathways leading to a specific phenotype in telomeropathies like DC; and thus (3) to identify new therapeutic targets. Recent studies on telomere biology and phenotype in iPSC, particularly from DC patients, showed conflicting results. Reprogramming methods and culture conditions may explain these opposite findings. Both Agarwal *et al*. and Batista *et al*. used retro/lentiviral constructs to overexpress the reprogramming factors. They also included only a few clones of each mutant iPSC line in their studies, and studied telomere dynamics over a limited observation period. Transgene removal was not performed. All these factors could lead to a clonal selection and may explain their divergent results and interpretations. Moreover, the effect of mutated dyskerin on tissue development, i.e. hematopoiesis, was not studied.

In this study I systematically investigated the telomere biology in a DC patient harboring a *DKC1* mutation using three patient-derived iPSCs clones over time. Additionally, I investigated how dysfunctional dyskerin affects hematopoietic development and differentiation. The developed model might be useful for further molecular studies on telomere biology but also could serve as platform to screen for molecules that potentially overcome the mutant phenotype.

2. OBJECTIVES

2. Objectives

2.1. General objective

The objective of this study is to characterize the telomere biology during the reprogramming of human cells carrying a *DKC1* gene mutation and their ability of hematopoietic differentiation.

2.2. Specific objectives

i. To derive pluripotent stem cells from somatic cells of a DC patient carrying a *DKC1* mutation;

ii. To investigate telomere length and telomerase activity during several passages of the patient's pluripotent stem cells;

iii. To investigate the capacity of the patient's pluripotent stem cells to differentiate into hematopoietic tissue.

3. MATERIAL AND METHODS

3. Material and methods

3.1. Material

3.1.1. Antibodies and immunostaining reagents

3.1.1.a – Primary antibodies

All the following antibodies were provided by Abcam (Cambridge, UK).

- Mouse anti-human **PML** protein primary antibody
- Rabbit anti-human **NANOG** IgG
- Rabbit anti-human **OCT4** IgG

3.1.1.b – Secondary antibodies

- **Alexa Fluor 555**: donkey anti-rabbit IgG – Invitrogen, Thermo Fisher Scientific (Waltham, MA, USA)
- **Alexa Fluor 594**: donkey anti-mouse IgG – Abcam (Cambridge, UK)

3.1.1.c – Conjugated antibodies

All the following antibodies were provided by BD Biosciences (Franklin Lakes, NJ, USA).

- Mouse anti-human **SSEA4** IgG3k **Alexa Fluor 555**
- Mouse anti-human **TRA-1-60** IgMk **Alexa Fluor 488**
- Mouse anti-human **TRA-1-81** IgMk **Alexa Fluor 488**

3.1.1.d – Immunostaining reagents

- 4′,6-diamidino-2-phenylindole (**DAPI**) solution – Thermo Fisher Scientific (Waltham, MA, USA)
- Bovine Serum Albumin Fraction V solution (**BSA**) – Gibco (Waltham, MA, USA)
- **Donkey serum** – Jackson ImmunoResearch (West Grove, PA, USA)
- **Paraformaldehyde** – Sigma-Aldrich (St. Louis, MO, USA)
- **Slide mounting medium** – Thermo Scientific (Waltham, MA, USA)

- **Vectashield** with 4′,6-diamidino-2-phenylindole (**DAPI**) – Vector Labs (Burlingame, CA, USA)

3.1.2. Bacteria, plasmids, and transfection reagents

3.1.2.a – Bacteria

- One Shot **Stbl3 Chemically Competent *E. coli*** – Invitrogen, Thermo Fisher Scientific (Waltham, MA, USA)

3.1.2.b – Plasmids

- **pMD2.G** plasmid, a gift from Didier Trono for Addgene (code: 12259) – Addgene (Cambridge, MA, USA)
- **psPAX2** plasmid, a gift from Didier Trono for Addgene (code: 12259) – Addgene (Cambridge, MA, USA)
- STEMCCA plasmid carrying *OCT4*, *SOX2*, *KLF4*, and *MYC* (**STEMCCA "four factors"**) – provided by G. Mostoslavsky (Boston University, Boston, MA, USA)
- STEMCCA plasmid carrying *mCherry* gene in place of *MYC* (**STEMCCA "mCherry"**) – provided by G. Mostoslavsky (Boston University, Boston, MA, USA)
- **cre-recombinase expressing vector** pCL20i4rEF1-Puro-T2A-cre-GFP – provided by Harry L. Malech (National Institute of Allergy and Infectious Diseases, Bethesda, MD, USA)

3.1.2.c – Transfection reagents

- **FuGENE 6 transfection reagent** – Promega (Madison, WI, USA)
- **Lipofectamine LTX & Plus Reagent** – Invitrogen (Waltham, MA, USA)
- **Polybrene** – Merck Millipore (Darmstadt, Germany)

3.1.3. Cells

3.1.3.a – Human cell lines

All cell lines are adherent, and were provided by American Type Culture Collection, ATCC (Manassas, VA, USA).

- **293T**: derived from embryonic kidney
- **HeLa**: derived from cervical adenocarcinoma
- **Saos-2**: derived from osteosarcoma
- **U2-OS**: derived from osteosarcoma
- WI 38 VA13 subline 2RA cells, so-called **VA13**: telomerase-deficient cell line

3.1.3.b – Human pluripotent stem cell lines

- **Ctrl iPSCs c26 and c26-3**: iPSCs derived from skin fibroblasts of 22 years old, male, and clinically healthy subject, presenting normal telomere length and no family history of telomere diseases. The iPSCs were kindly provided by Dr. Cynthia E. Dunbar and Dr. Thomas Winkler (NHLBI, NIH, Bethesda, MD, USA). Detailed information regarding derivation of these iPSCs is available in Winkler *et al*. (2013);
- **Ctrl iPSCs PBMCs c7**: iPSCs derived from peripheral blood mononuclear cells (PBMCs) of 29 years old, female, and clinically healthy subject, presenting normal telomere length and no family history of telomere diseases. The PBMCs were reprogrammed using episomal vectors as described by Chou *et al*, 2011 and Dowey *et al*., 2012. Experiments were performed by Maria Florencia Tellechea, master student under Dr. Calado's mentorship (unpublished data);
- **H1**: embryonic stem cell line – WiCell International Stem Cell Bank (Madison, WI, USA);
- *TERT*-mutant iPSCs, ***TERT*[R889X]m c20-8**: iPSCs derived from skin fibroblasts of 55 years old, male patients, presenting pulmonary fibrosis, hypocellular bone marrow (< 5%) with normal peripheral blood cells counts; telomerase function abolished due to mutation. The iPSCs were kindly provided by Dr. Cynthia E. Dunbar and Dr. Thomas Winkler (NHLBI, NIH, Bethesda, MD, USA). Detailed information regarding derivation of these iPSCs is available in Winkler *et al*. (2013).

3.1.3.c – Mouse Embryonic Fibroblasts

- **Mouse Embryonic Fibroblasts** (**MEFs**) mitotically arrested by irradiation – GlobalStem (Gaithersburg, MD, USA)

3.1.4. Cell culture and lab consumables

- 2, 5, 10, 25, and 50 mL **serological pipettes** – Kasvi (Curitiba, PR, Brazil)
- 5 and 10 mL **borosilicate glass pipettes** – Fisherbrand, Thermo Fisher Scientific (Waltham, MA, USA)
- **16-gauge** and **21-gauge needles** – BD Biosciences (Franklin Lakes, NJ, USA)
- 3, 5, and 20 mL **syringes** – BD Biosciences (Franklin Lakes, NJ, USA)
- **13 mm cover slips**, sterilized by immersion in 70% ethyl alcohol – Waldemar Knittel Glasbearbeitungs GmbH (Braunschweig, Germany)
- **Beckman centrifugation tubes** (for ultracentrifugation) – Beckman Coulter (Brea, CA, USA)
- Blot absorbent **filter paper** – Bio-Rad (Hercules, CA, USA)
- **Glass slides** – Precision Glass Line, CRAL (Cotia, SP, Brazil)
- **Parafilm M** – Bemis (Oshkosh, WI, USA)
- **Positively charged nylon membrane** – Roche (Basel, Switzerland)

Labware provided by Corning brands (Corning, NY, USA):

- 25, 75, and 165 cm^2 cell culture treated **flasks** – Corning Falcon
- 35 mm and 100 mm cell culture treated **dishes** – Corning Falcon
- 6-well, 12-well, 24-well, and 96-well flat bottom cell culture treated **plates** – Corning Costar
- 15 and 50 mL **tubes** – Corning Falcon
- 2 mL **cryogenic vials** – Corning
- 0.2, 0.5, 1.5, and 2 mL **microcentrifuge tubes** – Corning Axygen
- 10, 20, 50, 100, 200, and 1000 µL **filtered pipette tips** – Corning Axygen
- **70 *µ*m cell strainer** – Corning Falcon
- Bottle-top **vacuum filter system** (0.22 µm pore filter) – Corning

- **Erlenmeyer flask** – Corning Pyrex
- Ultra-low attachment 6-well **plates** – Corning Costar

3.1.5. Cell culture media

3.1.5.a – Media and matrixes

- Dulbecco's Modified Eagle Medium (**DMEM**) **high glucose** (4.5 g/L) – Gibco (Waltham, MA, USA)
- **DMEM low glucose** (1 g/L) – Gibco (Waltham, MA, USA)
- **DMEM/F12** – Gibco (Waltham, MA, USA)
- **Essential 6** – Gibco (Waltham, MA, USA)
- **Essential 8** – Gibco (Waltham, MA, USA)
- Iscove's Modified Dulbecco's Medium (**IMDM**) – Gibco (Waltham, MA, USA)
- **Knock Out DMEM** Optimized for ES cells – Gibco (Waltham, MA, USA)
- LB nutrient **agar powder** – Bio-Rad (Hercules, CA, USA)
- **LB nutrient broth medium** – Gibco (Waltham, MA, USA)
- **Matrigel** basement membrane matrix – Corning Life Sciences (Corning, NY, USA)
- **MethoCult H4435** – STEMCELL Technologies (Vancouver, Canada)
- **mTeSR** – STEMCELL Technologies (Vancouver, Canada)
- STEMdiff Albumin Polyvinyl alcohol Essential Lipids (**APEL**) basal medium – STEMCELL Technologies (Vancouver, Canada)

3.1.5.b – Reagents and medium supplements

- **β-mercaptoethanol** – Sigma-Aldrich (St. Louis, MO, USA)
- **Accutase** cell detachment solution – Merck Millipore (Darmstadt, Germany)
- **Ampicillin** Ready Made Solution – Sigma-Aldrich (St. Louis, MO, USA)
- **Collagenase II** – Gibco (Waltham, MA, USA)
- **Collagenase IV** – Gibco (Waltham, MA, USA)
- Dimethyl sulfoxide (**DMSO**) – Sigma-Aldrich (St. Louis, MO, USA)
- **Dispase** – Gibco (Waltham, MA, USA)

- Ethylenediaminetetraacetic acid (**EDTA**) – Sigma-Aldrich (St. Louis, MO, USA)
- Fetal Bovine Serum (**FBS**); used heat-inactivated at 56°C for 30 min, and filtered – Gibco (Waltham, MA, USA)
- **HyClone FBS defined**; used heat-inactivated at 56°C for 30 min, and filtered – Thermo Scientific (Waltham, MA, USA)
- Knockout serum replacement (**KSR**) – Gibco (Waltham, MA, USA)
- **L-glutamine** – Gibco (Waltham, MA, USA)
- **MycoAlert Mycoplasma Detection** kit – Lonza (Rockland, ME, USA)
- Nonessential amino acids (**NEAA**) – Gibco (Waltham, MA, USA)
- Penicillin-Streptomycin-Glutamine (**PSG**) – Gibco (Waltham, MA, USA)
- **Phosphate Buffered Saline (PBS)**, 1×, pH = 7.2 – Gibco (Waltham, MA, USA)
- **Polyvinyl alcohol** – Sigma-Aldrich (St. Louis, MO, USA)
- **Puromycin** – Sigma-Aldrich (St. Louis, MO, USA)
- **ROCK inhibitor** (Y-27632) – Merck Millipore (Darmstadt, Germany)
- **Trypsin** (used at 0.05% in 1×PBS) – Gibco (Waltham, MA, USA)
- Ultra-pure water with **0.1% gelatin** – EDM Millipore, Merck Millipore (Darmstadt, Germany)
- **Valproic acid** – Stemgent (Cambridge, MA, USA)

3.1.5.c – Media preparation

- **ESC medium**

	Final concentration
DMEM/F12	n/a
KSR	20%
bFGF	10 ng/mL
NEAA	0.1 mM
L-glutamine	1 mM
β-mercaptoethanol	0.1 mM

- **D10 medium**

	Final concentration
DMEM low glucose	n/a
FBS	10%
PSG	1%

- **D20 medium**

	Final concentration
DMEM low glucose	n/a
FBS	20%
PSG	1%

- **D-MEF medium**

	Final concentration
DMEM high glucose	n/a
FBS	10%
NEAA	0.1 mM

- **I10 medium**

	Final concentration
IMDM	n/a
FBS	10%
PSG	1%

3.1.6. Cytokines

- Recombinant human fibroblast-like growth factor-basic (**bFGF**) – PeproTech (Rocky Hill, NJ, USA)

All the following cytokines were provided by R&D Systems (Minneapolis, MN, USA):

- **Activin A**
- Bone Morphogenetic Protein 4 (**BMP4**)
- FMS-like tyrosine kinase 3 Ligand (**Flt3L**)
- Granulocyte-colony stimulating factor (**G-CSF**)
- Interleukin-3 (**IL-3**)
- Interleukin-6 (**IL-6**)
- Stem Cell Factor (**SCF**)
- Vascular Endothelial Growth Factor (**VEGF**)

3.1.7. DNA sequencing

- **BigDye Terminator** Cycle Sequencing kit – Applied Biosystems (Waltham, MA, USA)
- **DyeEx 2.0 spin** kit – QIAGEN (Valencia, CA, USA)
- **Hi-Di formamide** – Applied Biosystems (Waltham, MA, USA)

3.1.8. Electrophoresis

- **1 kb plus DNA ladder** – Invitrogen (Waltham, MA, USA)
- **Agarose powder** – Sigma-Aldrich (St. Louis, MO, USA)
- Ethidium bromide (**EtBr**) – Amresco (Solon, OH, USA)
- GeneRuler **DNA Ladder Mix** – Thermo Fisher Scientific (Waltham, MA, USA)

3.1.9. Equipment

- **−80°C freezer** Forma 88000 series – Thermo Scientific, Thermo Fisher Scientific (Waltham, MA, USA)
- **−20°C freezer** Bosch Intelligent Freezer 32 – Robert Bosch GmbH (Gerlingen, Germany)
- **4°C refrigerator** Bosch Intelligent All Refrigerator 39 – Robert Bosch GmbH (Gerlingen, Germany)
- 2, 10, 20, 50, 100, 200, and 1000 µL **micropipettes** – Eppendorf (Hamburg, Germany)
- **2100 Bioanalyzer** – Agilent Technologies (Santa Clara, CA, USA)
- 7500 **Real-Time PCR System** – Applied Biosystems, Thermo Fisher Scientific (Waltham, MA, USA)
- ABI Prism 3100 **DNA sequencer** – Applied Biosystems, Thermo Fisher Scientific (Waltham, MA, USA)
- ABI Prism 7000 **Sequence Detection System** – Applied Biosystems, Thermo Fisher Scientific (Waltham, MA, USA)
- **Analytical balance** – Scientific Industries (Bohemia, NY, USA)
- **Centrifuge** 5430 R (benchtop microcentrifuge) – Eppendorf (Hamburg, Germany)

- **Centrifuge** 5810 R – Eppendorf (Hamburg, Germany)
- **CO_2 cell culture incubator** maintained at 37°C, 21% O_2, 5% CO_2, and humid – Thermo Scientific, Thermo Fisher Scientific (Waltham, MA, USA)
- CoolCell Alcohol-free **Cell Freezing Container** – BioCision (San Rafael, CA, USA)
- **Cytospin centrifuge** Cytospin 3 – Shandon Southern Instruments Limited (Runcorn, Cheshire, England)
- **DNA SpeedVac Concentrator** Savant – Thermo Scientific, Thermo Fisher Scientific (Waltham, Massachusetts, USA)
- Electronic **pipette controller** Easypet 3 – Eppendorf (Hamburg, Germany)
- **Electrophoresis unit** – Bio-Rad (Hercules, CA, USA)
- **Fluorescence microscope** AxioImager.M2 – Carl Zeiss (Oberkochen, Germany)
- **Hot plate** C-MAG HS 7 – IKA (Wilmington, NC, USA)
- **ImageQuant** imaging system – GE Healthcare Life Sciences (Little Chalfont, UK)
- **Inverted microscope** Axiovert 40 CFL – Carl Zeiss (Oberkochen, Germany)
- **Liquid nitrogen CryoPlus Storage System** – Thermo Scientific, Thermo Fisher Scientific (Waltham, MA, USA)
- LSR II **Flow Cytometer** System – BD Biosciences (Franklin Lakes, NJ, USA)
- **Microscope** Lx400 – Labomed (Los Angeles, CA, USA)
- Milli-Q Plus PF **water purification system** – EDM Millipore, Merck Millipore (Darmstadt, Germany)
- **NanoDrop ND1000 spectrophotometer** – Thermo Scientific, Thermo Fisher Scientific (Waltham, MA, USA)
- **Neubauer chamber** Improved Double – Precision Glass Line, CRAL (Cotia, SP, Brazil)
- **Orbital shaker** – Thermo Scientific, Thermo Fisher Scientific (Waltham, MA, USA)
- **QIAgility** robotic workstation for automated PCR setup – QIAGEN (Valencia, CA, USA)
- **Rotor-Gene Q** real-time PCR cycler – QIAGEN (Valencia, CA, USA)
- SpectraMax **fluorometer** – Molecular Devices (Sunnyvale, CA, USA)
- **Stereomicroscope** S4 E – Leica (Wetzlar, Germany)
- **Sterile cell culture laminar-flow hood** (class II biosafety cabinet) – Thermo Scientific, Thermo Fisher Scientific (Waltham, MA, USA)
- **Thermal cycler** Veriti – Applied Biosystems, Thermo Fisher Scientific (Waltham, MA, USA)

- ThermoStat Plus **shaker and thermoblock for microcentrifuge tubes** – Eppendorf (Hamburg, Germany)
- **Ultracentrifuge** Optima L8-70M, SW 28 Ti rotor – Beckman Coulter (Brea, CA, USA)
- **UV crosslinker** – Amersham Biosciences Corp., GE Healthcare Life Sciences (Little Chalfont, UK)
- **Vortex** Genie 2 – Scientific Industries (Bohemia, NY, USA)
- Victor3 **luminometer** – Perkin Elmer (Boston, MA, USA)
- **Water bath** – Fanem (Guarulhos, SP, Brazil)

3.1.10. Nucleic acids isolation

- **DNase I** – Gibco (Waltham, MA, USA)
- **DNeasy** Blood & Tissue kit – QIAGEN (Valencia, CA, USA)
- **Ethanol**, absolute – Merck (Darmstadt, Germany)
- **Isopropanol**, absolute – Merck (Darmstadt, Germany)
- **Plasmid Purification** Mega kit – QIAGEN (Valencia, CA, USA)
- **Proteinase K** – Invitrogen (Waltham, MA, USA)
- **RNA 6000 Nano** kit – Agilent Technologies (Santa Clara, CA, USA)
- **RNeasy** Mini kit – QIAGEN (Valencia, CA, USA)

3.1.11. Other chemicals, kits, and reagents

- **Genome-Wide Human SNP CytoScan HD Arrays** – Affymetrix (Santa Clara, CA, USA)
- **TeloTAGGG Telomere Length Assay** kit – Roche (Basel, Switzerland)
- **TRAPeze XL Telomerase Detection** kit – Merck Millipore (Darmstadt, Germany)
- **Pierce BCA Protein Assay** kit – Thermo Scientific (Waltham, MA, USA)

All the following reagents were provided by Sigma-Aldrich (St. Louis, MO, USA):

- 4-(1,1,3,3-Tetramethylbutyl)phenyl-polyethylene glycol (**Triton X-100**)
- **Acetate** solution

- **Formamide**
- Hydrochloric acid (**HCl**)
- Polyethylene glycol sorbitan monolaurate (**Tween 20**)
- Potassium chloride (**KCl**)
- Ribonuclease A (**RNase**)
- Sodium chloride (**NaCl**)
- **Sodium citrate**
- Sodium dodecyl sulfate (**SDS**)
- Tergitol-type NP-40 (**NP-40**)
- Tris(hydroxymethyl)aminomethane (**Tris base**)
- **Wright's stain**

3.1.12. PCR reagents and kits

- **2× TaqMan Gene Expression Master Mix** – Applied Biosystems (Waltham, MA, USA)
- **dATP**, **dGTP**, and **dTTP** – Invitrogen (Waltham, MA, USA)
- **dNTP** Set (100 mM) Solution – Invitrogen (Waltham, MA, USA)
- **DTT**, Molecular Grade (DL-Dithiothreitol) – Promega (Madison, WI, USA)
- **High-capacity cDNA Reverse Transcription** kit – Applied Biosystems (Waltham, MA, USA)
- Magnesium chloride (**$MgCl_2$**) – Sigma-Aldrich (St. Louis, MO, USA)
- **phi29 DNA Polymerase** kit – New England BioLabs (Ipswich, MA, USA)
- **Platinum PCR SuperMix High Fidelity** kit – Invitrogen (Waltham, MA, USA)
- **Platinum Taq DNA Polymerase** – Invitrogen (Waltham, MA, USA)
- **QIAquick PCR purification** kit – QIAGEN (Valencia, CA, USA)
- Ribonuclease H (**RNase H**) – Thermo Fisher Scientific (Waltham, MA, USA)
- **RNaseOUT** Recombinant Ribonuclease Inhibitor – Invitrogen (Waltham, MA, USA)
- **Rotor-Gene SYBR Green PCR Master Mix** – QIAGEN (Valencia, CA, USA)
- **SuperScript II Reverse Transcriptase** kit – Invitrogen (Waltham, MA, USA)
- **SYBR Green PCR Master Mix** – Applied Biosystems (Waltham, MA, USA)
- **TaqMan Universal Master Mix** – Applied Biosystems (Waltham, MA, USA)
- **Ultra-pure water**, molecular grade

3.1.13. Primers and probes

- 10× TaqMan probe for ***TERT*** (Hs99999022_m1), ***TERC*** (Hs03454202_s1), ***DKC1*** (Hs00154737_m1), and ***GAPDH*** (Hs4333764) – Applied Biosystems, Thermo Fisher Scientific (Waltham, MA, USA)
- **PNA telomere FISH probe** (TelG-FITC) – PNA Bio (Thousand Oaks, CA, USA)
- **Random Hexamers** (50 μM) – Invitrogen, Thermo Fisher Scientific (Waltham, MA, USA)

All the following primers sequences were synthetized by Integrated DNA Technologies, IDT (Coralville, IA, USA):

- Primers and probes sequences for detection of copy numbers of STEMCCA vector integrated in the genome of iPSCs.

HIV RRE	Forward	5′ GGGAGCAGCAGGAAGCAC 3′
	Reverse	5′ TTGTCTGGCCTGTACCGTCA 3′
	Probe	5′ ATGGGCGCAGCGTCAATGACG 3′
STP	Forward	5′ GGTGCCCTTCCTTGAGTTCA 3′
	Reverse	5′ CCCCTTGCACCCAGGAC 3′
	Probe	5′ CCCCAGGGATTCCCTCAGGTGTGT 3′

- Primers for amplifying exon 11 of the *DKC1* gene.

***DKC1* – exon 11**	
Forward	5′ GCACCCTCTTAGTGAATGAACC 3′
Reverse	5′ CCCAGTACCACTTACCTTTGGA 3′

- Primers for expression of pluripotency, endoderm, mesoderm, and ectoderm markers. F: forward; R: reverse.

Marker	Gene	Primer sequence
Pluripotency (endogenous)	*OCT4*	F – 5′ CCTCACTTCACTGCACTGTA 3′
		R – 5′ CAGGTTTTCTTTCCCTAGCT 3′
	SOX2	F – 5′ CCCAGCAGACTTCACATGT 3′
		R – 5′ CCTCCCATTTCCCTCGTTTT 3′
	KLF4	F – 5′ GATGAACTGACCAGGCACTA 3′
		R – 5′ GTGGGTCATATCCACTGTCT 3′
	MYC	F – 5′ TGCCTCAAATTGGACTTTGG 3′
		R – 5′ GATTGAAATTCTGTGTAACTGC 3′
	NANOG	F – 5′ TGAACCTCAGCTACAAACAG 3′
		R – 5′ TGGTGGTAGGAAGAGTAAAG 3′
Endoderm	*AFP*	F – 5′ AGCTTGGTGGTGGATGAAAC 3′
		R – 5′ CCCTCTTCAGCAAAGCAGAC 3′
	GATA4	F – 5′ CTAGACCGTGGGTTTTGCAT 3′
		R – 5′ TGGGTTAAGTGCCCCTGTAG 3′
Mesoderm	*RUNX1*	F – 5′ CCCTAGGGGATGTTCCAGAT 3′
		R – 5′ TGAAGCTTTTCCCTCTTCCA 3′
	CD34	F – 5′ TGAAGCCTAGCCTGTCACCT 3′
		R – 5′ CGCACAGCTGGAGGTCTTAT 3′
Ectoderm	*NCAM*	F – 5′ ATGGAAACTCTATTAAAGTGAACCTG 3′
		R – 5′ TAGACCTCATACTCAGCATTCCAGT 3′
	NES	F – 5′ GCGTTGGAACAGAGGTTGGA 3′
		R – 5′ TGGGAGCAAAGATCCAAGAC 3′
Housekeeping	*ACTB*	F – 5′ TGAAGTGTGACGTGGACATC 3′
		R – 5′ GGAGGAGCAATGATCTTGAT 3′

- Primer sequences for telomere repeats (T) and 36B4 gene (S).

T	Forward	5′ ACACTAAGGTTTGGGTTTGGGTTTGGGTTTGGGTTAGTGT 3′
	Reverse	5′ TGTTAGGTATCCCTATCCCTATCCCTATCCCTATCCCTAACA 3′
S	Forward	5′ CAGCAAGTGGGAAGGTGTAATCC 3′
	Reverse	5′ CCCATTCTATCATCAACGGGTACAA 3′

3.1.14. Restriction enzymes

- FastDigest restriction enzymes: ***Bam*HI**, ***Eco*RI**, ***Hinc*II**, ***Hind*III**, ***Hinf*I**, ***Not*I**, and ***Rsa*I** – Thermo Scientific, Thermo Fisher Scientific (Waltham, Massachusetts, USA)

3.1.15. Software

- **Applied Spectral Imaging** software (acquisition of fluorescent images) – Applied Spectral Imaging Ltd. (Carlsbad, CA, USA)
- **Cell^{F}** software (acquisition of cell culture images) – Olympus (Shinjuku, Tokyo, Japan)
- **CLC Main Workbench** software, version 5.7 (analysis of chromatograms from sequencing) – CLC bio (Aarhus, Denmark)
- **FlowJo** software (flow cytometry analysis) – FlowJo, LLC (Ashland, OR, USA)
- **GraphPad Prism** software, version 5.0c (statistics and graph plotting) – GraphPad Software (La Jolla, CA, USA)
- **ImageQuant** software (acquisition of gel and chemiluminescence images) – GE Healthcare Life Sciences (Little Chalfont, UK)
- The Chromosome Analysis Suite (**ChAS**) software (SNP arrays analysis) – Affymetrix (Santa Clara, CA, USA)
- **SoftMax** software (acquisition of fluorometric measurements) – Molecular Devices (Sunnyvale, CA, USA)

3.1.16. Solutions and buffers

- **50× TAE buffer** (for electrophoresis)

2 M Tris-acetate, 0.05 M EDTA pH 8, in deionized water

1× TAE buffer was prepared diluting the 50× TAE buffer in deionized water.

- **HCl solution** (for Southern blot)

0.25 M HCl in Milli-Q water

- **Denaturation solution** (for Southern blot)

0.5 M NaOH, 1.5 M NaCl, in Milli-Q water

- **Neutralization solution**, pH 7.5 (for Southern blot)

0.5 M Tris-HCl, 3 M NaCl, in Milli-Q water

- **20× SSC buffer**, pH 7.0 (for Southern blot, and C-circle assay)

3 M NaCl, 0.3 M Sodium citrate, in Milli-Q water

2× and 0.2× SSC buffers were prepared diluting the 20× SSC buffer in Milli-Q water

- **Stringent wash buffer I** (for Southern blot, and C-circle assay)

2× SSC plus 0.1% SDS

- **Stringent wash buffer II** (for Southern blot, and C-circle assay)

0.2× SSC plus 0.1% SDS

- **Lysis buffer** (for C-circle assay)

0.05 M KCl, 0.01 M Tris-HCl, 2 mM $MgCl_2$, 0.45% NP-40, 0.45% Tween 20, in Milli-Q water.

3.2. Methods

3.2.1. Derivation of patient skin fibroblasts

Skin from punch biopsy of the upper medial arm was used to derive dermal fibroblasts. Biopsy was performed at the Clinical Hospital at Ribeirão Preto Medical School (HCFMRP, Ribeirão Preto, SP, Brazil) under approval of ethics committee (HCRP 8723/2006) following written informed consent in accordance with the Declaration of Helsinki of patient's legal guardian. Biopsy was cut into pieces of approximately 1 mm^3 size and placed in 10 mL 1×PBS containing 100 mg/mL collagenase II, 2.5 U/mL dispase and 10 U/μL DNase I. Skin fragments were incubated for 50 min in an orbital shaker (200 rpm) at 37°C. Fragments were washed with D20 medium. Each fragment was transferred to one well of a 6-well tissue culture plate, and then covered with a sterile glass slip. Skin fragments were cultured in D20 for approximately 10 days. All cell lines and iPSCs were cultured in incubators with ambient oxygen pressure and 5% CO_2. Fibroblasts that grew out of the tissue were enzymatically dissociated from the tissue culture plate and glass slips. For this purpose, wells containing fibroblasts were washed once with 1×PBS, and then treated with 0.5 mL 0.05% trypsin for 3 min at 37°C. After adding 4 mL D20 medium, the entire content was transferred to 25 cm^2 tissue culture flasks previously prefilled with 5 mL of warmed D20 medium. Medium change occurred every 3 days. After reaching approximately 75% confluence, the fibroblasts were passaged using 0.05% trypsin.

For expansion, trypsinized fibroblasts were centrifuged (300 × *g* for 5 min), counted with a Neubauer chamber, and seeded in a 75 cm^2 cell culture flask at a concentration of 5×10^5 cells per flask.

For freezing, aliquots of 1×10^6 cells were centrifuged (300 × *g* for 5 min) and resuspended in 1 mL of cold freezing medium containing 10% DMSO in FBS. Aliquots were transferred to cryogenic vials and immediately placed into a cell freezing container in the −80°C freezer. After 24 h, vials were transferred to a liquid nitrogen storage system for long-term storage.

Frozen cells were thawed separately. Immediately after removed from liquid nitrogen, the vial was quickly thawed in water bath at 37°C for 2 min. The content was transferred dropwise to a 15 mL tube containing 9 mL of pre-warmed (37°C) D20. The tube was centrifuged (300 × *g* for 5 min), the supernatant was removed, and cell pellet was resuspended in 10 mL of D20, homogenized by pipetting, and transferred to a 165 cm^2 cell

culture flask and cultured as described above. All steps of cell manipulation described in the present study were performed under sterile conditions in a cell culture laminar-flow hood (class II biosafety cabinet).

3.2.2 Testing cell cultures for mycoplasma contamination

Cell cultures were routinely tested for mycoplasma contamination using the MycoAlert Mycoplasma Detection kit according to manufacture's recommendations. Approximately 1 mL of supernatant was taken from culture cells preferably at high confluences and without medium change for 48 h. Supernatant was transferred to a 1.5 mL tube and centrifuged at 200 × *g* for 5 min. An aliquot of 100 µL of cleared supernatant was placed in a well of 96-well plate and added to 100 µL MycoAlert Reagent, then incubated at room temperature for 5 min in order to lyse possible mycoplasma in the supernatant. The reaction of ATP in the cell supernatant with luciferin emits light that can be detected with standard luminometers. The levels of ATP measured as luminescence (reading A), were read on the Victor3 luminometer. After, 100 µL MycoAlert Substrate was added and incubated at room temperature for 10 min. In the presence of mycoplasmal enzymes, the substrate reacts with the enzymes catalyzing the conversion of ADP to ATP. Again, the levels of ATP were read on the luminometer (reading B). The ratio of reading B to reading A was used to determine whether a cell culture was contaminated by mycoplasma, in which ratios greater than 1 were interpreted as contamination. A positive control provided in the kit was always run in each round of analysis. Contaminated cell cultures were immediately removed from the incubator and discarded.

3.2.3. Bacterial transformation

Plasmids containing viral packing information and the reprogramming transgenes were expanded after transformation in *E. coli* strain Stbl3. Detailed plasmid maps are shown in Figure 3.1 and Figure 3.2.

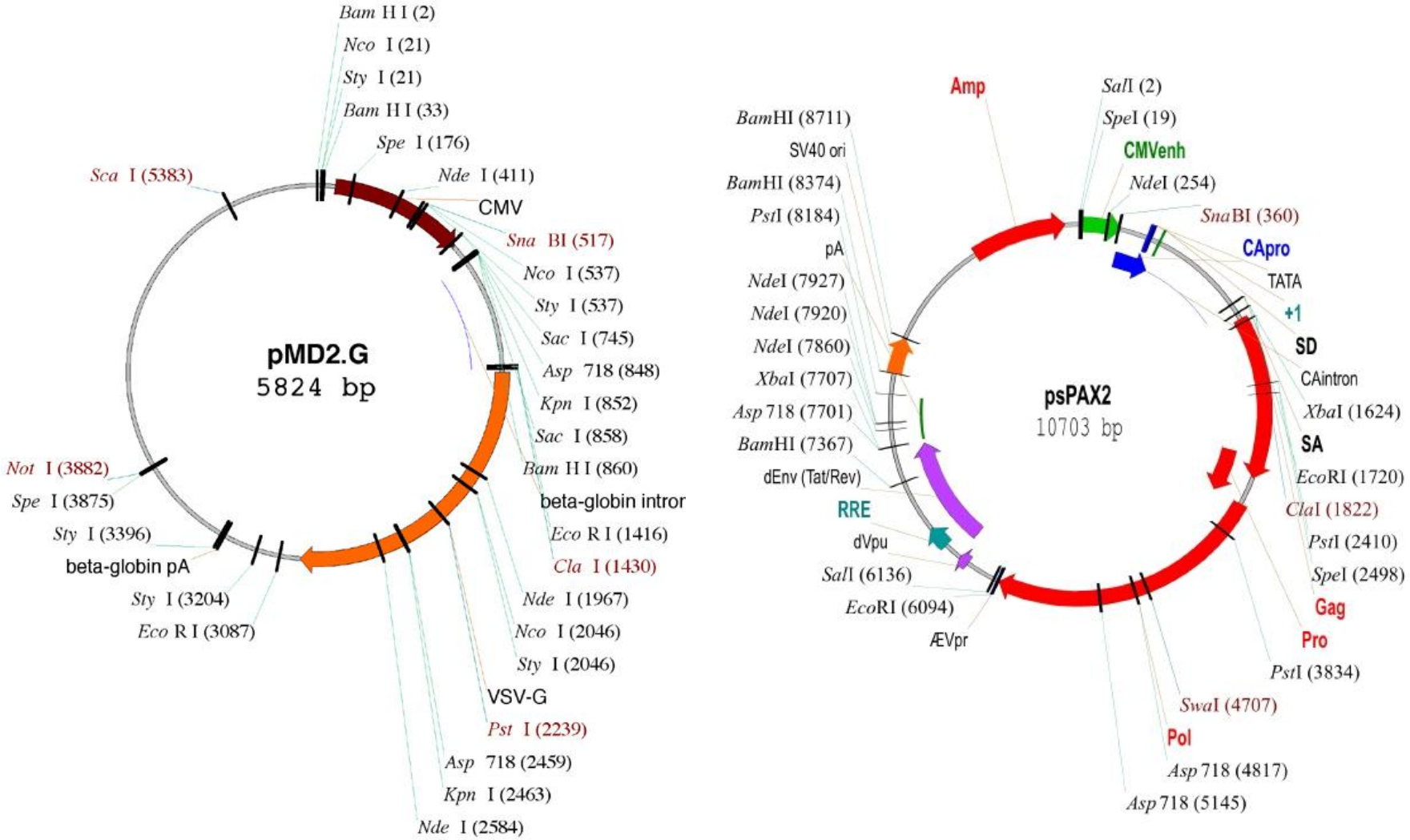

Figure 3.1 – Maps of plasmids pMD2.G and psPAX2. Maps showing restriction sites as well as genes for VSV-G envelope (pMD2.G), and lentiviral packing (psPAX2). Transformed bacteria present resistance to ampicillin (Amp). In parentheses are the positions relative to the origin of replication (SV40 ori) expressed in base pairs (bp). Images provided by the depositor, Didier Trono (available at www.addgene.org).

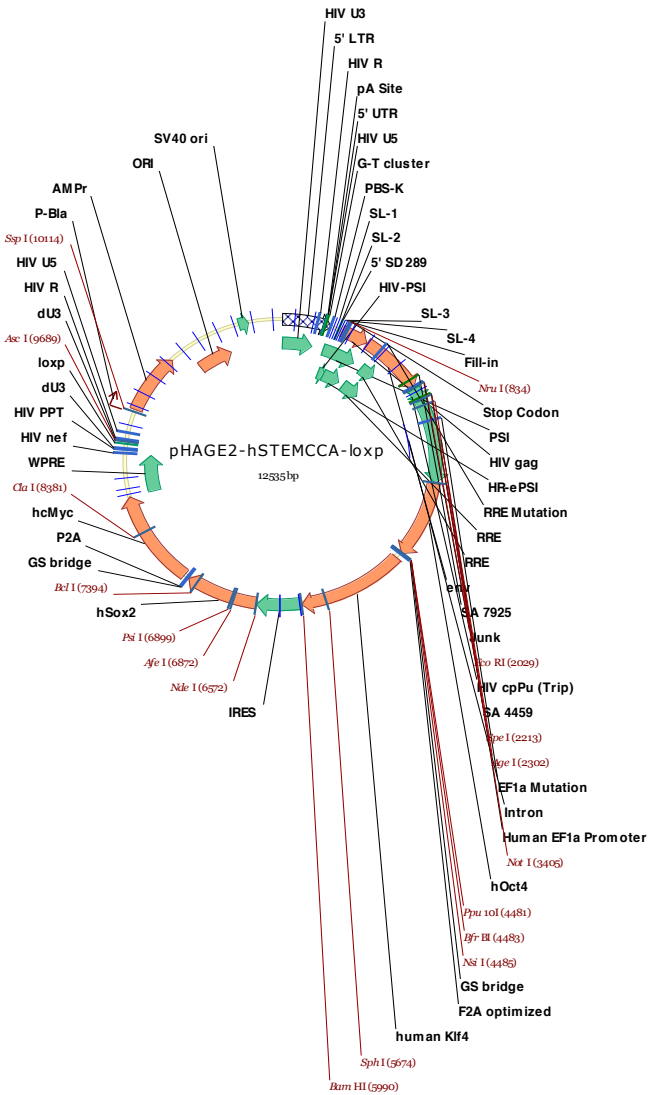

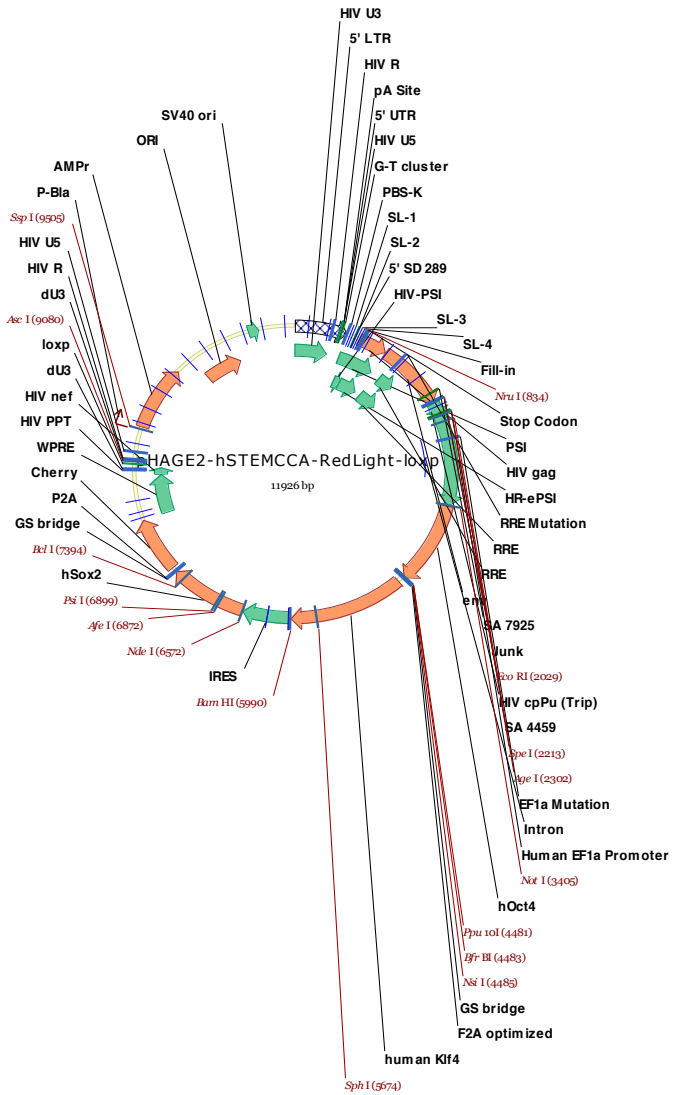

Figure 3.2 – Maps of STEMCCA plasmids. Maps showing restriction sites as well as the four reprogramming transcription factors (hSTEMCCA, left) or the *mCherry* gene in place of *MYC* (hSTEMCCA-RedLight, right). Transformed bacteria present resistance to ampicillin. In parentheses are the positions relative to the origin of replication (SV40 ori) expressed in base pairs (bp). Images kindly provided by G. Mostoslavsky (Boston University, Boston, Massachusetts, USA).

Competent bacteria (Stbl3 *E. coli*) were transformed with each plasmid as follows: bacteria were thawed on ice for about 2 min; 100 ng of plasmid DNA was added and gently mixed; vials were incubated on ice for 30 min, then heat-shocked for 45 s at 42°C, and then, placed for 2 min on ice; 250 µL of pre-warmed S.O.C. medium was added to each vial and incubated at 37°C for 1 h in a shaking incubator (225 rpm). After, 100 µL of each transformation reaction was spread on a pre-warmed LB agar plate (100 mm dish) containing 100 µg/mL ampicillin for selection. Dishes were inverted and incubated overnight at 37°C. One individual colony per plasmid was picked and transferred to 10 mL LB nutrient broth medium containing 100 µg/mL ampicillin and incubated for 8 h at 37°C in an orbital shaker (300 rpm). From this starter culture, 1 mL was placed in an Erlenmeyer flask containing 500 mL LB nutrient broth medium with 100 µg/mL ampicillin, and incubated overnight at 37°C in a orbital shaker (300 rpm). The bacterial cells were harvested by centrifugation (6,000 × *g* for 15 min at 4°C). The supernatant was discarded and the plasmid DNA from cell pellet was isolated.

3.2.4. Plasmid DNA purification

For isolating the plasmid DNA from bacteria, the Plasmid Purification Mega kit was used according to manufacture's recommendations with modifications. First, cells were lysed by adding buffer P1 plus LyseBlue reagent and simultaneously vortexing and pipetting up and down until disrupt all cell clumps. Buffer P2 was added and vigorously homogenized by inverting 5 times, and then incubated at room temperature for 5 min. Chilled buffer P3 was added and homogenized by inversion, and incubated on ice for 30 min. The lysate was filtered using filter paper in order to clear supernatant containing plasmid DNA. The supernatant was applied to a QIAGEN-tip (from kit, previously equilibrated with buffer QBT) and allowed to enter the resin by gravity flow. The DNA was bound to the resin in this step. The QIAGEN-tip was washed with buffer QC to remove remaining contaminants from resin. Then, DNA was eluted from resin by adding buffer QF. The DNA was precipitated from the eluate by adding 0.7 volumes of room-temperature isopropanol, and centrifuging at 6,000 × *g* for 1 h at 4°C. The supernatant was carefully decanted. The DNA pellet was washed with 70% ethanol at room temperature, and centrifuged at 6,000 × *g* for 20 min at 4°C. The supernatant was decanted and the pellet was air-dried for 30 min. Finally, DNA was dissolved in 1 mL ultra-pure water and quantified using the NanoDrop spectrophotometer.

The identity of the purified plasmids was confirmed by restriction digest. The plasmid DNA of each sample was digested with a set of restriction enzymes (Figure 3.3). Agarose gel electrophoresis was used to analyze the length of the digested products. FastDigest enzymes were used following manufacture's recommendations with modifications. For each reaction, 500 ng of plasmid was added to 2 µL 10× FastDigest buffer, 1 µL FastDigest enzyme (1 µL of each enzyme for double digestion), and ultra-pure water (to complete a final volume of 20 µL). Samples were incubated for 30 min at 37°C in the water bath. The pMD2.G plasmid was digested with *Hind*III alone, *Not*I alone, and both *Hind*III and *Not*I. The psPAX2 plasmid was digested with *Bam*HI alone (cleaving at three different sites), and *Eco*RI alone (cleaving at two different sites). STEMCCA "four factors" was digested with *Bam*HI alone, *Eco*RI alone, and both *Bam*HI and *Eco*RI. STEMCCA "mCherry" was digested with *Hinc*II (cleaving at two different sites).

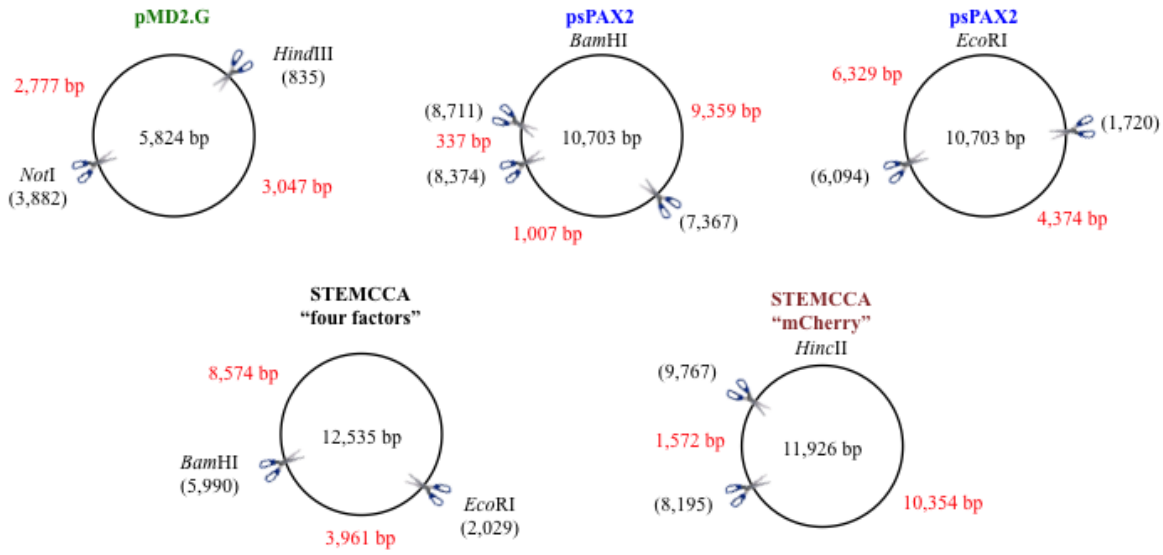

Figure 3.3 – Restriction enzymes and digestion sites of plasmids. Different restriction enzymes were selected for each plasmid according to the sizes of digestion sites. In parentheses are the sites of recognition and cleavage in base pairs (bp), represented in the plasmid maps as scissors. Numbers in red represent the sizes of fragments produced after digestion.

The products of digested as well as non-digested plasmids, along with a molecular weight ladder (1 kb), were loaded in a 1% agarose gel containing 0.5 µg/mL EtBr, and run in an electrophoresis unit filled with 1× TAE buffer (80 V for 30 min). The DNA fragments (bands) in the gel were visualized through a device emitting UV light (ImageQuant imaging

system and software).

3.2.5. Production and titration of lentiviral particles

The production of viral particles was done as described by Sommer *et al*. (2009). First, 293T-packaging cells were cultured in 165 cm^2 cell culture flasks and I10 medium until achieving a confluence about 70%. On the day previous to transfection (day −1), cells were enzymatically removed from the flask using 0.05% trypsin (as described in the previous section for fibroblasts culture). Cells were centrifuged (300 × *g* for 5 min), counted using a Neubauer chamber, and seeded in 100 mm cell culture dishes, 5×10^6 cells per dish, in I10. The next day, media was replaced with fresh I10 and an ideal confluence of 70-80% was expected: a too high cell density impairs transfection whereas a too low density leads to poor cell survival after transfection. For each dish, transfection medium (final volume of 200 µL) was composed of serum free IMDM plus 12 µL FuGENE 6 transfection reagent. The following reagents and plasmids were added: 0.2 µg pMD2.G, 1.8 µg psPAX2, and 2 µg STEMCCA plasmids, either STEMCCA "four factors" or STEMCCA "mCherry" (incubated for 15 min at room temperature). The transfection mixture was added dropwise to the cells. Cells were incubated overnight. After 24 h, the cells supernatant was collected and replaced with fresh I10. In order to separate cell debris from viral particles, the supernatant was filtered using 0.22 µm pore filter systems. The viral particles were concentrated 100× by ultracentrifugation (20,000 × *g* at 4°C for 2 h). Virus particles were resuspended in serum free IMDM, aliquoted in 1.5 mL tubes and stored in the −80°C freezer. This procedure was repeated after 48 h. STEMCCA "mCherry" was produced parallel to the STEMCCA "four factors" in order to facilitate titration through measuring the red fluorescence emitted by the mCherry protein.

For titration, HeLa cells were transduced with viruses STEMCCA "mCherry" at different concentrations. In detail, one day prior to transduction, HeLa cells were seeded in 12-well cell culture plates at 3×10^4 cells per well in D10 medium. Right before the transduction, the number of cells per well was estimated as follows: three wells were harvested using trypsin (as described for derivation of fibroblasts). The cells were counted using a Neubauer chamber. The cells numbers were averaged and later used to calculate the viral titer at transduction. The cells were transduced with four serial dilutions of concentrated virus (n = 4) diluted in D10 medium containing 6 µg/mL polybrene: 4 µL, 1.6 µL, 0.64 µL,

and 0.256 µL. The transduction was performed for both viruses collected 24 h and 48 h post transfection. Five days after transduction, fluorescence emitted by mCherry was assessed by flow cytometry. Assuming that one virus infects a cell that emits fluorescence, virus titer could be determined as:

$$\text{Titer (virus/µL)} = \frac{1}{n} \sum_{i=1}^{n} \frac{\text{Total number of cells} \times \% \text{ of mCherry}^{+} \text{ cells}}{\text{Volume of serial dilution}}$$

Since the viral production of STEMCCA "mCherry" and STEMCCA "four factors" was done in parallel using the exact same cells and conditions, equal titers between the two viruses can be assumed.

3.2.6. Generation of iPSCs

Induced pluripotent stem cells (iPSCs) were generated from dermal fibroblasts by forced expression of the reprogramming transcription factors *OCT4*, *SOX2*, *KLF4*, and *MYC* using a "stem cell cassette" (STEMCCA "four factors"), a single polycistronic lentiviral vector expressing the factors (Sommer *et al*., 2009). One day prior to lentiviral transduction, patient fibroblasts in culture, that tested negative for mycoplasma contamination, were harvested with trypsin as previously described (section "3.2.1. Derivation of skin fibroblasts"). Cells were centrifuged (300 × *g* for 5 min), counted with a Neubauer chamber, and seeded in a 6-well cell culture plate, 1×10^5 cells per well, in D20, and maintained in a CO_2 cell culture incubator. Fibroblasts were seeded at passage 7. The next day, cells were transduced with STEMCCA "four factors" lentiviruses. First, one representative well of the plate was selected for cell counting. This well was rinsed with 1×PBS and trypsinized, incubated at 37°C and rinsed with D20. Cells were counted using a Neubauer chamber. The number of cells in this well was used as an estimate for the other wells. Based on this number, the amount of viruses needed per well was calculated. Two multiplicity of infection (MOI) were tested: 2.5 and 5. The MOI corresponds to the number of transduced viruses per cell (e.g. MOI = 5 means that the number of viruses used in transduction was 5 times the estimate number of cells in the well). Although virtually one virus is sufficient for reprogramming one cell, MOI higher than 1 is commonly used in order to increase the efficiency of reprogramming experiments. The

use of a MOI below 10 is recommended to prevent that many viruses integrate into the genome of the target cell. After calculating the amount of both STEMCCA "four factors" and STEMCCA "mCherry" lentiviruses needed per well (based on titration of STEMCCA "mCherry", as described in the previous section), the transduction medium was prepared: 1 mL D20, 6 μg/mL polybrene, and lentiviruses. Fibroblasts medium was replaced with transduction medium as follows:

- Well number 1: STEMCCA "four factors", MOI = 2.5;
- Well number 2: STEMCCA "four factors", MOI = 5;
- Well number 3: STEMCCA "mCherry", MOI = 2.5;
- Well number 4: transduction medium without virus (negative control);
- Well number 5: harvested for cell counting;
- Well number 6: empty.

Plate was incubated for 6 h in a CO_2 cell culture incubator. Then, transduction medium was replaced with D20. Five days after transduction, fibroblasts were enzymatically removed from wells using trypsin and counted as previously described. Fibroblasts transduced with STEMCCA "mCherry" were analyzed in a flow cytometer in order to calculate the percentage of transduced cell in the STEMCCA "four factors" conditions. This calculation considered the percentage of cells that emitted the mCherry red fluorescence and also provided information about transduction efficiency. The percentage of STEMCCA "four factors" was assumed to be similar to the one observed for STEMCCA "mCherry". The well containing transduction medium without virus was used as negative control in the flow cytometry analysis, in order to estimate and subtract the autofluorescence emitted by the cells. Based on transduction efficiency of mCherry, the fibroblasts transduced with STEMCCA "four factors" (MOI = 5) were transferred to two 100 mm gelatin-coated culture dishes (1×10^5 and 1.5×10^5 cells per dish, respectively) and D20 medium. The dishes were pre-seeded the day before with mouse embryonic fibroblasts (MEFs) mitotically arrested by irradiation (methods for preparing MEFs plates are described in the section "3.2.7.b – Preparation of feeder plates"). In the next day, D20 medium was replaced with ESC medium. In the first seven days after the transference to feeder cells (MEFs), the transduced fibroblasts were cultured in ESC media supplemented with 0.5 mM valproic acid in order to induce cell reprogramming, since valproic acid promotes DNA demethylation. Dishes were kept in a cell incubator under normoxic condition. Medium was replaced everyday.

On day 13 post transduction, MEFs were added in the dishes. As MEFs do not

proliferate and a good number of these cells plated before has detached due to apoptosis or senescence, the addition of MEFs was needed in order to maintain sufficient amounts of feeder cells for the emerging iPSCs. For this purpose, one vial containing 2×10^6 MEFs was thawed as previously described (section "3.2.1. Derivation of skin fibroblasts"), centrifuged (300 × *g* for 5 min), the supernatant was removed, and cell pellet was resuspended in 30 mL of ESC medium, and homogenized by pipetting. The medium from each dish was replaced with 10 mL ESC medium plus MEFs (circa 6×10^5 MEFs per dish) and incubated. On day 24, ESC medium was replaced with "conditioned" ESC medium, replaced everyday (methods for preparing this medium are provided in the section "3.2.7.a – Preparation of conditioned ESC medium").

On day 29, individual colonies presenting ESC-like morphology were mechanically collected. To collect the colonies manually, the dish was placed in a stereomicroscope inside the cell culture hood. Each colony was scraped using sterile 50 μL tips, and fragmented in small clumps containing circa 100 cells. The fragments of each colony were collected and transferred to one well of a 12-well cell culture plate containing MEFs (prepared the day before collecting colonies) and ESC medium supplemented with 10 μM ROCK inhibitor (an inhibitor of apoptosis that increases survival of dissociated human pluripotent stem cells). Since each colony was reprogrammed from virtually one parental fibroblast, each colony was referred to as one clone. After 48 h, medium was replaced with ESC medium daily. Seven days after first passage, iPSCs colonies were enzymatically dissociated into small aggregates of cells using collagenase IV (methods for passaging iPSCs with collagenase are provided in the section "3.2.7.c – Passage of PSCs in feeder cultures"). The content of each well was transferred to one well of a 6-well cell culture plate containing MEFs. The iPSCs were maintained on MEFs and ESC medium, expanded and frozen. An overview of reprogramming experiment is provided on Figure 3.4.

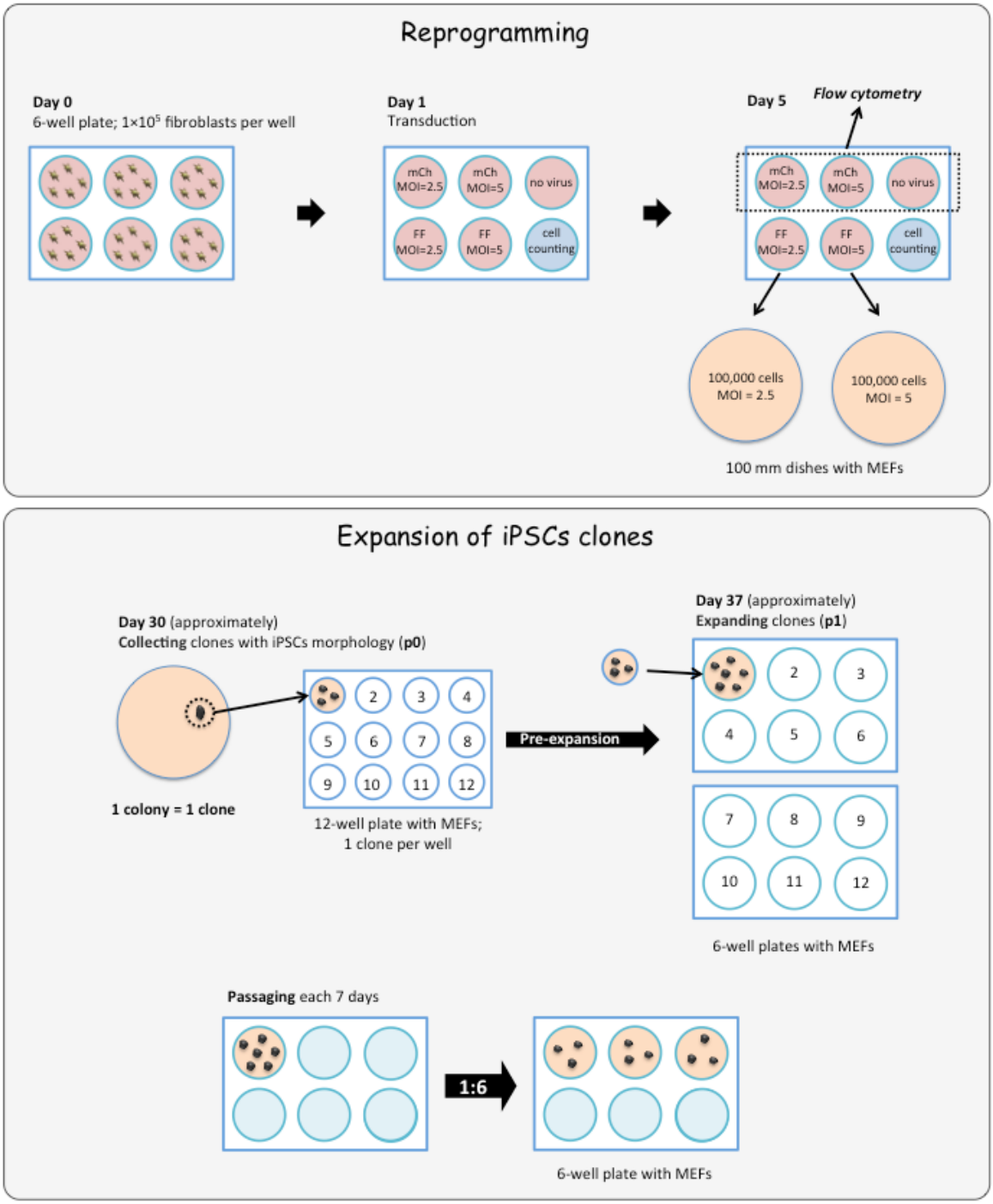

Figure 3.4 – Overview of reprogramming experiment and expansion of the first iPSCs. One day previous to transduction, fibroblasts are seeded in 6-well plates. Fibroblasts are transduced with STEMCCA "four factors" (FF), and "mCherry" (mCh) at different multiplicities of infection (MOI). Five days later, fibroblasts are harvested and either analyzed by flow cytometry (mCh) or seeded in 100 mm dishes pre-plated with MEFs (FF). Colonies resembling ESC-morphology are collected and expanded: first transferred to 12-well, then 6-well plates. The iPSCs are maintained in 6-well plates, and passaged each 7 days, approximately, at a 1 to 6 ratio (depending on confluence in the well).

The efficiency of derivation of iPSCs was calculated as follows:

$$\text{Efficiency (\%)} = \frac{\text{Number of iPSC clones}}{\text{Number of transduced cells}} \times 100$$

3.2.7. Culturing pluripotent stem cells (PSCs)

After the establishment of the patient iPSCs cultures, and in order to avoid MEFs interference in further experiments, iPSCs were transferred to a feeder-independent platform using Matrigel basement membrane matrix. The patient iPSCs were cultured for several passages with daily media change. Clones at different passages were frozen and kept in a liquid nitrogen storage system for long-term storage. Induced pluripotent stem cells derived from healthy subjects as well as H1, a human ESC (hESC) line, were used as controls for the experiments. Detailed information regarding these cells is provided in the "3.1.3.b – Human pluripotent stem cell lines" section. The pluripotent stem cells (PSCs), that include both iPSCs and ESCs, were maintained and manipulated under the same culture conditions and methods. Detailed methods for PSCs maintenance, passaging, freezing, and thawing (for both feeder and feeder-independent platforms) are provided below.

3.2.7.a – Preparation of conditioned ESC medium

To prepare conditioned ESC medium, 4×10^6 MEFs mitotically arrested by irradiation were thawed and seeded in one 165 cm^2 cell culture flask containing D-MEF medium. Cells were maintained in a cell incubator overnight. Next day, medium was removed; cells were rinsed once with 1×PBS and 40 mL ESC medium without bFGF was added. ESC medium without bFGF was replaced and collected for 10 days. Next, the conditioned medium was filtered using 0.22 μm pore filter systems, and supplemented with 10 ng/mL bFGF.

3.2.7.b – Preparation of feeder plates

First, 1 mL ultra-pure water with 0.1% gelatin was added to each well of 6-well plates. Plates were incubated for 1 h at 37°C. Meanwhile, 2×10^6 MEFs mitotically arrested by irradiation were thawed, centrifuged (300 × *g* for 5 min), supernatant was discarded, and pellet was resuspended in 37 mL D-MEF medium. The exceeding liquid was aspirated from

the wells, and immediately replaced with 2 mL D-MEF medium plus MEFs (circa 1×10^5 cells) per well. Plates were placed in a cell incubator overnight. Immediately before being used, wells were rinsed twice with 1×PBS, and then filled with ESC medium (2 mL per well of 6-well plates). When the use of different plates or flasks was necessary, volumes were adapted for the surface area and the same procedures were performed.

3.2.7.c – Passage of PSCs in feeder cultures

For a proper passage procedure of PSCs cultured in MEFs, colonies were enzymatically dissociated into small aggregates of cells using collagenase IV resuspended in Knock Out DMEM (about 3×10^5 units per mL). The medium from each well was removed, and replaced with collagenase (1 mL per well of 6-well plates). Plates were incubated for 3 min at 37°C and then, collagenase was removed from each well (Figure 3.5-B). Each well was rinsed with 3 mL ESC medium and scraped with glass pipettes until disrupting colonies into clumps of about 50 to 100 cells (Figure 3.5-C). The content of each well was transferred to a 10 mL tube and centrifuged (200 × *g* for 5 min); supernatant was removed and pellet was carefully resuspended in 6 mL ESC medium, in a way that prevented the disruption of cell clumps. Cells were seeded in a 6-well feeder plate (usually 1 mL per well) depending on the confluence before the passage, and then maintained in the cell culture incubator. ESC medium was replaced every day (2.5 mL per well of 6-well plates). Cells were passaged every seven days, at a confluence of 75% (approximately).

Figure 3.5 – Passaging PSC colonies maintained in feeder cultures. (**A**) Wells at confluence of 75% (approximately) were passaged every seven days. (**B**) Colony displaying detaching border after 3 min of collagenase treatment at 37°C. (**C**) Size of cell aggregates after plating; too small aggregates may not adhere in the plate; on the other hand, large aggregates may differentiate in a few days after seeding the cells. Scale bars = 500 μm.

Spontaneous differentiation is a common feature of PSCs. The correct maintenance of the cultures is indispensable in order to maintain the PSC lines in an undifferentiated state (Figure 3.6-A). The differentiated cells can be easily recognized and are usually darker than the pluripotent cells. These cells tend to be clustered in the colony (e.g. in the center), as a darker and flat region, or forming three-dimensional ball-shaped structures like embryoid bodies (Figure 3.6-B). In addition, cells exhibiting morphologies different from the classical PSC morphology (cells with large nuclei and scant cytoplasm, and tightly arranged into the colony), such as cells with fibroblastoid shape, are also differentiated (Figure 3.6-C). Colonies that displayed regions of differentiation were manually removed prior to collagenase treatment using 50 μL tips and a stereomicroscope inside the cell culture hood. This removal of differentiated cells was necessary since they trigger cell signaling for differentiation of the adjacent pluripotent cells.

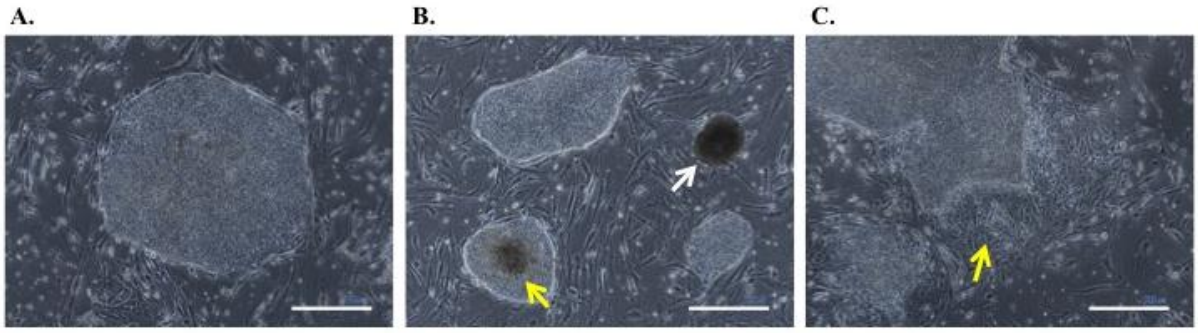

Figure 3.6 – PSC colonies maintained in feeder cultures and displaying regions of spontaneous differentiation. (**A**) An example of a colony without signs of differentiated cells. (**B**) Spontaneous differentiation recognized as darker cells clustered in the center of the colony, as shown by the yellow arrow; differentiated cells that formed a three-dimensional structure like a EB, as shown by the white arrow. (**C**) Region of spontaneous differentiation formed by cells exhibiting morphologies different than the morphology of pluripotent cells. Scale bars = 500 μm.

3.2.7.d – Preparation of feeder-independent plates

The PSCs maintained in feeder-independent cultures were plated in Matrigel basement membrane matrix and either Essential 8 (hereafter referred as E8) or mTeSR medium. To prepare Matrigel aliquots, Matrigel bottles were thawed overnight at 4°C. In the next day, the same volume of cold Knock Out DMEM was added to the bottle, which was quickly homogenized with pre-chilled pipettes, and immediately transferred to cold microcentrifuge

tubes placed on ice (1 mL per tube). Aliquots were maintained in the −80°C freezer and thawed overnight at 4°C prior to use. In order to prepare Matrigel plates, one aliquot of Matrigel (1 mL) was diluted in 27 mL of cold Knock Out DMEM, and then 1.5 mL of this dilution was plated in each well of 6-well plates. Plates were wrapped in parafilm (to avoid that the liquid dried out) and stored at 4°C for up to 10 days. Prior to use, plates were incubated at 37°C for 15 min or at room temperature for 30 min. Wells were rinsed once with 2 mL Knock Out DMEM, and then filled with either E8 or mTeSR medium (2 mL per well of 6-well plates). When the use of different plates or flasks was necessary, volumes were adapted for the surface area and the same procedures were performed.

3.2.7.e – Passage of PSCs in feeder-independent cultures

In feeder-independent platform, PSCs were passaged using an enzyme-free dissociation buffer containing 0.5 mM EDTA and 0.03 M NaCl in 1×PBS (hereafter referred as dissociation buffer). Firstly, PSCs were rinsed twice with 1×PBS, then covered with dissociation buffer (1 mL per well of 6-well plates), and incubated for 4 min at room temperature. Dissociation buffer was removed and the well was rinsed with 2 mL of either E8 or mTeSR medium (depending on the medium that cells had been cultured), without the need of scraping the colonies. Detached colonies were carefully pipetted and dissociated into clumps of about 50 to 100 cells (Figure 3.7-B). Medium containing cell clumps was transferred to Matrigel plates, usually in the ratio 1:5, depending on the confluence of the cells before the passage procedure, then maintained in the cell culture incubator. Medium was replaced every day (2.5 mL per well of 6-well plates). Cells were passaged every three or four days, at a confluence of 75% (approximately).

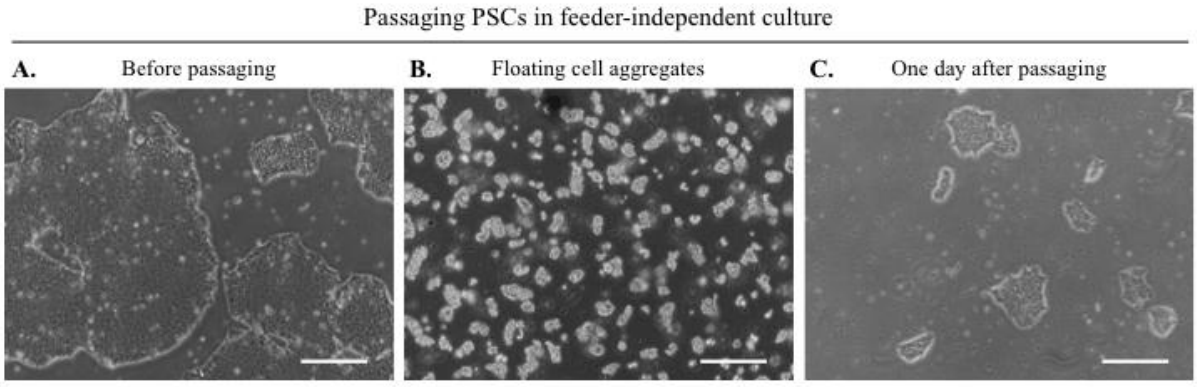

Figure 3.7 – Passaging PSC colonies maintained in feeder-independent cultures. (**A**) Wells at confluence about 75% were passaged every four days. (**B**) Size of cell aggregates after EDTA treatment and pipetting. (**C**) Size of the colonies one day after seeding the cells. Scale bars = 500 μm.

Although media for feeder-independent platform exert positive selection on undifferentiated cell, colonies may present regions of differentiation, usually visualized as lighter spots in the colony or regions of cells with fibroblastoid shape (Figures 3.8-B and C). However, spontaneous differentiation is feeder-independent platform is observed at a lower frequency than in feeder platform. Colonies with regions of differentiation were manually removed prior to passage procedure using 50 μL tips and a stereomicroscope inside the cell culture hood.

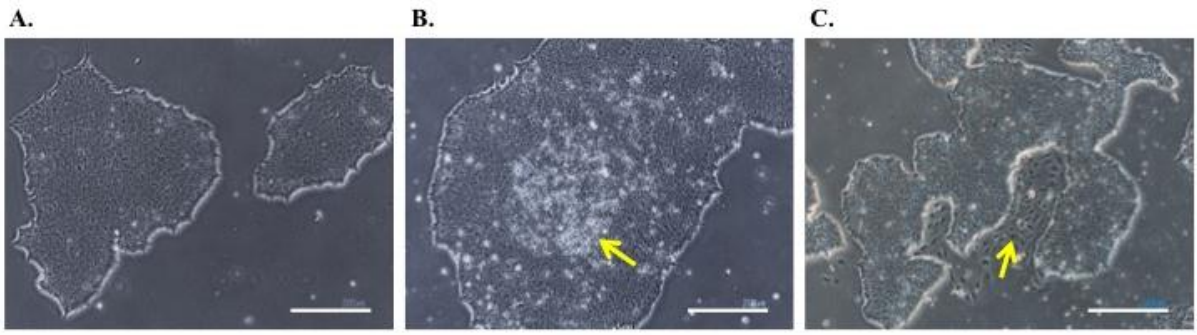

Figure 3.8 – PSC colonies maintained in feeder-independent cultures and displaying regions of spontaneous differentiation. (**A**) An example of two colonies without signs of differentiated cells. (**B**) Spontaneous differentiation recognized as lighter cells scattered in the colony, as indicated by the arrow. (**C**) Region of spontaneous differentiation formed by cells exhibiting morphologies different from the morphology of pluripotent cells. Scale bars = 500 μm.

3.2.7.f – Transition between feeder and feeder-independent cultures

The patient-derived iPSCs were first established and maintained in feeder cultures, and then transferred to a feeder-independent platform in order to avoid MEFs interference in further experiments. The iPSCs maintained in different platforms display peculiarities such as differences in the colony format: colonies maintained in feeder cultures tend to exhibit rounded formats (Figure 3.9-A), while colonies in feeder-independent culture may be rounded or did not exhibit defined formats, occasionally resembling geographical maps (Figure 3.9-B). In order to transfer iPSCs in feeders to a feeder-independent culture, cells were passaged following procedures of feeder passaging, but were seeded in Matrigel plates instead of feeder plates, in ESC medium at the ratio 1:1. The next day, medium was replaced with either E8 or mTeSR.

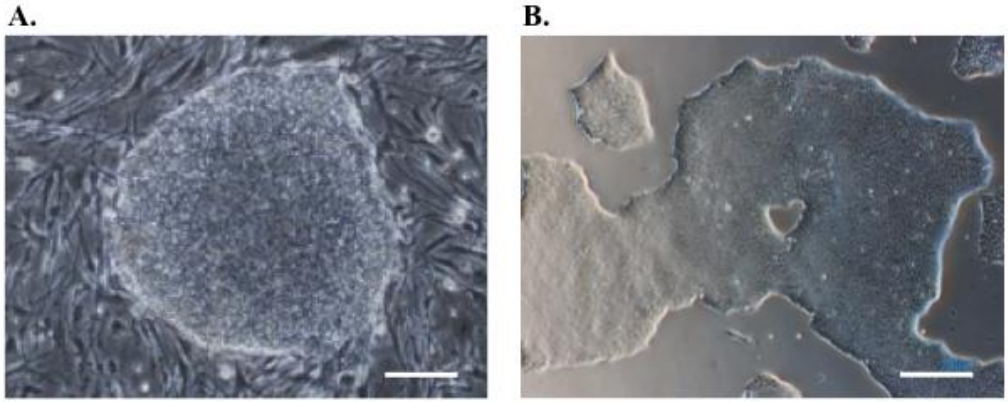

Figure 3.9 – iPSC clones maintained in feeder and feeder-independent cultures. (**A**) An example of a colony in feeder culture, displaying well-defined and rounded delimitation. (**B**) An example of colonies in feeder-independent culture, displaying different sizes, and varied formats, though also displaying well-defined borders. Scale bars = 500 μm.

3.2.7.g – Freezing PSCs

To freeze both feeder and feeder-independent PSCs, cells were collected as described above for regular passaging. In case of PSCs in feeders, after centrifugation and removal of supernatant, the remaining pellet was resuspended in ESC medium, 0.5 mL per well collected (e.g. if three wells were collected and centrifuged, pellet was resuspended in 1.5 mL ESC medium). In case of PSCs feeder-independent, after removing dissociation buffer, each well was rinsed with 0.6 mL E8 (or mTeSR). In both platforms, 0.5 mL aliquots (cell clumps in

medium) were transferred to cryogenic vials, following addition of 0.5 mL 2× freezing medium (20% DMSO in HyClone FBS). Vials were inverted to mix and immediately placed into a cell freezing container in the −80°C freezer. After 24 h, cryogenic vials were transferred to a liquid nitrogen storage system for long-term storage. For both culture platforms, the content of one confluent well (approximately 75%) of 6-well plates was frozen in one vial. In addition, the clumps collected to be frozen were bigger than the clumps at the moment of seeding, since these clumps would be pipetted several times before being seeded again.

3.2.7.h – Thawing PSCs

To thaw PSCs, each cryogenic vial was manipulated separately. Immediately after being removed from liquid nitrogen, the cryogenic vial was quickly thawed in water bath at 37°C for 2 min. The content was transferred dropwise to a 15 mL tube containing 9 mL of pre-warmed (37°C) medium (the same medium in which cells were cultured before being frozen). The tube was centrifuged (200 × *g* for 5 min), the supernatant was removed, and cell pellet was resuspended in 2 mL of medium supplemented with 10 μM ROCK inhibitor. Cell clumps were carefully pipetted, and transferred to one well of a 6-well plate (MEFs or Matrigel plate, depending on the platform that cells had been cultured before being frozen), then maintained in the cell culture incubator. Daily media change was started the following day. Usually, the content of one vial was thawed in one well of 6-well plates. PSCs frozen from feeder-independent culture recover faster (usually in five days), while PSCs frozen from feeders take about two weeks to recover after freezing process. However, the recovering depends on the confluence of the cells before freezing (high confluences recover fast), as well as size of clumps (small clumps of cells usually do not adhere, and large clumps start differentiating after a few days of thawing).

3.2.8. Nucleic acids isolation from iPSCs

Pellets from the iPSCs in feeder-independent culture were collected and stored for DNA and RNA isolation. iPSCs were harvested with dissociation buffer similarly to passage procedures. After dissociation, cells were rinsed from wells with medium, centrifuged (200 × *g* for 5 min), and the supernatant was removed. The pellet was washed once with 1×PBS,

centrifuged (200 × *g* for 5 min), and all PBS was carefully removed. Pellets were maintained in the −80°C freezer until proceeding to extraction.

3.2.8.a – DNA extraction

Total DNA was extracted from pellets containing around 1×10^6 cells using the DNeasy Blood & Tissue kit according to manufacturer's recommendations. First, each pellet was resuspended in 200 µL 1×PBS and 20 µL proteinase K; 200 µL buffer AL was added, sample was vortexed, and incubated at 56°C for 10 min; 200 µL ethanol 100% was added and sample was vortexed; the mixture was pipetted into the DNeasy Mini spin column (provided in the kit) placed in a collection tube and centrifuged (6,000 × *g* for 1 min). The flow-through was discarded; 500 µL buffer AW1 was added and centrifuged (6,000 × *g* for 1 min). The flow-through was discarded; 500 µL buffer AW2 was added and centrifuged (20,000 × *g* for 3 min) to dry the column membrane. Finally, the column was placed in a 1.5 mL microcentrifuge tube; 30 µL ultra-pure water was pipetted directly onto the column membrane and incubated at room temperature for 1 min, then centrifuged (6,000 × *g* for 1 min) to elute DNA from membrane. DNA samples were stored in the −20°C freezer.

3.2.8.b – RNA extraction

Total RNA was extracted from pellets containing around 1×10^6 cells using the RNeasy Mini Kit according to manufacturer's recommendations. First, cells were lysed by adding 350 µL buffer RLT plus 35 µL β-mercaptoethanol, and vigorously pipetted; 350 µL ethanol 70% was added to the lysate and sample was homogenized by pipetting; 700 µL of the sample was transferred to an RNeasy spin column (provided in the kit) placed in a collection tube and centrifuged (8,000 × *g* for 15 s). The flow-through was discarded; 700 µL buffer RW1 was added to wash the column membrane and centrifuged (8,000 × *g* for 15 s). The flow-through was discarded; 500 µL buffer RPE was added to wash the column membrane and centrifuged (8,000 × *g* for 15 s); the flow-through was discarded; 500 µL buffer RPE was added a second time to wash the column membrane and centrifuged (8,000 × *g* for 2 min); the flow-through was discarded. Finally, the column was placed in a 1.5 mL microcentrifuge tube; 30 µL RNase-free ultra-pure water was pipetted directly onto the column membrane and centrifuged (8,000 × *g* for 1 min) to elute the RNA from membrane. RNA samples were stored in the −80°C freezer.

3.2.8.c – Quantification and purity of DNA and RNA samples

DNA and RNA samples were quantified using the NanoDrop spectrophotometer. Quantification was based on absorbance values at 260 nm (A_{260}). Absorbance values at 230 nm (A_{230}) and 280 nm (A_{280}) were also acquired in order to estimate the DNA and RNA purity. The ratio A_{260}/A_{280} provides an estimate of purity concerning contaminants that absorb in the UV spectrum, such as proteins, while the ratio A_{260}/A_{230} provides an estimate of purity concerning organic compounds contaminants, such as phenol. Ideal values for both ratios should be close to 2. Ratios ranging from 1.8 to 2.1 were considered acceptable for either DNA or RNA samples.

3.2.9. Excision of exogenous reprogramming transgenes in the iPSCs

The lentiviral vector used for derivation of patient iPSCs (the STEMCCA "four factors") is flanked by loxP sites that allow the excision of integrated reprogramming genes by Cre-LoxP mediated recombination (Somers *et al*., 2010). In order to produce transgene-free clones, the patient iPSCs were transfected with the non-integrating plasmid pCL20i4rEF1-Puro-T2A-cre-GFP, which promotes transient cre-recombinase expression. First, iPSCs cultured in feeder platform were passaged and directly seeded in Matrigel-coated 12-well plates in conditioned ESC medium containing 10 μM ROCK inhibitor. When cells achieved confluence of 75% (three days after passaging), medium was replaced with 1 mL transfection medium (DMEM/F12 supplemented with 1% L-glutamine and 1% NEAA) per well. Next, 1 μg of plasmid was added to 100 μL DMEM/F12, and 1 μL PLUS Reagent to dilute the DNA. The mixture was incubated for 5 min at room temperature. Then, 6 μL Lipofectamine LTX was added to the diluted DNA mixture, vortexed and incubated for 30 min at room temperature. Finally, 100 μL of the DNA mixture was dropwise added to each well containing iPSCs, and the plate was incubated for 6 h at 37°C. Cells that were effectively transfected with the plasmid started expressing cre-recombinase and were positively selected by puromycin treatment for three days. To select these cells, the day following transfection, medium was replaced with conditioned ESC medium containing 3 μg/mL puromycin. The next two days, medium was replaced with conditioned ESC medium containing 2 μg/mL

puromycin. After selection, MEFs were added in the wells and ESC medium was changed daily until individual cells form colonies. Assuming that one colony was formed by the expansion of one single iPSC that was transfected, cre-excised, and selected, each colony was referred to as one subclone that has arisen from the iPSC clone. The colonies with ESC-like morphology were mechanically collected and expanded on MEFs and ESC medium for several passages and then transferred to feeder-independent culture.

A multiplex polymerase chain reaction (multiplex PCR) was performed in DNA samples from three iPSC clones before excision in order to assess copy numbers of STEMCCA vectors integrated into the genome of reprogrammed cells. Multiplex PCR was also performed after cre-excision in the subclones in order to verify whether the removal of transgenes was successfully performed. PCR reactions were prepared using the TaqMan Universal Master Mix according to the manufacturer's recommendations. Reactions were done in duplicates; each one consisted of the kit-supplied master mix, 160 ng DNA, primer-probe mixes for *HIV* (FAM) and housekeeping gene *STP* (VIC/TAMRA), 0.8 μM each primer and 0.08 μM each probe. Conditions for reaction were: 50°C for 2 min, 95°C for 10 min, followed by 40 cycles of 95°C for 15 s and 60°C for 1 min, concluding with a 4°C incubation. Number of copies was calculated as $2^{-\Delta\Delta C_T}$, normalized by an iPSC control known as carrying one copy of the transgenes, as follows:

$$\Delta C_{T\ sample} = C_{T(\textbf{\textit{HIV RRE}})\ sample} - C_{T(\textbf{\textit{STP}})\ sample}$$

$$\Delta\Delta C_{T\ sample} = \Delta C_{T\ sample} - \Delta C_{T\ \textbf{iPSC one copy}}$$

$$2^{-\Delta\Delta C_{T\ sample}} = \text{number of transgene copies}$$

3.2.10. iPSCs characterization

In order to demonstrate that the iPSCs derived from the patient fibroblasts resembled hESCs and genotypic characteristics from patient, three excised iPSCs subclones were selected for further characterization, which encompassed karyotyping, immunocytochemistry, gene sequencing, embryoid bodies (EBs) formation assay, and quantitative PCR for checking the expression of endogenous markers.

3.2.10.a – Immunocytochemistry

Immunocytochemistry for endogenous markers of pluripotency was performed in iPSC clones as well as H1 hESC line (positive control). Cells were cultured in 96-well plate for 2 days in MEFs (negative control) and ESC medium. Cells were washed once with 1×PBS and fixed with 4% paraformaldehyde for 30 min at room temperature, and washed three times with 1×PBS. Cells were permeabilized with 0.2% Triton X-100 for 30 min at room temperature followed by another step of washing three times with 1×PBS. Cells were blocked in blocking buffer (1×PBS containing 3% BSA and 5% donkey serum) for 2 h at room temperature. Blocking buffer was removed. Primary antibodies against human OCT4, NANOG, SSEA4, TRA-1-81, and TRA-1-60 were diluted in blocking buffer (1:100) and added, then incubated at 4°C overnight. The next day, primary antibodies were removed and cells were washed three times with 1×PBS. Secondary antibodies diluted in blocking buffer (1:500) were added and cells were incubated at 4°C for 3 h in the dark. Secondary antibodies were removed and cells were washed three times with 1×PBS. Nuclei were stained using Vectashield with DAPI, one drop per well, incubated for 10 min. Finally, 1×PBS was added in the wells. Cell images were acquired in a fluorescence microscope.

3.2.10.b – Embryoid bodies (EBs) formation assay

In vitro differentiation assay (embryoid body formation) was performed in iPSCs and H1 hESC line. Cells cultured in feeder-independent platform and mTeSR medium were passaged at confluence of 75% (approximately) using dissociation buffer as previously described (section "3.2.7.e – Passage of PSCs in feeder-independent cultures"). The content of one well was split into three wells in a Matrigel plate (6-well plates). Cells were grown for two days with daily medium change. Next, PSCs were incubated in mTeSR medium supplemented with 10 μM ROCK inhibitor for 1 h at 37°C. Medium was removed and cells were rinsed twice with 1×PBS, and incubated with dissociation buffer for 5 min at room temperature. The dissociation buffer was removed and PSCs aggregates were rinsed with mTeSR medium containing 30 μM polyvinyl alcohol, carefully pipetted to avoid dissociation of aggregates, which should be bigger in size than aggregates seeded in passage procedure (about 500 cells per clump). The content of two wells of cells was transferred to one well of ultra-low attachment 6-well plates and placed into the cell culture incubator. In the following day, plates were checked for embryoid bodies (EBs) formation. Two days later, medium was

changed for Essential 6, in which EBs were cultured for 15 days, with medium change in each 3 days. Then, EBs were collected and washed once with 1×PBS, followed by RNA extraction as previously described (section "3.2.8.b – RNA extraction").

3.2.10.c – Quantitative PCR of pluripotency and differentiation markers

The expression of endogenous pluripotency markers (*OCT4*, *SOX2*, *KLF4*, *MYC*, and *NANOG*), as well as differentiation markers for endoderm (*AFP* and *GATA4*), mesoderm (*RUNX1* and *CD34*), and ectoderm (*NCAM* and *NES*) was assessed in RNA samples from EBs. In order to compare gene expression in EBs with the cells in the pluripotent state, RNA samples of the PSCs prior to EBs formation were also analyzed. First, reverse transcription polymerase chain reactions (RT-PCR) were performed. For each reaction, 500 ng RNA, 100 ng random primer, 2 µL dNTP, and ultra-pure water (enough for final volume of 20 µL) were mixed and incubated at 65°C for 5 min. After, 4 µL 10× buffer, 5 mM $MgCl_2$, 10 mM DTT, and 2 µL RNaseOUT were added and incubated at 25°C for 2 min. Then, 2 µL SuperScript II Reverse Transcriptase was added. Samples were incubated in the thermal cycler at 25°C for 10 min, 42°C for 50 min, and 70°C for 15 min. Finally, 2 µL RNase H was added and incubated 37°C for 20 min.

The cDNA obtained in RT-PCR was used for quantitative PCR (qPCR). Reactions were prepared in duplicate in 96-well plates, each one containing 2 µL cDNA (diluted 6 times in ultra-pure water), 7.5 µL SYBR Green PCR Master Mix, 0.14 µM primer forward, 0.14 µM primer reverse, and 5 µL ultra-pure water. The ABI Prism 7000 equipment was used for amplification and detection. The reaction conditions were: 95°C for 10 min followed by 40 cycles of 95°C for 15 s and 60°C for 1 min, concluding with a 4°C incubation. The expression levels of each gene were calculated as $2^{\Delta C_T}$, normalized by *ACTB* expression, in which ΔC_T was calculated as follows:

$$\Delta C_{T\ sample} = C_{T(\boldsymbol{GENE})\ sample} - C_{T(\boldsymbol{ACTB})\ sample}$$

3.2.10.d – Karyotyping

The reprogramming process is a putative source of acquisition of cytogenetics abnormalities, and karyotyping is a regular procedure to test the cytogenetics integrity in iPSCs. Karyotyping was performed by WiCell Research Institute (Madison, WI, USA). For

each iPSC subclone, a total of 20 metaphases were counted and 8 analyzed; 4 metaphases were karyotyped in a band resolution of either 425-450 or 450-475.

3.2.10.e – Gene sequencing

In order to confirm the *DKC1* mutation previously detected in the patient at the diagnosis, the exon 11 of this gene was sequenced in the iPSCs subclones. For this purpose, total genomic DNA was extracted from cell pellets as described in the section "3.2.8.a – DNA extraction". Exon 11 was amplified by PCR using Platinum PCR SuperMix High Fidelity kit. For each PCR reaction, 200 ng DNA was added to 45 µL Platinum PCR Mix, 0.2 µM *DKC1* primer forward, 0.2 µM *DKC1* primer reverse, and ultra-pure water to complete a final volume of 50 µL. Samples were incubated in the thermal cycler at 94°C for 2 min, followed by 35 cycles of 94°C for 30 s, 55°C for 30 s, and 68°C for 1 min, concluding with a 4°C incubation.

Next, PCR products were purified using the QIAquick PCR purification kit according to manufacture's recommendations. First, one volume of PCR reaction was added to five volumes of buffer PB. The mixture was added to a QIAquick column (provided in the kit) placed into a collection tube. The DNA was bound to the column by centrifuging sample (17,900 × *g* for 1 min); the flow-through was discarded. To wash, 750 µL buffer PE was added to the column and centrifuged (17,900 × *g* for 1 min). The flow-through was discarded. The column was dried by centrifugation (17,900 × *g* for 1 min). To elute DNA from membrane, 30 µL ultra-pure water was pipetted directly onto the column membrane and incubated at room temperature for 1 min, then centrifuged (17,900 × *g* for 1 min). Purified DNA was quantified using the NanoDrop spectrophotometer.

In order to check the integrity and the size of the purified PCR products, 5 µL PCR products were added to 1 µL 5× Loading Dye (from the kit). Samples along with a molecular weight ladder (GeneRuler DNA Ladder Mix) were loaded in a 1% agarose gel containing 0.5 µg/mL EtBr, and run in an electrophoresis unit filled with 1× TAE buffer (80 V for 30 min). The DNA fragments (bands) in the gel were visualized through a device that emits UV light (ImageQuant imaging system and software).

Next, the sequencing reactions were prepared with 20 ng DNA, 0.5 µM *DKC1* primer forward, 3 µL BigDye Terminator, and ultra-pure water to complete a final volume of 10 µL. Samples were incubated in the thermal cycler at 94°C for 2 min, followed by 35 cycles of

94°C for 10 s, 50°C for 5 s, and 60°C for 4 min. The sequencing reactions were purified using the DyeEx 2.0 spin kit. For this purpose, the spin column provided in the kit was first gently vortexed to resuspend the resin, then placed into a collection tube and centrifuged (1,000 × *g* for 3 min). The column was transferred to a 1.5 mL microcentrifuge tube. The sequencing reactions (10 µL) were slowly applied into the gel bed in the column and centrifuged (1,000 × *g* for 3 min). The purified DNA was dried in a vacuum concentrator for 30 min at high speed. The dried products were resuspended in 15 µL Hi-Di formamide. Finally, products were loaded in the sequence analyzer ABI Prism 3100. The chromatograms were analyzed with CLC Main Workbench software.

3.2.11. Quantitative PCR for telomere length

Three patient iPSC clones were cultured in feeder-independent platform for 42 passages (represented as p*x*, for cells passaged in a number *x* of times). Cell pellets were collected in intervals of approximately six passages and total genomic DNA was extracted and quantified as previously described (section "3.2.8.a – DNA extraction"). Genomic DNA from parental fibroblasts (fibroblasts at p7 collected immediately before reprogramming experiment) was also extracted. The integrity of DNA samples was tested through agarose gel electrophoresis: 50 ng of each DNA sample, along with a molecular weight ladder (1 kb), was loaded in a 1.5% agarose gel containing 0.5 µg/mL EtBr, and run in an electrophoresis unit filled with 1× TAE buffer (80 V for 30 min). The DNA fragments (bands) in the gel were visualized through a device emitting UV light (ImageQuant imaging system and software).

The qPCR for telomere length was adapted from methods described by Cawthon (2002) and Callicott and Womack (2006). Each experiment of qPCR for telomere length consisted of two qPCR assays: one using primers for annealing and amplifying the telomere (referred as T), and the other assay using primers for a gene known to have a single copy in the genome, the *36B4* gene (referred as S). The qPCR reaction for T consisted of 8 µL DNA at 0.2 ng/µL (a total of 1.6 ng DNA per reaction), 10 µL 2× Rotor-Gene SYBR Green PCR Master Mix, 900 nM primer $T_{forward}$, and 900 nM primer $T_{reverse}$ (final volume = 20 µL). Conditions for reactions were: 95°C for 5 min followed by 25 cycles of 98°C for 7 s and 60°C for 10 s, concluding with a 4°C incubation. The qPCR reaction for S consisted of 8 µL DNA at 0.2 ng/µL (a total of 1.6 ng DNA per reaction), 10 µL 2× Rotor-Gene SYBR Green PCR Master Mix, 900 nM primer $S_{forward}$, and 1.5 µM primer $S_{reverse}$ (final volume = 20 µL). Conditions

for reactions were: 95°C for 5 min followed by 35 cycles of 98°C for 7 s and 58°C for 10 s, concluding with a 4°C incubation. A standard curve was run in each assay using a control DNA at serial concentrations (10, 5, 2.5, 1.25, and 0.625 ng per reaction). An experiment was only accepted if standard curve had a correlation coefficient (r^2 value) ≥ 0.9 for both T and S assays. As validation samples, the control DNA as well as DNA from an umbilical cord blood were run along with samples. PCR reactions were pipetted using the QIAgility robotic workstation. The amplification and quantification was performed in the Rotor-Gene Q real-time PCR cycler. The threshold was set during the exponential phase of amplification, and the number of amplification cycles needed to reach the threshold fluorescence was denoted as cycle threshold (C_T). C_T values for both T and S assays were acquired for each sample. Samples were pipetted in triplicate, and the C_T value for a given sample was represented as the average of C_T values of triplicates. The telomere length was represented as a relative T/S ratio, which was inferred based on the relative quantification calculated using the $2^{-\Delta\Delta C_T}$ method (Livak and Schmittgen, 2001), as follows:

$$\Delta C_{T\ sample} = C_{T(\mathbf{T})\ sample} - C_{T(\mathbf{S})\ sample}$$
$$\Delta\Delta C_{T\ sample} = \Delta C_{T\ sample} - \Delta C_{T\ curve}$$
$$2^{-\Delta\Delta C_{T\ sample}} = \mathbf{T/S\ ratio}\ \text{for}\ \textit{sample}$$

The $\Delta C_{T\ curve}$ represents the average of the ΔC_T values obtained for each one of the five points in the standard curve. Three independent qPCR experiments were performed for each sample. The final T/S ratio for a given sample represents the mean and the standard deviation (SD) of the three experiments.

3.2.12. Southern hybridization for telomere length

In order to validate qPCR results, the mean terminal restriction fragment (TRF) length was assessed by Southern blot analysis. TRF length was measured in six iPSCs samples as well as parental fibroblasts. The TeloTAGGG Telomere Length Assay kit was used according to the manufacturer's protocols. The solutions used in this technique (and that were not provided in the TeloTAGGG kit) were detailed in the section "3.1.13. Solutions and buffers". First, a total amount of 800 ng of genomic DNA per sample (from the same DNA aliquots used for qPCR) was digested with restriction enzymes: 2 µL *Hinf*I, 2 µL *Rsa*I, and

2.5 µL 10× digestion buffer (final volume of 25 µL in ultra-pure water). The samples were incubated in the thermal cycler at 37°C for 90 min. Next, fragments of digested DNA were separated by gel electrophoresis. For this purpose, the samples were loaded in a 0.8% agarose gel. A molecular weight ladder (2 µL DIG molecular weight, 6 µL ultra-pure water, and 2 µL 5x loading buffer) was loaded in both extremities of the gel (5 µL molecular weight ladder per lane). Samples and ladder were run in an electrophoresis unit filled with 1× TAE buffer at 80 V for 4 h. The gel was carefully transferred to a recipient and washed with solutions and gentle agitation. First, gel was submerged in HCl solution for 15 min, and then rinsed twice with water. Second, gel was submerged two times in denaturation solution for 15 min (each), and then rinsed twice with water. Third, gel was submerged two times in neutralization solution for 15 min (each). The blotting was prepared: the DNA fragments were transferred from the gel to a positively charged nylon membrane by capillary action in 20× SSC buffer overnight. For this procedure, a tray was placed upside down inside a reservoir filled with 20× SSC buffer. Sheets of filter paper soaked in buffer were mounted on the tray's surface, and in contact with the buffer. The gel was placed on the filter paper (the DNA side facing up), and the nylon membrane was placed on the gel, in contact with the DNA side. Sheets of filter paper and paper towels were pilled on the membrane, and a glass bottle filled with water was placed on the top such as a weight. The buffer carried the DNA from the gel to the membrane by capillarity, as the dry filter papers and paper towels absorbed the buffer from the reservoir, passing through the gel and the membrane. As membrane was positively charged, the DNA was bound to it on contact.

The following day, the membrane was washed with 2× SSC buffer (always, DNA side up). The transferred DNA was permanently attached to the membrane by UV-crosslinking (1200J). Next, the membrane was washed one more time with 2× SSC buffer. The telomere sequences were hybridized with a telomere-specific probe. For this step, the membrane was submerged in pre-warmed DIG Easy Hyb solution (from kit) and incubated at 42°C for 1 h with gentle agitation. The solution was removed and replaced by hybridization solution composed of 1.8 µL digoxigenin (DIG)-labeled hybridization probe in 15 mL pre-warmed DIG Easy Hyb solution. The membrane was incubated in the hybridization solution at 42°C for 3 h with gentle agitation. Next, the hybridization solution was removed and the membrane was washed twice with stringent wash buffer I (5 min each) with gentle agitation. The membrane was washed twice with stringent wash buffer II (20 min each) at 50°C with gentle agitation. Membrane was washed once with washing buffer for 5 min. The membrane was submerged in blocking solution (containing maleic acid, from kit) and incubated for 1 h, and

then incubated for 30 min in Anti-DIG-Alkaline Phosphatase solution (from kit). The membrane was washed twice with washing buffer (15 min each), and equilibrated with detection buffer (from kit) by incubation for 5 min. The buffer was removed and 4 mL substrate solution (from kit) was dropwise applied to the membrane, with the DNA side facing up. The excess of substrate solution was removed, and the membrane was wrapped in plastic film, spreading the remaining substrate solution homogeneously over the membrane, and avoiding the formation of air bubbles. Finally, the chemiluminescence detection was performed in the ImageQuant imaging system and software with exposure time of 30 min. The mean TRF length was calculated as:

$$\overline{TRF} = \frac{\Sigma (OD_i)}{\Sigma (OD_i / L_i)}$$

OD_i represents the chemiluminescent signal and L_i is the length of the TRF at position *i*.

3.2.13. Telomeric repeat amplification protocol (TRAP) for telomerase activity

In vitro telomerase activity was assessed by TRAP assay using the TRAPeze XL Telomerase Detection kit according to manufacturer's instructions. First, pellets containing around 1×10^6 cells were collected from iPSC clones maintained in feeder-independent culture at different passages (p). Pellets from parental fibroblasts (p6) and fully undifferentiated hESC line H1 (p35) were also collected and used as negative and positive controls, respectively, for the telomerase activity of iPSCs. HeLa cells were used as normalizers. Proteins from cell pellets were extracted adding 200 µL of CHAPS lysis buffer (from kit) per sample; samples were incubated on ice for 30 min, and then centrifuged (12,000 × *g* for 20 min at 4°C); 160 µL of the supernatant was transferred to microcentrifuge tubes placed on ice.

One aliquot of each sample was used to determine the protein concentration, which was performed using the Pierce BCA Protein Assay kit according to the manufacturer's instructions. First, 50 parts of BCA Reagent A was mixed to 1 part of BCA Reagent B; 25 µL of each protein sample was added to 200 µL of this mixture. BSA protein standards of known concentration were prepared in serial dilutions of 2, 1, 0.5, 0.25, and 0.125 µg/µL such as the samples: 25 µL of standard was added to 200 µL mixture. A blank standard was prepared adding 25 µL CHAPS buffer to 200 µL mixture. Samples and standards were pipetted in

duplicate in a 96-well plate. The plate was incubated at 37°C for 30 min. The absorbance was measure at 562 nm on the SpectraMax fluorometer and analyzed on the SoftMax software. For calculating protein concentrations, the average of 562 nm absorbance measurement of the blank standard duplicates from the 562 nm absorbance measurement of all other individual standard and unknown samples duplicates. A standard curve was potted with the absorbance measurements of standards. An assay was only accepted if standard curve had a correlation coefficient (r^2 value) $\geq$ 0.9. The protein concentration of each unknown sample was determined using the standard curve. The final concentration of a given sample was calculated as the average of the duplicates. The protein samples were diluted in CHAPS buffer to a final concentration of 150 ng/μL, and stored in the −80°C freezer.

The activity of telomerase was detected by fluorometry. First, the telomerase enzymes present in each protein extract sample were allowed to add telomeric repeats in a given substrate oligonucleotide. Then, Taq polymerase was provided to synthesize the complimentary strands of the extended products using fluorescein-labeled primers, in which the fluorescence emitted was directly proportional to the amount of telomeric repeats products generated, corresponding to an estimative of telomerase activity. For performing this assay, qPCR reactions were prepared with 2 μL proteins (300 ng), 10 μL 5× TRAPeze XL Reaction Mix, 2 units of Taq polymerase (Platinum Taq DNA Polymerase), and ultra-pure water to a final volume of 50 μL per reaction. Dilutions of a control template (TSR8) instead of sample extracts were prepared to generate a standard curve (0.4, 0.08, 0.016, and 0.0032 amoles per reaction). The TSR8 is an oligonucleotide sequence composed of eight telomeric repeats. Telomerase positive control (HeLa cells protein extract), minus telomerase control (CHAPS instead of protein samples), minus Taq polymerase control (ultra-pure water instead of Taq polymerase), and no template control (ultra-pure water instead of protein samples) were also prepared. Reactions were pipetted in duplicate, and thermal cycled as follows: 30°C for 30 min (for telomerase extension), and a 4-step PCR of 36 cycles at 94°C for 30 s, 59°C for 30 s, and 72°C for 1 min, then a extension step at 72°C for 3 min, and 55°C for 25 min, concluding with a 4°C incubation.

For fluorescence measurements, 50 μL PCR products were added to 150 μL buffer solution (10 mM TrisHCl pH 7.4, 0.15 M NaCl, 2 mM $MgCl_2$) and acquired in the SpectraMax fluorometer and SoftMax software, using the excitation/emission parameters for fluorescein (495 nm/516 nm) and sulforhodamine (600 nm/620 nm). To calculate the increase of fluorescence emission, the “minus telomerase control” was subtracted from the fluorescein emission (ΔFL), and the “minus Taq polymerase” was subtracted from the

sulforhodamine emission (ΔR) in each reaction. The $\log_{10}$ of the relative ratio of fluorescence increase was calculated for each reaction: $\log_{10}$ (ΔFL/ΔR). In order to generate a standard curve, the $\log_{10}$ (ΔFL/ΔR) calculated for each TSR8 dilution was plotted on the Y-axis against the $\log_{10}$ value of the corresponding concentration of TSR8 (0.4, 0.08, 0.016, or 0.0032 amoles) on the X-axis. Since 1 amole of TSR8 corresponds to 1,000 TPG units (which are the units for measurement of telomerase activity), the linear equation generated from standard curve was applied for the calculation of the number of TPG units for each sample. One TPG (total product generated) unit corresponds to the number of primers (in 10^{-3} amole) extended with at least 3 telomeric repeats. An experiment was only accepted if standard curve had a correlation coefficient (r^2 value) ≥ 0.9. Relative telomerase activity was determined by setting the HeLa activity as 100%. The telomerase activity value of a given sample represents the mean and SD of two independent experiments.

3.2.14. Expression of *TERT*, *TERC*, and *DKC1*

Cell pellets were collected from patient iPSC clones and subclones maintained in feeder-independent culture at early and late passages (p), as well as parental fibroblasts (p5), the negative control; hESC line H1 (p61) was used for calculating relative gene expression. First, total RNA was extracted and quantified as described in the section "3.2.8. Nucleic acids isolation from iPSCs". The RNA integrity was checked by loading 1.2 µL RNA into microfluidic chips of the RNA 6000 Nano kit, and then analyzed on a 2100 Bioanalyzer instrument according to the manufacturer's recommendations. RNA samples with Integrity Number (RIN) ≥ 7.0 were used for RT-PCR. The reactions were performed using 500 ng RNA and the High-capacity cDNA Reverse Transcription kit according to the manufacturer's recommendations. Each RNA sample was mixed with 2 µL 10× RT buffer, 4 mM dNTP mix, 2 µL 10× RT random primers, 1 µL MultiScribe Reverse Transcriptase, and ultra-pure water (to complete a final volume of 20 µL). Reactions were incubated in the thermal cycler at 25°C for 10 min, 37°C for 120 min, and 85°C for 5 min, concluding with a 4°C incubation. The cDNA obtained in RT-PCR was diluted in ultra-pure water (20 µL cDNA and 80 µL water). The expression levels of the *TERT*, *TERC*, and *DKC1* genes were assessed by qPCR, using the expression levels of the *GAPDH* housekeeping gene as normalizer.

The qPCR reactions were prepared in duplicate, each one containing 2.5 µL cDNA, 5 µL 2× TaqMan Gene Expression Master Mix, 1 µL 10× TaqMan probe, and 1.5 µL ultra-pure

water. Conditions for qPCR reactions were: 50°C for 2 min, and 95°C for 10 min, followed by 40 cycles of 95°C for 15 s and 60°C for 1 min, concluding with a 4°C incubation. Data were acquired on a 7500 Real-Time PCR System. The threshold was set during the exponential phase of amplification, and the number of amplification cycles needed to reach the threshold fluorescence was denoted as cycle threshold (C_T). The quantification of gene expression in the iPSCs (relative to H1) was calculated using the $2^{-\Delta\Delta C_T}$ method (Livak and Schmittgen, 2001), as follows:

$$\Delta C_{T\ sample} = C_{T(\boldsymbol{GENE})\ sample} - C_{T(\boldsymbol{GAPDH})\ sample}$$

$$\Delta\Delta C_{T\ sample} = \Delta C_{T\ sample} - \Delta C_{T\ \mathbf{H1}}$$

$$2^{-\Delta\Delta C_{T\ sample}} = \text{expression of } \textit{sample} \text{ (relative to H1)}$$

3.2.15. SNP arrays for high-resolution genome-wide DNA copy number analysis

A next-generation cytogenetics study was carried out through SNP arrays using the Genome-Wide Human SNP CytoScan HD Arrays according to the manufacturer's recommendations. First, total genomic DNA was extracted from three iPSC clones maintained in long-term culture in feeder-independent platform, according to methods described in the section "3.2.8. Nucleic acids isolation from iPSCs". The integrity of DNA samples was tested through agarose gel electrophoresis: 50 ng of each DNA sample, along with a molecular weight ladder (1 kb), was loaded in a 1.5% agarose gel containing 0.5 µg/mL EtBr, and run in an electrophoresis unit filled with 1× TAE buffer (80 V for 30 min). The DNA fragments (bands) in the gel were visualized through a device emitting UV light (ImageQuant imaging system and software).

Then, 250 ng DNA was digested with the *Nsp*I restriction enzyme (as part of the Digestion Master Mix) at 37ºC for 2 h, and 65ºC for 20 min. The samples were ligated to Nsp I adaptors in a reaction containing T4 DNA ligase, incubated in the thermal cycler at 16ºC for 3 h, and 70ºC for 20 min. The ligated DNA was amplified in a PCR reaction containing 2.5 mM of each dNTP, PCR primer, GC-melt reagent, buffer, and Titanium Taq DNA Polymerase. The reactions were incubated in the thermal cycler at 94ºC for 3 min, followed by 30 cycles of 94ºC for 30 s, 60ºC for 45 s, and 68ºC for 15 s, and one cycle at 68ºC for 7 min. The samples amplification was confirmed by running 3 µL of each PCR product on a

2% agarose gel. The PCR products were purified using magnetic beads. The purified samples (45 µL) were fragmented with 10 µL fragmentation buffer and reagent (containing DNase I) at 37ºC for 35 min, and 95ºC for 15 min. Again, fragmentation reactions were loaded in a 4% agarose gel. After, terminal regions of the fragments were labeled with biotin, and hybridized to the SNP CytoScan HD chips. The chips were automated washed, scanned, read, and analyzed in "The Chromosome Analysis Suite (ChAS)" software (Affymetrix). First, non-cloning uniparental disomy (UPD) areas as well as chromosomal deletions and insertions previously identified in SNP arrays in the population as genomic variants were excluded using the Database of Genomic Variants (Center for Applied Genomics – http://projects.tcag.ca/variation/). For detection of copy number variants in the samples, filter was set at >300 kbp for lesions and number of probes >50.

3.2.16. C-circles assay

The assessment of DNA C-circles in the patient iPSCs was carried out according to methods described by Henson *et al*. (2009). The patient parental fibroblasts and the iPSC control were also evaluated. The human osteosarcoma cell lines U2-OS and Saos-2 were used as positive controls. The lysis buffer and solutions used in this technique were detailed in the section "3.1.13. Solutions and buffers". First, pellets containing 1×10^5 cells were collected from fibroblasts and iPSC clones maintained in feeder-independent culture at different passages (p). The DNA was extracted from cells by lysing them with addition of 47.5 µL lysis buffer and 2.5 µL of proteinase K per sample. Samples were incubated in a shaker at 56°C and 1,400 rpm for 1 h. Then, proteinase was inactivated at 70°C and 1,400 rpm for 20 min. Genomic DNA was digested using 2 µL of each restriction enzyme, *Hinf*I and *Rsa*I, and 25 ng of RNase, incubated at 37°C for 90 min. The reaction for amplification of the DNA C-circles (when present) was performed. For each reaction, 10 µL of digested DNA was combined with 10 µL BSA (0.2 mg/mL), 0.1% Tween 20, 1 mM each dATP, dGTP, and dTTP, 1× phi29 buffer and 7 U phi29 DNA polymerase. Reaction were incubated in the thermal cycler at 30°C for 8 h then 65°C for 20 min. The final product was diluted in 60 µL of 2× SSC and blotted to a positively charged nylon membrane using a 96-well holder attached to vacuum. After applying the samples, the membrane was air-dried.

The membrane was washed with 2× SSC buffer (always, DNA side up). The transferred DNA was permanently attached to the membrane by UV-crosslinking (1200J). Next, the

membrane was washed one more time with 2× SSC buffer. The telomere sequences were hybridized with a telomere-specific probe. For this step, the membrane was submerged in pre-warmed DIG Easy Hyb solution (from TeloTAGGG Telomere Length Assay kit) and incubated at 42°C for 1 h with gentle agitation. The solution was removed and replaced by hybridization solution composed of 1.8 μL digoxigenin (DIG)-labeled hybridization probe in 15 mL pre-warmed DIG Easy Hyb solution. The membrane was incubated in the hybridization solution at 42°C for 3 h with gentle agitation. Next, the hybridization solution was removed and the membrane was washed twice with stringent wash buffer I (5 min each) with gentle agitation. The membrane was washed twice with stringent wash buffer II (20 min each) at 50°C with gentle agitation. Membrane was washed once with washing buffer for 5 min. The membrane was submerged in blocking solution (containing maleic acid, from kit) and incubated for 1 h, and then incubated for 30 min in Anti-DIG-Alkaline Phosphatase solution (from kit). The membrane was washed twice with washing buffer (15 min each), and equilibrated with detection buffer (from kit) by incubation for 5 min. The buffer was removed and 4 mL substrate solution (from kit) was dropwise applied to the membrane, with the DNA side facing up. The excess of substrate solution was removed, and the membrane was wrapped in plastic film, spreading the remaining substrate solution homogeneously over the membrane, and avoiding the formation of air bubbles. Finally, the chemiluminescence detection was performed in the ImageQuant imaging system and software with exposure time of 20 min.

3.2.17. Detection of telomere-associated promyelocytic leukemia bodies

The Alternative Lengthening of Telomeres (ALT)-associated promyelocytic leukemia bodies (APBs) assay was performed on patient iPSC clones and subclones at different passages, as well as iPSCs control and H1 hESCs. Patient fibroblasts were set as negative control, and telomerase-deficient VA13 cell line was set as positive control. First, PSCs from confluent 6-well plates in feeder-independent culture were dissociated in single cells. For this purpose, cells were rinsed once with 1×PBS and detached with 1 mL per well of Accutase cell detachment solution, incubated for 10 min at 37°C. Cells were pipetted in order to dissociate colonies, and then resuspended in 10 mL DMEM/F12 medium, transferred to a 15 mL tube and centrifuged (200 × *g* for 5 min). An aliquot of cells was prepared to be counted in the Neubauer chamber. After centrifugation, the supernatant was removed and cells were

resuspended in mTeSR medium containing 10 μM ROCK inhibitor; 3×10^5 cells were seeded in one well of 24-well plates previously covered with 13 mm coverslips and coated with Matrigel matrix (as described in "3.2.7.d – Preparation of feeder-independent plates"). PSCs were incubated overnight in the cell culture incubator. Next, media were aspirated and cells were washed once with 1×PBS, following fixation with pre-warmed (37°C) 2% paraformaldehyde in 1×PBS for 10 min at room temperature. Cells were washed twice with 1×PBS and permeabilized with 0.5% Triton X-100 in 1×PBS for 10 min at room temperature, and washed three times with 1×PBS. Cells were blocked in blocking buffer (1% BSA in 1×PBS) for 1 h at 37°C, and then incubated overnight at 4°C with the mouse anti-human PML protein primary antibody diluted in blocking buffer (1:200). The primary antibody was removed and cells were washed three times with 1×PBS. Diluted secondary antibody (1:500 in blocking buffer) donkey anti-mouse IgG Alexa Fluor 594 was added and cells were incubated at room temperature for 1 h. Secondary antibody was removed and cells were washed twice with 1×PBS, proceeding then to telomere fluorescence *in situ* hybridization (telomere FISH). For this purpose, cells were fixed again with 2% paraformaldehyde in 1×PBS for 2 min at room temperature, following two steps of washing with 1×PBS for 3 min. Cells were dehydrated with cold ethanol series (70%, 85%, and 100%) for 2 min each step. Coverslips containing cells were pre-warmed in a hot plate (85°C) for 5 min in the dark. Meanwhile, pre-warmed (85°C) hybridization buffer (70% formamide, 3 mM Tris, and 0.01% BSA in 1×PBS) was added to 200 nM PNA telomere FISH probe (TelG-FITC). The mix was applied to the coverslips, then incubated for 15 min on the hot plate at 85°C. For hybridization, the coverslips were incubated in a humid chamber at room temperature for 2 h in the dark. Then, coverslips were washed with washing solution (2× SSC plus 0.1% Tween-20) at 56°C for 15 min, and washed twice with 1×PBS. Nuclei were counterstained with 1.5 μg/mL DAPI solution for 15 min at room temperature, and then washed with 1×PBS. Coverslips were removed from 24-well plates and placed upside down in slides using 6 μL mounting medium. Slides were analyzed under a fluorescence microscope, in which cell images were acquired.

3.2.18. Hematopoietic Stem Cell differentiation

Hematopoietic stem cell (HSC) differentiation was carried out in mutant iPSCs and controls. The differentiation of each PSC line was performed in at least two independent

experiment sets. The differentiation protocol was adapted from Ng *et al*. (2008) and Chadwick *et al*. (2003). In order to generate EBs prior to differentiation, cells cultured in feeder-independent platform and mTeSR medium were passaged at confluence of 75% (approximately) using dissociation buffer as previously described (section "3.2.7.e – Passage of PSCs in feeder-independent cultures"). The content of one well was split into three wells in a Matrigel plate (6-well plates). Cells were grown for two days with daily medium change. After, PSCs were incubated in mTeSR medium supplemented with 10 μM ROCK inhibitor for 1 h at 37°C. Medium was removed and cells were rinsed twice with 1×PBS, and incubated with dissociation buffer for 5 min at room temperature. The dissociation buffer was removed and PSCs aggregates were rinsed with mTeSR medium containing 30 μM polyvinyl alcohol, carefully pipetted to avoid dissociation of aggregates, which should be bigger in size than aggregates for passaging (about 500 cells per clump). The content of two wells of cells was transferred to one well of ultra-low attachment 6-well plates and placed into the cell culture incubator. In the next day, plates were checked for EBs formation and medium was changed for STEMdiff APEL basal medium supplemented with a series of cytokines combinations in specific timing and concentration. First, in order to induce EBs to the mesodermal germ layer, cells were exposed for four days to basal medium containing 30 ng/mL VEGF, 30 ng/mL BMP4, 40 ng/mL SCF, and 50 ng/mL Activin A. Then, in order to induce mesodermal cells to the hematopoietic lineages, cells were exposed for nine days to basal medium containing 300 ng/mL SCF, 300 ng/mL Flt3L, 10 ng/mL IL-3, 10 ng/mL IL-6, 50 ng/mL G-CSF, and 25 ng/mL BMP4). Medium was replaced in each three days (3 mL per well in the ultra-low attachment 6-well plates).

At the end of day 13 of HSC differentiation, EBs were collected and dissociated using 0.05% trypsin. For this purpose, EBs were collected with glass pipettes, placed in 15 mL tubes, rinsed once with 1×PBS and decanted by gravity. Supernatant was removed and 500 μL trypsin was added per tube. Tubes were incubated at 37°C in the water bath for 6 min, with regular pipetting in each 2 min. Trypsin was inactivated by addition of 1 mL D10. For complete dissociation of EBs, the cells were homogenized five times using 21-gauge needles attached to syringes, then filtered using 70 μm cell-strainers placed into 50 mL tubes. An aliquot of the single cells was collected for counting in the Neubauer chamber. Cells were centrifuged (200 × *g* for 5 min) and resuspended in 1×PBS to a final concentration of 1×10^3 cells per 1 μL PBS, proceeding immediately to colony-forming cell (CFC) assay.

For the CFC assay, 1.5×10^5 cells (150 μL) were pipetted into aliquots of 3 mL methylcellulose medium with recombinant cytokines (MethoCult H4435); 2.5 mL of

methylcellulose medium containing cells was aspirated using 16-gauge needles attached to syringes; the medium was carefully dispensed into 35 mm cell culture dishes, 1 mL per dish (5×10^4 cells per dish), avoiding bubbles. Four dishes were prepared per PSC line in each differentiation experiment. Dishes were placed in the cell culture incubator. Fourteen days after seeding cells in the methylcellulose medium, the CFUs (colony-forming units) that have grown were identified and counted under an inverted microscope according to the standard morphological criteria. Colonies composed of at least 50 cells were considered for counting. The criteria classify colonies as follows: CFU-GM, CFU-granulocyte, macrophage; CFU-G, CFU-granulocyte; CFU-M, CFU-macrophage; BFU-E, burst forming unit erythroid; CFU-E, CFU-erythroid; CFU-GEMM, CFU-granulocyte, erythrocyte, monocyte, megakaryocyte; CFU-F, CFU-fibroblast. First, the average of the four dishes counting was calculated for a PSC line in each independent experiment. The results of CFU counting for a given PSC line express the average and standard deviation of at least two independent experiments.

The Figure 3.10 provides a schematic timeline of the steps performed in the HSC differentiation experiments.

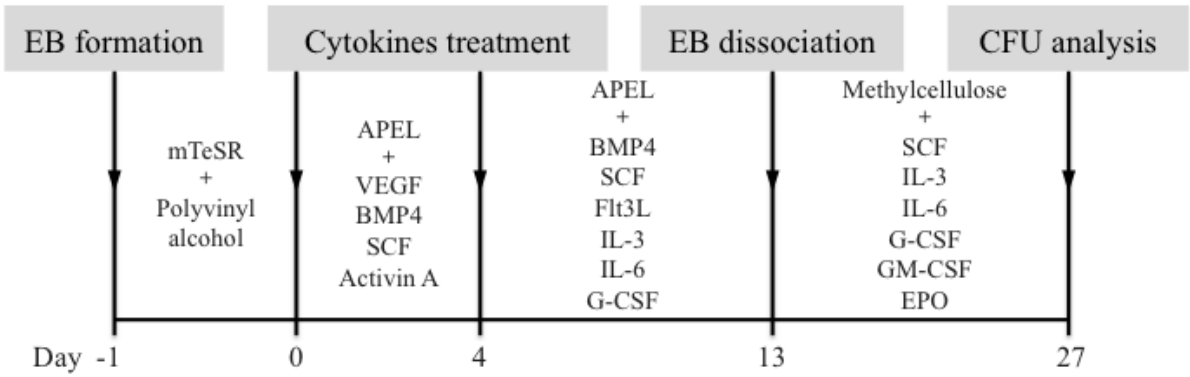

Figure 3.10 – Overview of the HSC differentiation in the PSCs. First, EBs were derived from the PSCs colonies one day before starting cytokines treatment. Next, EBs were guided to mesodermal differentiation with specific cytokines for three days (day 0 to 3). By day 4, medium was replaced with a different cytokines cocktail in order to promote maturation of the hematopoietic stem and progenitor cells. On day 13, EBs were harvested and dissociated, and cells were seeded in semi-solid medium (methylcellulose) containing cytokines. CFUs formed after 14 days in methylcellulose were classified and counted.

After CFU counting, representative colonies were collected using 50 µL pipettes and tips, washed three times with 1×PBS, centrifuged (200 × *g* for 5 min), counted, and transferred to slides for morphological analysis. For preparing slides, 1×10^5 cells were resuspended in 200 µL 1×PBS, and spun at 200 × *g* for 10 min in a cytospin centrifuge. Then, cells were fixed on slides using 4% paraformaldehyde for 10 min. Cells were stained

with Wright's stain by covering slides with the staining solution and incubating for 7 min. Slides were washed with 1×PBS, and analyzed under a microscope.

3.2.19. Statistical analysis

The GraphPad Prism software was used for statistics and graph creation. Linear regression was applied in Southern blot and qPCR results. Coefficient of variance was calculated for *TERT*, *TERC*, and *DKC1* expression levels. One-way analysis of variance (ANOVA) was applied for the comparison of telomere elongation rates. Nonparametric statistics (Kruskal-Wallis and Dunn's post test) were used for comparison of grouped samples (for expression of pluripotency and differentiation markers, as well as for telomerase activity). The p-values bellow 0.05 were considered statistically significant.

4. RESULTS

4. Results

4.1. Patient clinical characteristics

In order to investigate the telomere dynamics in the reprogramming process of cells from DC patients, a 3-year-old male patient previously diagnosed with DC was selected. The patient displayed the classical triad that characterizes the disease (leukoplakia of the tongue, nail dystrophy, and auricular hyperpigmentation), as well as recurrent pneumonia, cerebellar hypoplasia, pancytopenia, and hypocellular bone marrow suggesting aplastic anemia. Southern blot was used to measure telomere length of the patient in his blood leukocytes, resulting in a length of seven kilobases (kb). This telomere length is below the tenth percentile of the telomere length curve obtained for healthy subjects. The Figure 4.1 displays the telomere length (kb) from leukocytes of 205 healthy blood donors, in which the DC patient was highlighted.

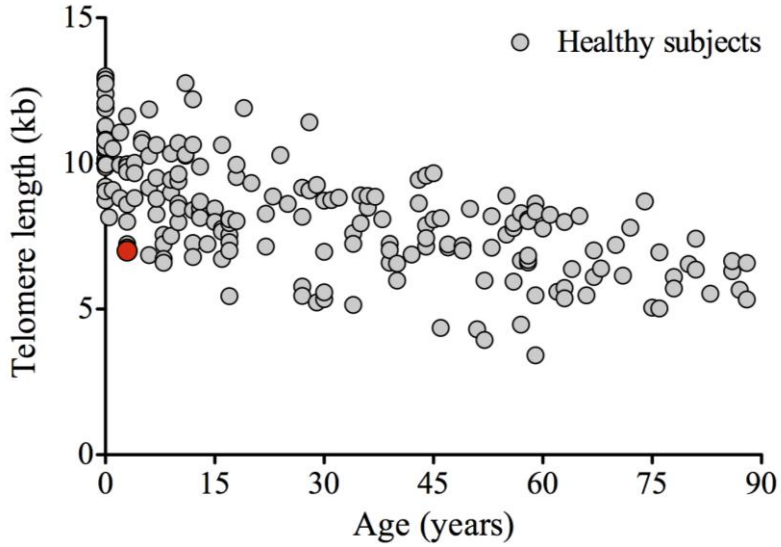

Figure 4.1 – Telomere length from leukocytes as a function of age. Telomere lengths were measured by Southern blot from leukocytes of 205 healthy blood donors (grey circles); the DC patient was represented as a red circle, displaying shorter telomeres adjusted for his age. The telomere lengths from healthy subjects were provided by Scatena, 2014, master's dissertation.

The sequencing of *DKC1* gene identified a nucleotide substitution C>T at position 1058 (exon 11) (Figure 4.2), which is responsible for the A353V amino acid missense substitution in the dyskerin, the protein encoded by the *DKC1* gene. Because the patient's mother was

clinically healthy and did not present any mutation in the *DKC1* gene (Figure 4.2), the nucleotide substitution was classified as a *de novo* mutation.

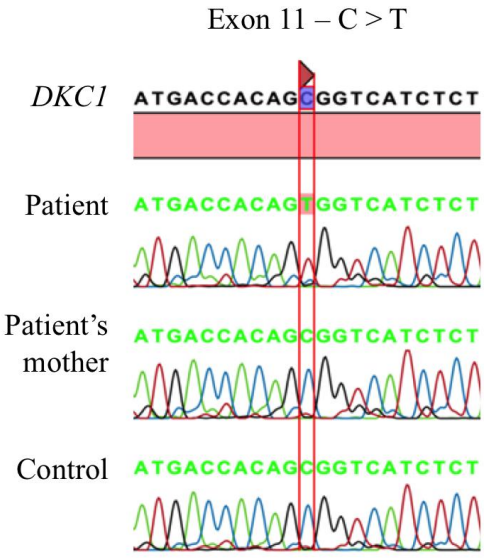

Figure 4.2 – Detection of a *DKC1* mutation in the patient. A nucleotide substitution C>T at position 1058 (exon 11) was identified in the *DKC1* gene in the patient's leukocytes, which resulted in the missense mutation A353V. The patient's mother did not display the alteration.

4.2. Reprogramming

4.2.1. Virus production

4.2.1.a – Plasmid expansion and preparation

Competent cells (Stbl3 *E. coli*) were transformed with the following plasmids: pMD2.G, psPAX2, STEMCCA "four factors", and STEMCCA "mCherry". The plasmid DNA was isolated and restriction digestion was performed to exclude recombination events and confirm the identity of the plasmids. The Figure 4.3 shows the image of the agarose gel with the digested plasmid samples.

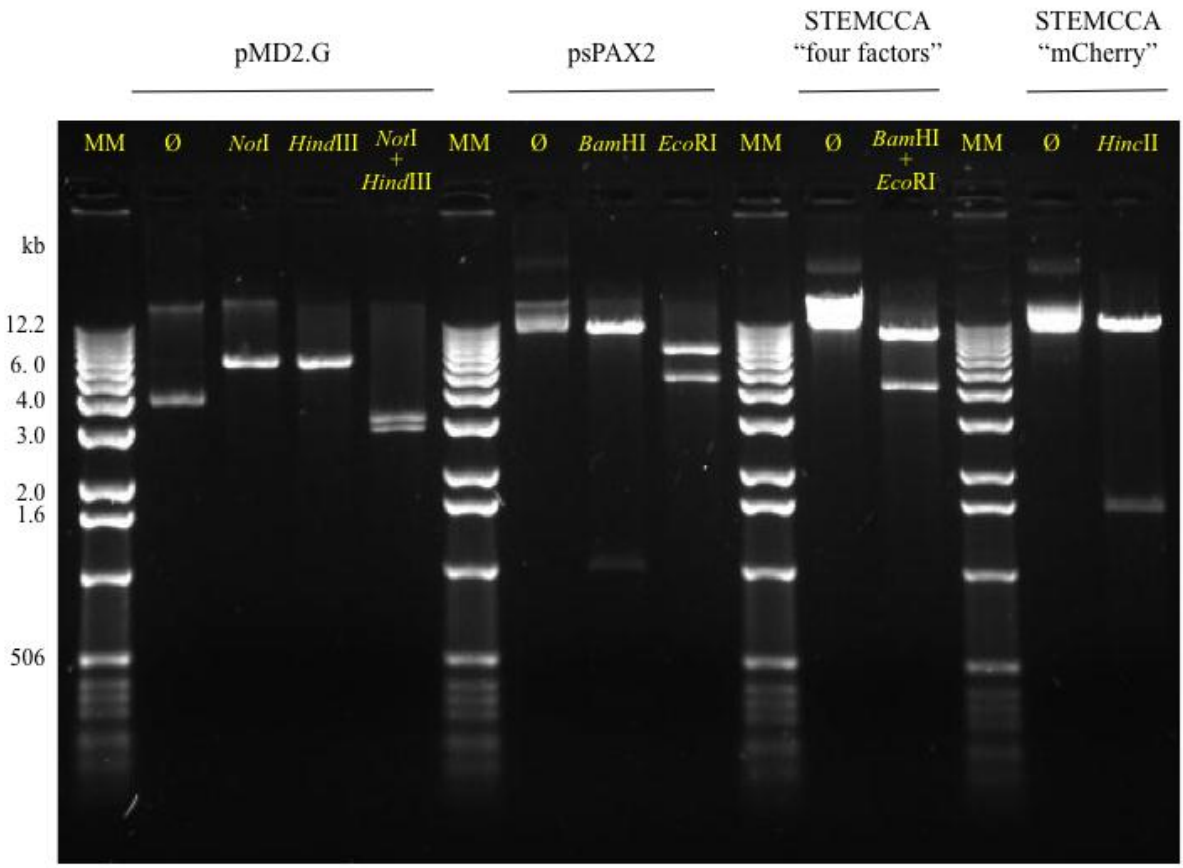

Figure 4.3 – Plasmid DNA digested with specific restriction enzymes. Plasmid pMD2.G without digestion (Ø), digested with *Not*I alone, *Hind*III alone, and both (*Not*I + *Hind*III); plasmid psPAX2 without digestion (Ø), digested with *Bam*HI alone, and *Eco*RI alone; plasmid STEMCCA "four factors" without digestion (Ø), and digested with both *Bam*HI and *Eco*RI; plasmid STEMCCA "mCherry" without digestion (Ø), and digested with *Hinc*II. MM: molecular marker; kb: kilobases.

In general, the results on the gel matched the predicted sizes inferred from the plasmid maps (provided in Figures 3.1 and 3.2). Table 4.1 provides a summary of the results.

Table 4.1 – Fragment sizes expected and observed for plasmids after digestion with restriction enzymes.

Plasmid	Lane	Restriction enzyme	Fragment size (kb)	
			Expected	Observed (approx.)
pMD2.G	2	None	5.8	5
	3	*Not*I	5.8	6
	4	*Hind*III	5.8	6
	5	*Not*I and *Hind*III	2.7 and 3	2.7 and 3
psPAX2	7	None	10.7	10
	8	*Bam*HI	0.3, 1, and 9.3	1 and 9
	9	*Eco*RI	4.3 and 6.3	4 and 6
STEMCCA "four factors"	11	None	12.6	12
	12	*Bam*HI and *Eco*RI	4 and 8.6	4 and 9
STEMCCA "mCherry"	14	None	11.9	12
	15	*Hinc*II	1.6 and 10.3	1.5 and 10

4.2.1.b – Production and titration of lentiviral particles

Lentiviral particles were produced in 293T-packaging cells through transfection of plasmids expressing VSV-G envelope (pMD2.G plasmid), HIV-based lentiviral packaging system (psPAX2 plasmid), and either STEMCCA carrying *OCT4*, *SOX2*, *KLF4*, and *MYC* (STEMCCA "four factors"), or STEMCCA carrying *mCherry* gene in place of *MYC* (STEMCCA "mCherry"). Virus particles were collected 24 h and 48 h after transfection, and concentrated by ultracentrifugation. The purpose of producing STEMCCA "mCherry" along with the "four factors" virus was to estimate the number of viral particles in the "four factors" batch that does not have a marker to easily visualize transduced cells. Figure 4.4 shows high mCherry expression in the cell line 293T indicating a good transfection efficiency and possibly production of viral particles.

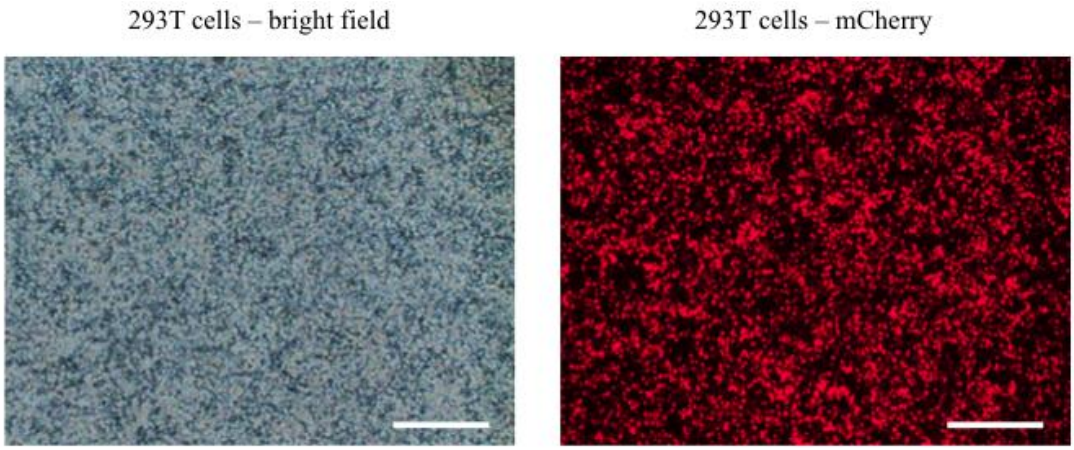

Figure 4.4 – The fluorescence emitted by mCherry protein in 293T cells transfected with STEMCCA "mCherry". The cells were visualized under a fluorescence microscope 48 h after transfection with the plasmids for virus production. Scale bars = 500 µm.

Subsequently, the number of viral particles was determined through titration. HeLa cells were transduced with the STEMCCA "mCherry" viruses collected 24 h and 48 h after transfection with different volumes of concentrated viral supernatant (4 µL, 1.6 µL, 0.64 µL, and 0.256 µL). As negative control, the medium from one well was replaced with transduction medium without viruses. The cell number before transduction was 98,670 cells. Five days after transduction, the cells were harvested and the fluorescence emitted by mCherry was assessed by flow cytometry. The results of flow cytometry analysis, and steps of the calculation, as well as the final titration, are shown in Table 4.2. The average titer was calculated from sample showing mCherry expression between 3 to 35%. This is the linear range when, in average, one viral particle infects one cell. STEMCCA "four factors" and STEMCCA "mCherry" are very similar viruses with comparable transfection capabilities. Hence, the titration results from "mCherry" reflect the simultaneously produced "four factors" titer. The viruses collected 48 h after transfection in 293T cells were used for the following reprogramming experiments.

Table 4.2 – Titration of viral particles produced with STEMCCA "mCherry".

Time after transfection	Serial dilution	Volume of virus (μL)	mCherry$^+$ cells (%)	Correction *	Total viruses **	Titer (particles/mL) ***	Average (particles/mL) ****
24 h	No virus	0	0.4	n/a	n/a	n/a	2.7×10^6
	1	4	14.5	14.1	1.4×10^4	3.5×10^6	
	2	1.6	3.4	3	3.0×10^3	2.0×10^6	
	3	0.64	1.4	1	1.0×10^3	1.5×10^6	
	4	0.256	0.6	0.2	2.0×10^3	7.7×10^5	
48 h	No virus	0	0.4	n/a	n/a	n/a	7.6×10^6
	1	4	34.5	34.1	3.4×10^4	8.4×10^6	
	2	1.6	14.3	13.9	1.4×10^4	8.6×10^6	
	3	0.64	4.1	3.7	3.6×10^3	5.7×10^6	
	4	0.256	1.5	1.1	1.1×10^3	4.2×10^6	

* Subtraction of autofluorescence of cells (mCherry$^+$ cells from "no virus");
** Total cells at the beginning (98,670) × mCherry$^+$ cells;
*** Total viruses divided by the volume of transduced mCherry virus;
**** Virus 24 h: average of serial dilutions 1 and 2; virus 48 h: average of serial dilutions 1, 2, and 3.

4.2.2. Derivation of induced pluripotent stem cells (iPSCs) from *DKC1*[A353V] fibroblasts

Fibroblasts from the DC patient described in the section 4.1 were isolated from a skin biopsy and were cultured for several passages for expansion (Figure 4.5). For reprogramming experiments, passage 7 fibroblasts were transduced with STEMCCA "four factors". In parallel, fibroblasts were transduced with STEMCCA "mCherry" to monitor transduction efficiency.

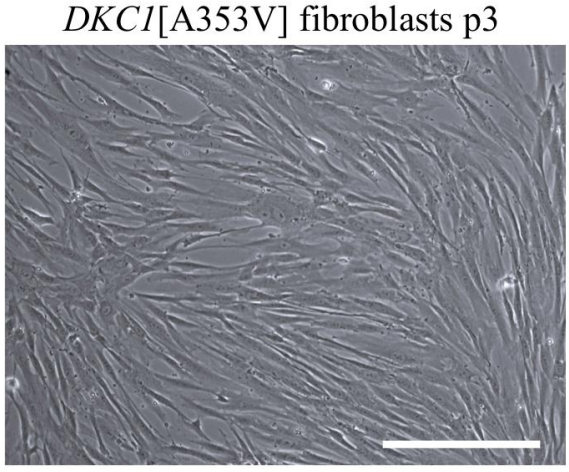

Figure 4.5 – *DKC1*-mutant fibroblasts. Dermal fibroblasts on passage 3 (p3) that were isolated from a skin biopsy of the DC patient. Scale bar = 500 μm.

Flow cytometry analysis of fibroblasts transduced with STEMCCA "mCherry" showed 26% positive cells on day 5 after transduction for the MOI of 2.5. Low reprogramming of cells from telomeropathy patients have been reported (about 0.002%; Agarwal *et al*., 2010; Batista *et al*., 2011), thus only fibroblasts transduced with STEMCCA "four factors" and MOI = 5 were used for iPSC derivation. Unlike in previous studies, all experiments were performed under normoxic conditions.

Small colonies resembling ESC morphology started to appear by day 10. The ESCs colonies are characterized by their tightly packed and flat formats, with rounded and well-defined borders, and consisting of hundreds to thousands cells with large nuclei and scant cytoplasm (Figure 4.6). The Figure 4.7 displays colonies at different days, illustrating their growth and morphology during early phase of reprogramming. The Figure 4.8 illustrates two colonies observed in the reprogramming experiment, one displaying the classical ESCs morphology (Figure 4.8-A), and the other, a non-classical morphology probably formed by the division of a not fully reprogrammed fibroblast (Figure 4.8-B).

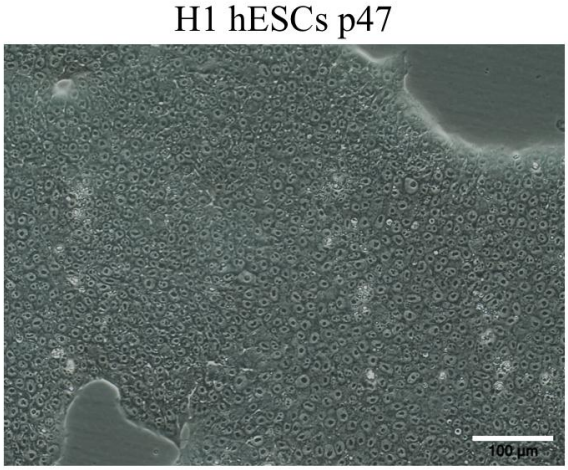

Figure 4.6 – H1 human embryonic stem cells (hESCs). Cells tightly packed forming a flat colony; pluripotent cells display large nuclei and scant cytoplasm; the colony was plated on feeder-independent culture, at p47. Scale bar = 100 µm.

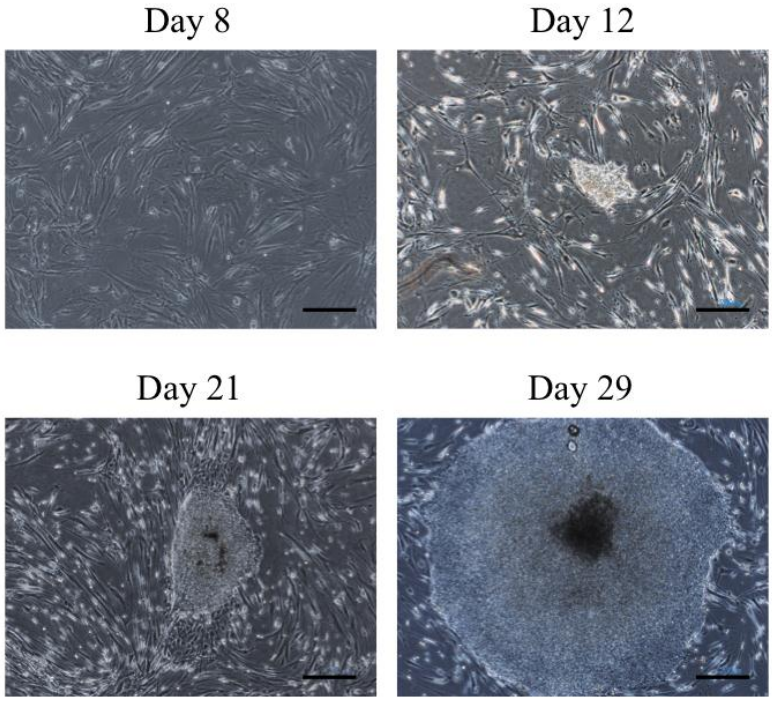

Figure 4.7 – *DKC1*-mutant colonies resembling ESCs at different days after transduction. *DKC1*-mutant fibroblasts were transduced with STEMCCA "four factors" and seeded in dishes coated with gelatin and feeder cells. At day 8, human fibroblasts could not be distinguished from MEFs. From day 10, small colonies were arising and growing on the feeders. Different colonies are shown on days 12, 21, and 29 after transduction. Scale bars = 500 μm.

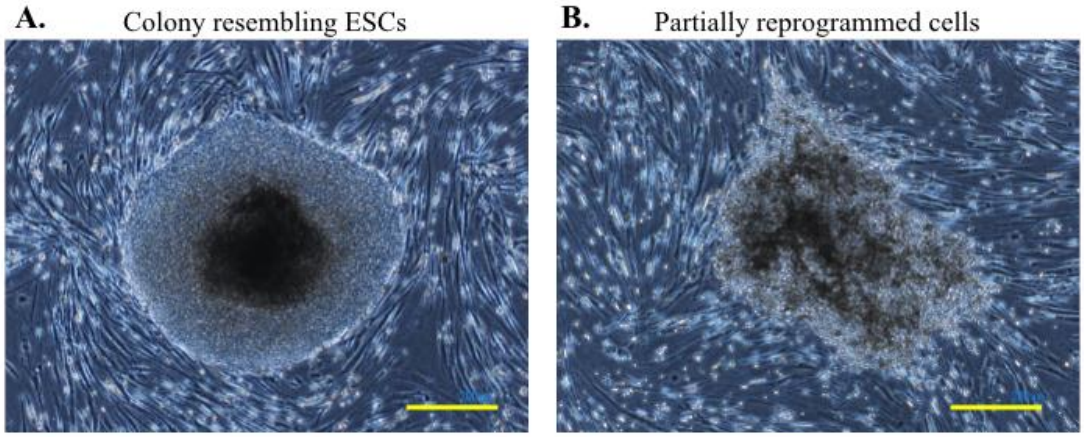

Figure 4.8 – *DKC1*-mutant colonies observed in the reprogramming experiment. Colonies observed at day 25 after transduction. (**A**) Colony resembling ESCs morphology, displaying well-defined and rounded border, and a flat format with tightly packed cells. The darker region in the center was composed of differentiated cells. (**B**) Colony formed by not compacted, darker cells, some of them displaying fibroblastoid morphology. Colony may be a result of a fibroblast that was infected but not completely reprogrammed to the pluripotent state. Scale bars = 500 μm.

At the day 29 after transduction, individual colonies with ESC-like morphology were counted in the two dishes. A total number of 27 iPSC colonies were identified, demonstrating

that the efficiency of reprogramming experiment was 0.01% (Table 4.3). Since each colony is thought to be derived from one single fibroblast, 27 clones (or 27 independent iPSC lines) were derived. The colonies were manually passaged and individually propagated.

Table 4.3 – Reprogramming experiments of *DKC1*-mutant fibroblasts.

Dish	Number of fibroblasts seeded*	Number of iPSC colonies**	Efficiency (%)***
1	1×10^5	11	0.01
2	1.5×10^5	16	0.01

* Fibroblasts seeded 5 days after transduction with viral particles STEMCCA "four factors";
** Colonies resembling ESCs morphology that were counted at day 29 after transduction;
*** Efficiency based on the number of transduced fibroblasts seeded and the number of iPSCs colonies on day 29.

4.2.3. Characterization of *DKC1*[A353V] iPSC clones

Three randomly selected *DKC1*-mutant iPSC clones, also referred to as *DKC1*[A353V] iPSCs, clones 4, 7, and 12 (hereafter referred as c4, c7, and c12) were further expanded and characterized. First, the expression of classic pluripotency markers OCT4, NANOG, SSEA4, TRA-1-81, and TRA-1-60 was confirmed by immunocytochemistry. All clones stained positive similar to the H1 hESC reference line (Figure 4.9). The selected clones were maintained in culture for several passages. At this stage, samples were obtained for later assessment of telomere length and telomerase function.

Epigenetic reprogramming is not completed when the colonies are identified, and several passages are required to complete this remodeling process. Therefore, excision of the transgenes should be performed at later passages. Also, complete characterization of the pluripotent state of derived cells should be performed after successful transgene removal.

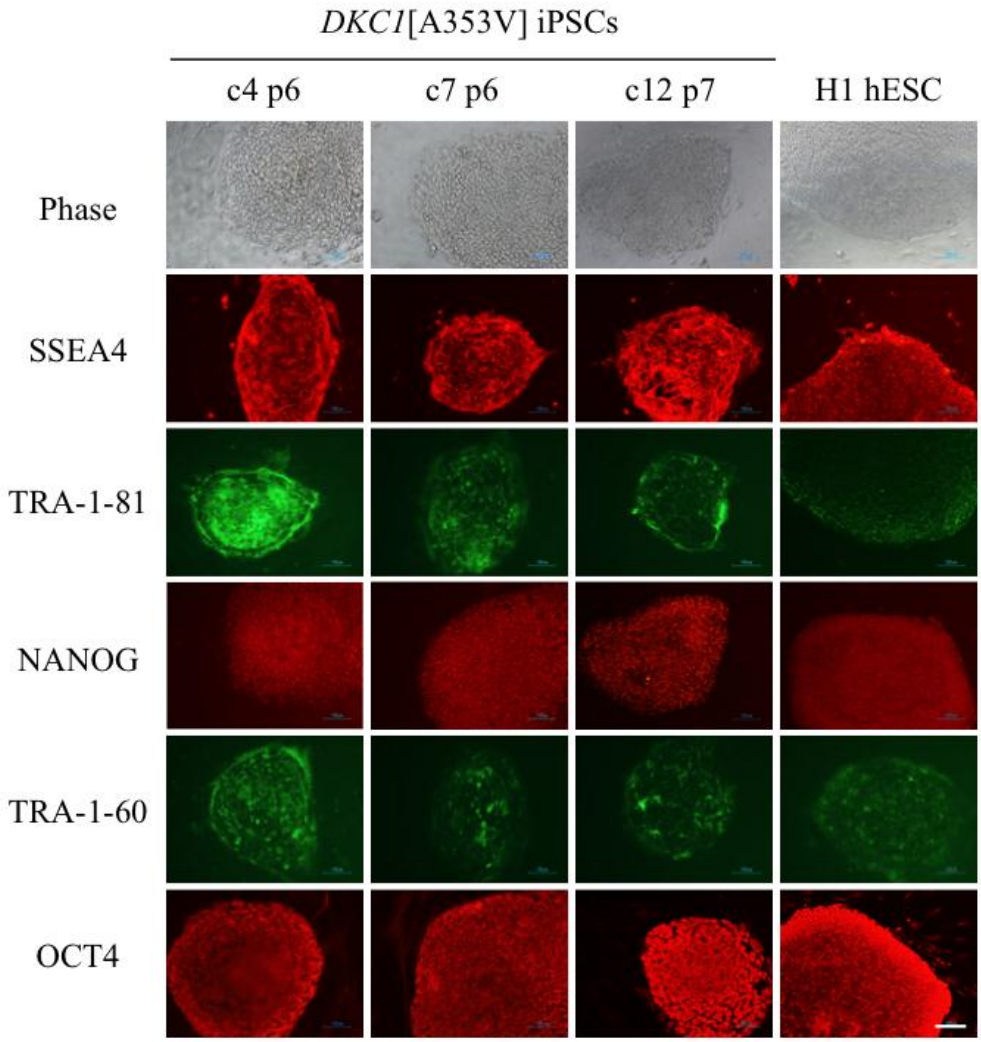

Figure 4.9 – Morphology and immunocytochemistry of *DKC1*[A353V] iPSC clones. Patient-derived iPSC clones (c) 4, 7, and 12, at specific passages (p), stained positive for the pluripotency markers SSEA4, TRA-1-81, NANOG, TRA-1-60, and OCT4. H1 hESC line is shown as positive control. Cells were grown on MEFs that expectedly did not stain with the selected markers (negative control). Scale bar = 100 μm.

4.2.4. Derivation of transgene-free *DKC1*[A353V] iPSCs

DKC1[A353V] iPSCs c4, c7, and c12 were maintained in culture for excision of the reprogramming transgenes by transient cre-recombinase expression. Before excision, a multiplex PCR was carried out in order to estimate vector copy number. Clones 4 and 12 contained one copy whereas clone 7 showed 3 integrated viruses (Figure 4.10).

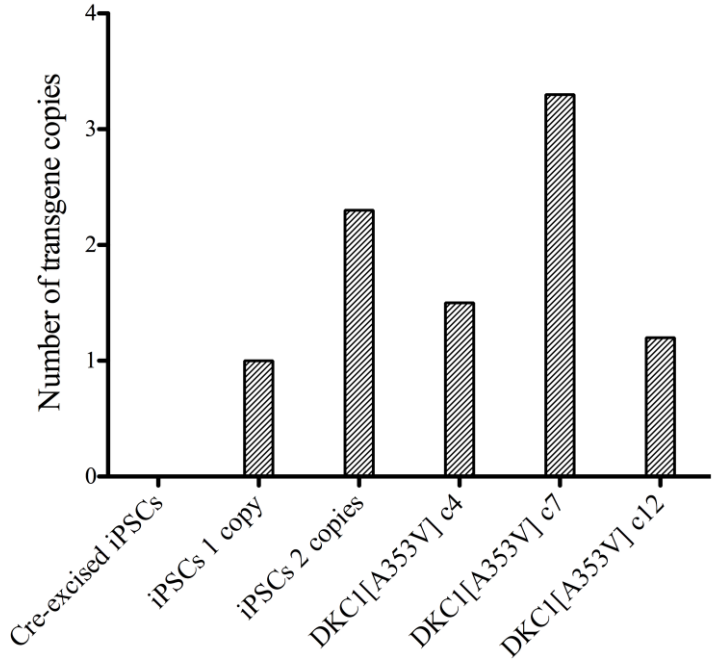

Figure 4.10 – Multiplex PCR for number of inserted transgenes into the iPSC clones. Three *DKC1*[A353V] iPSC clones (c4, c7, and c12) were compared to iPSCs previously known as containing none (cre-excised iPSCs), one (iPSCs 1 copy), or two copies (iPSCs 2 copies) of inserted transgenes. Data was normalized by "iPSCs 1 copy".

The iPSCs c4, c7, and c12 were transfected with a non-integrating vector transiently expressing cre-recombinase. After positive selection with puromycin for cells transduced with the cre-recombinase plasmid, it took about 15 days before iPSC colonies grew to size large enough for manual selection. Each colony was formed by the division of one single pluripotent cell that was successfully transfected and selected. Therefore, each new clone represents a subclone derived from a parental iPSC clone. Consequently, the subclones were named with the number of the parental clone and a new number. Table 4.4 displays the subclones derived from the parental iPSCs c4, c7, and c12.

Table 4.4 – Transgene-free subclones derived from the *DKC1*[A353V] iPSCs c4, c7, and c12.

Parental iPSCs (clone)	Amount of subclones	Nomenclature of subclones
4	8	4-1 to 4-8
7	8	7-1 to 7-8
12	5	12-1 to 12-5

One subclone from each parental line was maintained in culture for further characterization (c4-7, c7-4, and c12-5). Multiplex PCR confirmed efficient transgene removal (Figure 4.11).

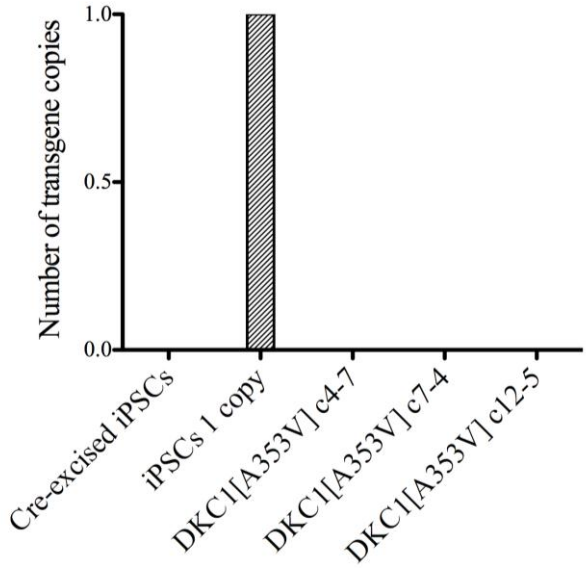

Figure 4.11 – Multiplex PCR for confirmation of transgene removal in the iPSC clones. Three *DKC1*[A353V] iPSC clones (c4-7, c7-4, and c12-5) were compared to iPSCs previously known as containing none (cre-excised iPSCs), or one copy (iPSCs 1 copy) of inserted transgenes. Data was normalized by "iPSCs 1 copy".

4.2.5. Characterization of transgene-free *DKC1*[A353V] iPSC clones

4.2.5.a – DKC1[A353V] iPSCs express pluripotency markers

Selected iPSCs expressed the pluripotent cell surface markers SSEA4, TRA-l-60, and TRA-1-81, as well as the nuclear markers OCT4 and NANOG. Expression resembled the reference hESC line H1 (Figure 4.12).

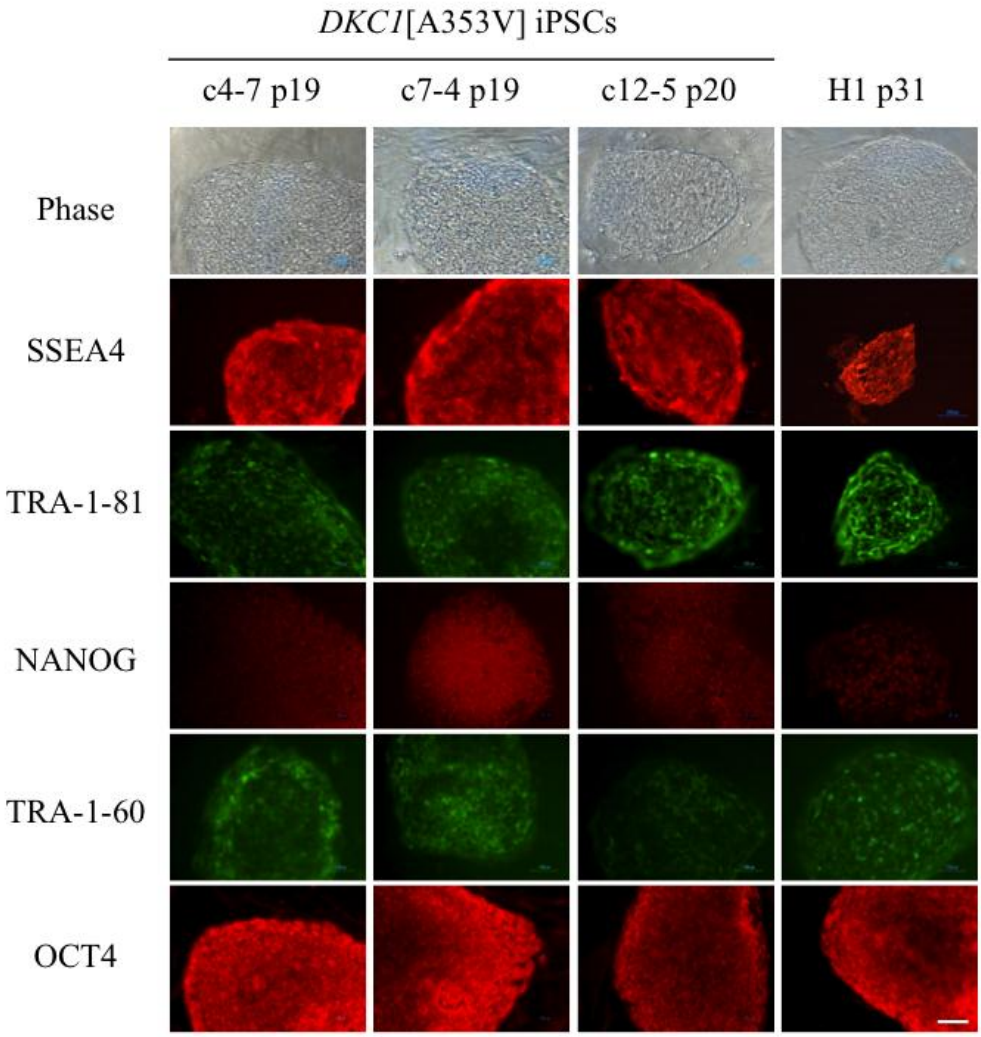

Figure 4.12 – Morphology and immunocytochemistry of *DKC1*[A353V] iPSCs c4-7, c7-4, and c12-5. The iPSCs stained positive for the pluripotency markers SSEA4, TRA-1-81, NANOG, TRA-1-60, and OCT4. H1 hESC line is shown as positive control. Cells were grown on MEFs that expectedly did not stain with the selected markers (negative control). Scale bar = 100 µm.

4.2.5.b – In vitro differentiation

Embryoid body (EB) differentiation was performed to evaluate the differentiation capacity and thus the pluripotency of the iPSCs *in vitro*. When transferred to low attachment plates, PSCs tend to form three-dimensional structures, the EBs, that further mature *in vitro* and may contain tissue from all three germ layers (Itskovitz-Eldor *et al*., 2000). The three iPSC clones readily differentiated to EBs in a similar manner and time scale to those observed in the H1 hESC line, as shown in the Figure 4.13.

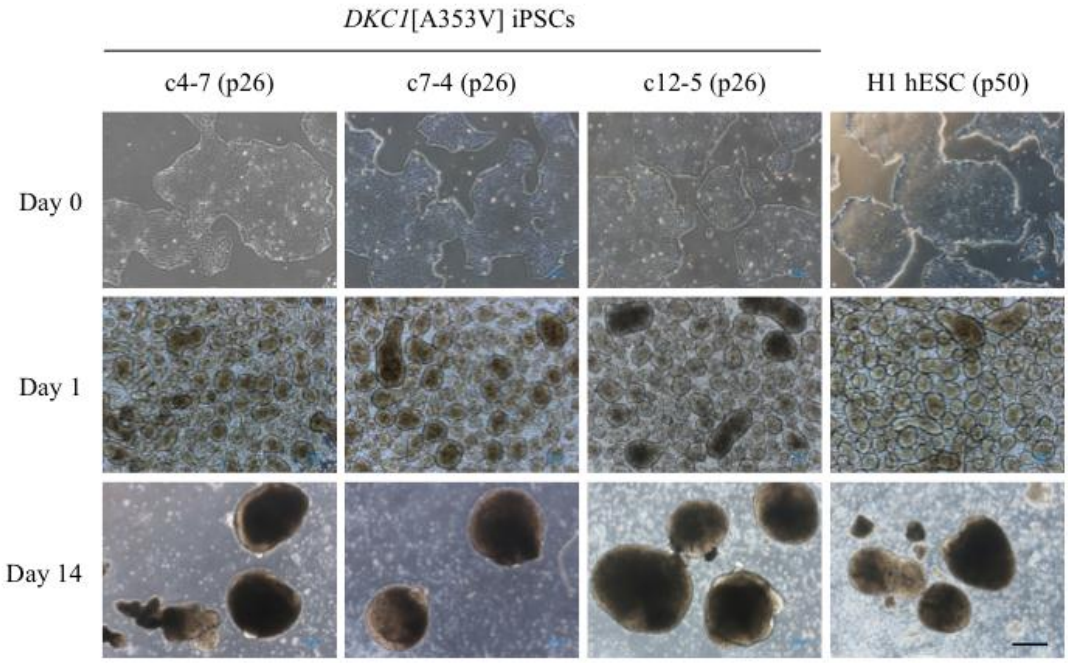

Figure 4.13 – Embryoid bodies formation performed in *DKC1*[A353V] iPSC clones. iPSCs and H1 hESC line (positive control) colonies on feeder-free culture prior to EBs formation assay are shown on Day 0; three-dimensional aggregates of pluripotent stem cells like EBs one day after passaging in medium containing polyvinyl alcohol are shown on Day 1; EBs after 2 weeks of maturation in culture are shown on Day 14. Scale bar = 500 μm.

Subsequently, mRNA was extracted from undifferentiated PSCs and EBs, and the expression of typical pluripotency-associated genes like *OCT4*, *SOX2*, *KLF4*, *MYC*, and *NANOG*, as well as markers of endoderm (*AFP* and *GATA4*), mesoderm (*RUNX1* and *CD34*), and ectoderm (*NCAM* and *NES*) were determined by RT-qPCR. All iPSCs showed expression of pluripotency markers *OCT4*, *SOX2*, *KLF4*, and *MYC* comparable to control ESCs (Figure 4.14). *NANOG* expression was higher in PSCs than in EBs. However, the expression of this marker was lower in iPSCs than in H1 hESCs. On the other hand, EB-differentiated cells exhibit lower or absent expression of pluripotency genes *OCT4*, *MYC*, and *NANOG* (Figure 4.14). The expression of *SOX2* and *KLF4* was higher in EBs than in PSCs. *KLF4* is not PSC-specific and is also involved in the differentiation of epithelial cells. *SOX2* is also involved in neural development. Thus, it may explain the higher expression of these transcription factors in EBs.

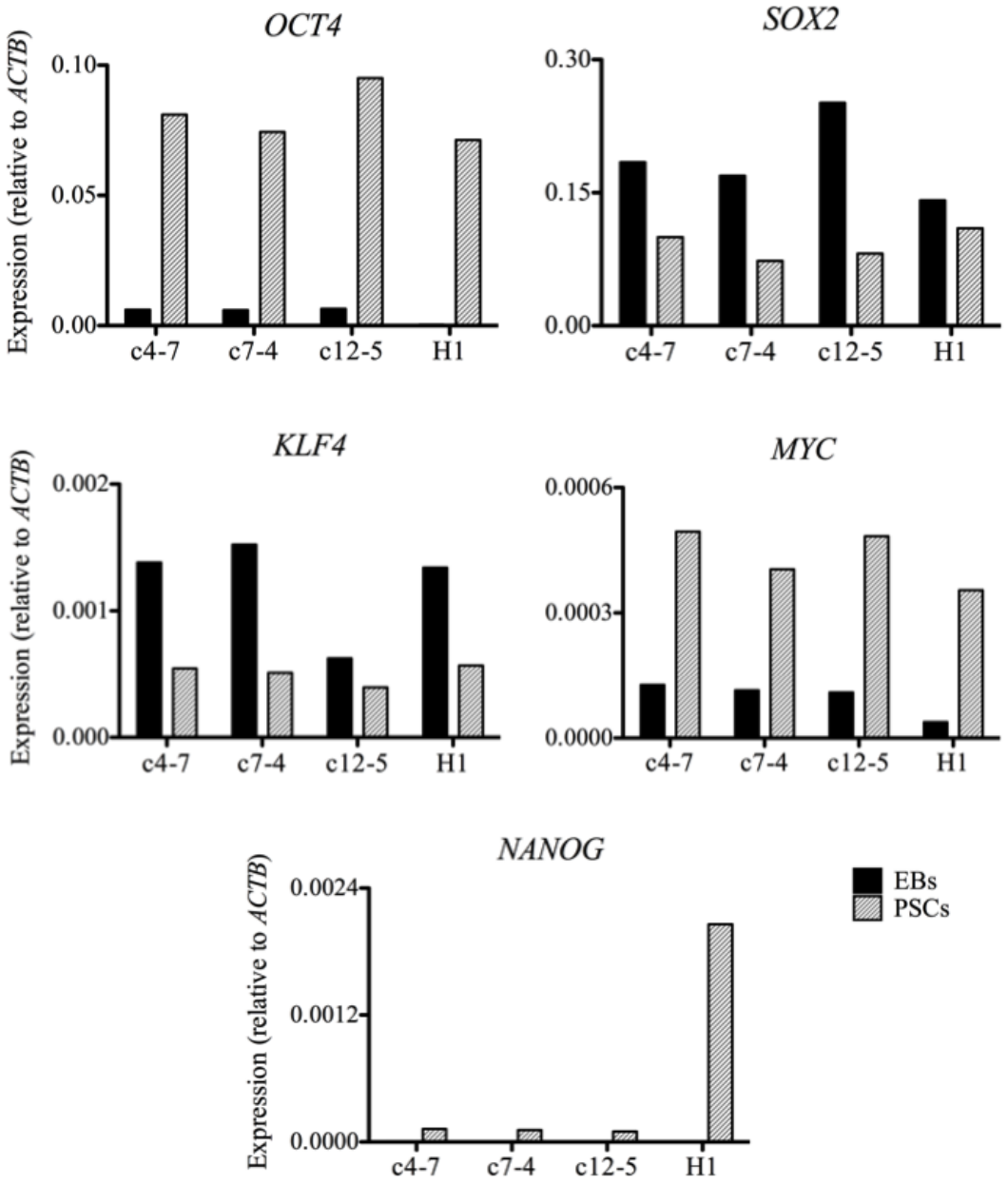

Figure 4.14 – Expression levels of endogenous pluripotency markers. Gene expression of EBs and iPSC clones (c) 4-7, 7-4, 12-5, as well as H1 (positive control); expression levels were normalized by *ACTB* (actin, beta). EBs = embryoid bodies; PSCs = pluripotent stem cells (iPSCs and H1 hESC line).

The expression levels of endoderm, mesoderm, and ectoderm markers are shown on Figure 4.15. The expression levels of *AFP* were higher in the pluripotent cells than in EBs, different from expected, though exhibiting similar expression patterns in the iPSC clones and positive control. iPSCs c4-7 displayed increased expression of *GATA4* in EBs compared to the other iPSCs and H1, which is indicative for the previously described clonal heterogeneity of iPSCs. The same clone also had a higher expression of the mesodermal transcription factor *RUNX1* and the hematoendothelial marker *CD34*. Both ectoderm markers *NCAM* and *NES*

were up-regulated in EBs compared to the undifferentiated state of the three iPSC clones. In general, there was no significant difference between expression patterns of iPSC clones and H1 hESC line for both biological conditions analyzed (EBs and undifferentiated cells).

Some discrepancies were observed in the expression levels of markers such as *SOX2* and *KLF4*, which were highly expressed in EBs than in PSCs (Figure 4.14), and *AFP*, which was highly expressed in PSCs than in EBs (Figure 4.15). However, these discrepancies were detected not just in the iPSC clones, but also in H1, the positive control. Thus, it suggests that a possible interference of one or more environmental factors, such as components of the medium in which the EBs were cultured, may have contributed to these patterns of gene expression.

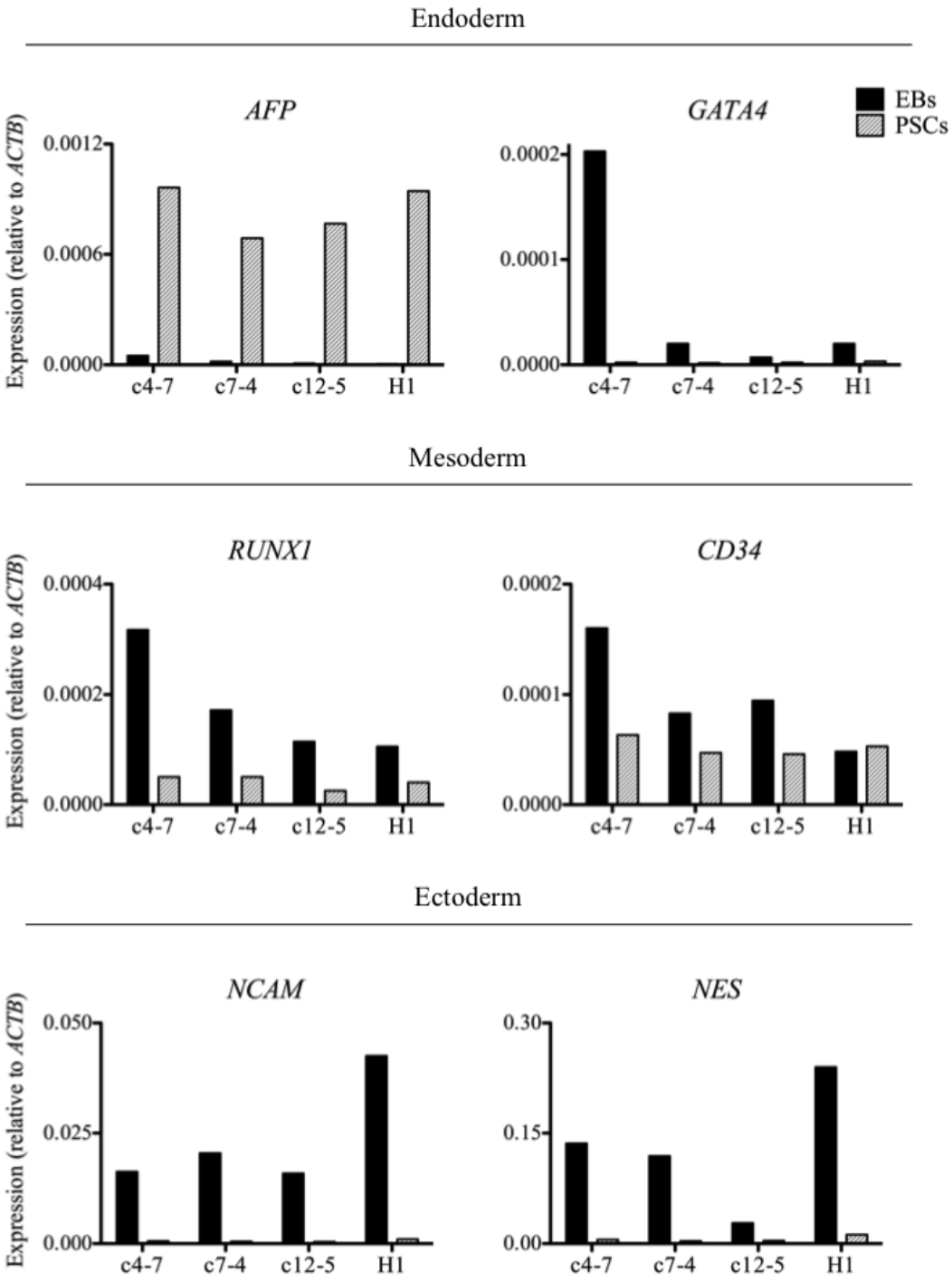

Figure 4.15 – Expression levels of endoderm, mesoderm, and ectoderm markers. Gene expression in EBs and iPSCs of clones c4-7, c7-4, c12-5, as well as H1 (positive control); expression levels were normalized by *ACTB* (actin, beta). EBs = embryoid bodies; PSCs = pluripotent stem cells (iPSCs and H1 hESC line).

4.2.5.c – No chromosomal abnormality was acquired in the DKC1[A353V] iPSC clones

Genotoxicity is a major concern for *in vitro* culture of somatic and pluripotent cells. Epigenetic reprogramming itself may also contribute to genomic instability and clonal selection of cells with aberrant genotype. All iPSCs retained a normal karyotype throughout reprogramming, initial passaging and transgene removal. Cells were examined by G-banding (Figure 4.16).

Figure 4.16 – Karyotyping of *DKC1*[A353V] iPSC clones 4-7, 7-4, and 12-5. The three iPSC clones presented 46, XY normal karyotype in the band resolution (BR) analyzed: c4-7, BR = 450-475; c7-4, and c12-5, BR = 425-450.

4.2.5.d – DKC1[A353V] iPSC clones retained the mutation of the parental fibroblasts

Exon 11 of the *DKC1* gene was sequenced in the three clones and results were compared to the parental fibroblasts and the reference genome. Sequencing analysis confirmed that the derived iPSCs retained the nucleotide substitution C>T at position 1058 of the gene (Figure 4.17), which leads to the A353V amino acid missense substitution in the dyskerin protein.

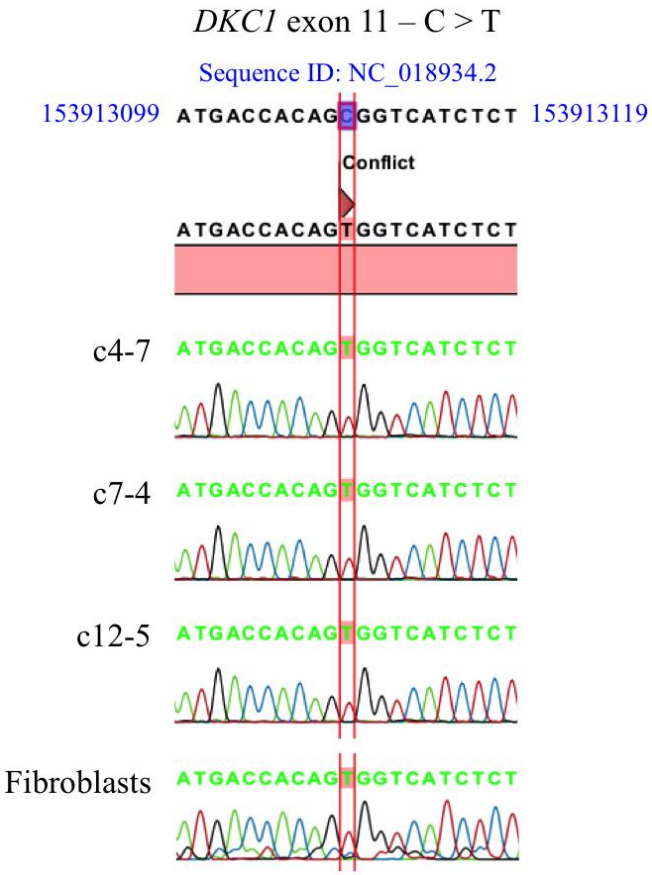

Figure 4.17 – Confirmation of the *DKC1* mutation in patient-derived iPSC clones. Patient-derived iPSCs retained the nucleotide substitution C>T at position 1058 (exon 11), previously identified in the parental fibroblasts.

4.3. *DKC1*[A353V] iPSCs can be maintained in long-term culture

The *DKC1*[A353V] iPSCs c4, c7, and c12 were cultured for several passages (p58, p46, and p45, respectively) in feeder-free platform in order to assess the ability of these cells to be maintained in long-term culture. The clones were capable of maintaining characteristics of pluripotent cells, as ESC-like morphology, and ability to remain in the undifferentiated state (Figure 4.18), which indicates self-renewal capacity. One of the clones (c4) is still been maintained in culture in the same conditions, currently at passage 140. Colonies of this clone

at passages 95 and 125 are shown in Figure 4.19 at different magnifications. This clone was positively stained for alkaline phosphatase, a cell surface marker that characterizes undifferentiated ESCs. The clone was tested at passage 111 (Figure 4.20).

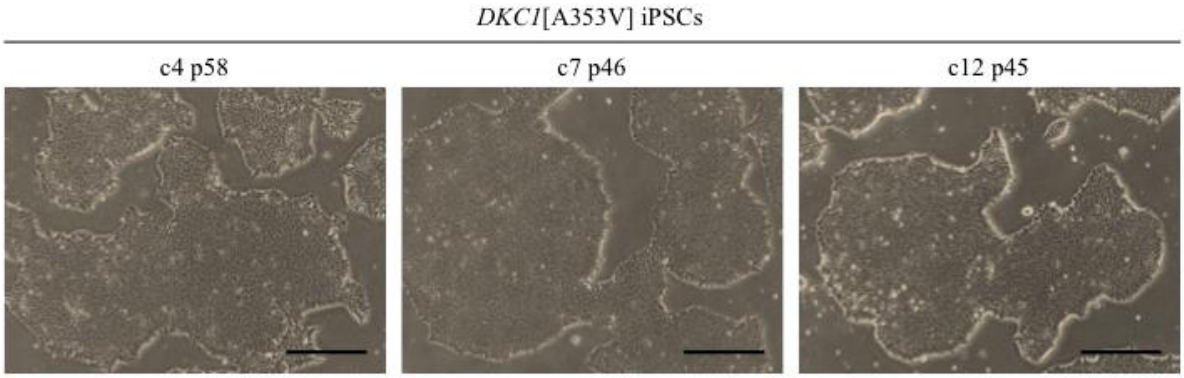

Figure 4.18 – *DKC1*[A353V] iPSC clones in long-term culture. iPSC clones (c) 4, 7, and 12 cultured for several passages (p) in feeder-independent conditions. Colonies of iPSCs displayed hESC-like morphology and absence of differentiated cells even at high confluences. Scale bars = 500 µm.

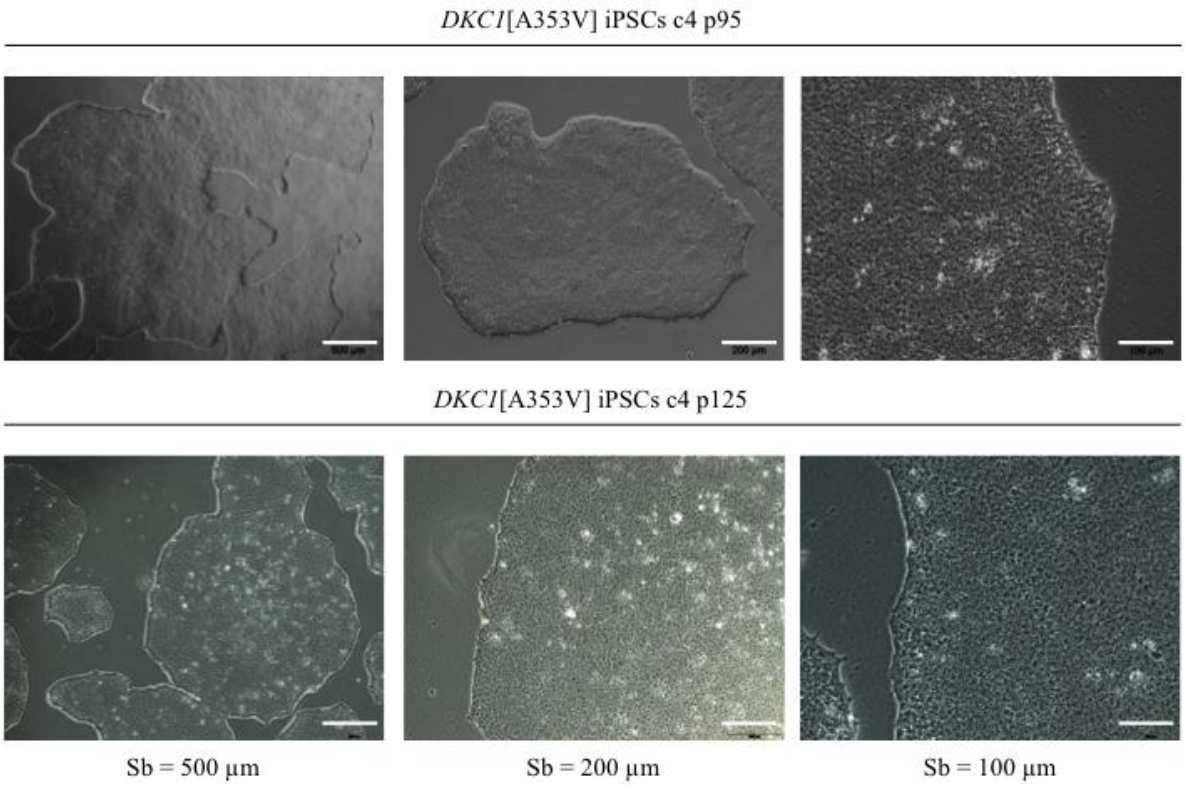

Figure 4.19 – *DKC1*[A353V] iPSC clone 4 at passages 95 and 125 at different magnifications. Colonies exhibited hESC morphology and no sign of differentiated cells. Sb = scale bar.

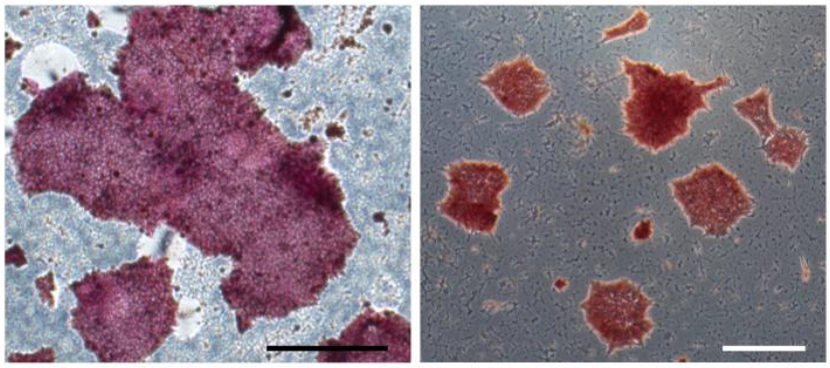

Figure 4.20 – *DKC1*[A353V] iPSC clone 4 at passages 111 stained for alkaline phosphatase. The colonies stained positive for the cell surface marker of undifferentiated ESCs. Black scale bar = 500 µm; white scale bar = 200 µm.

4.4. Dynamics of telomere length and telomerase activity in *DKC1*[A353V] iPSC clones

4.4.1. Telomere length is stabilized in *DKC1*[A353V] iPSC clones

Telomere length was determined using quantitative PCR. Serial samples of *DKC1*[A353V] iPSCs were collected and the telomere length was measured at different time points between passages 4 to 42. DNA integrity is crucial for accurate telomere measurements using qPCR. Samples analyzed did not show signs of degradation (Figure 4.21).

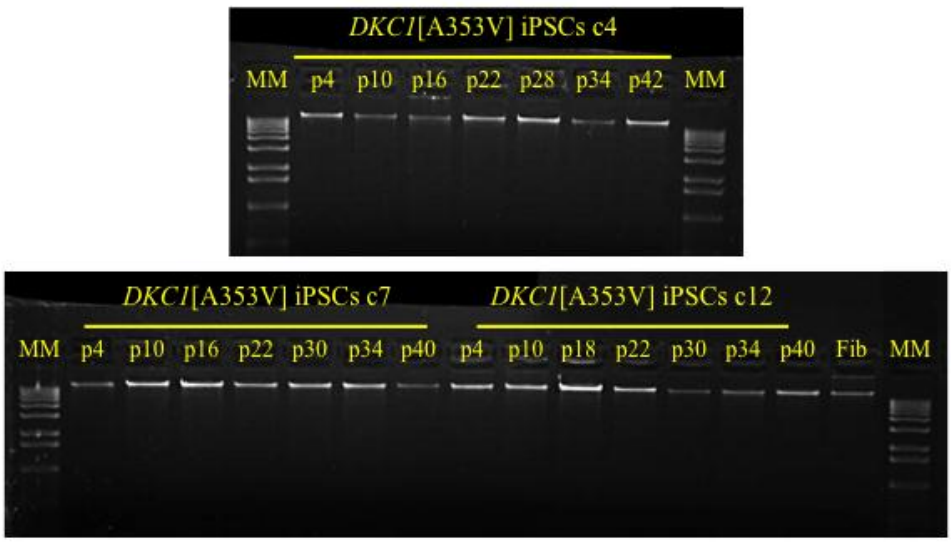

Figure 4.21 – Integrity of DNA samples checked through agarose gel electrophoresis. Aliquots of 50 ng DNA extracted from *DKC1*[A353V] iPSC clones 4, 7, and 12 at specific passages (p), as well as *DKC1*[A353V] fibroblasts (Fib) were loaded in an agarose gel. No smear was detected, which

confirmed the integrity of the DNA samples. MM: molecular marker.

Compared to parental fibroblast (time point 0) telomeres shortened during the first passages. However, starting around passage 20, when epigenetic remodeling is usually completed, telomere length plateaued. Telomere length displayed variation at lower levels and did not significantly changed upon prolonged culture (Figure 4.22). Clone 12 exhibited modest telomere elongation in the last two passages. In contrast to Batista *et al*. (2011), the shortening of telomeres was not associated with increased differentiation or decreased proliferation in later passages. Clone 4 was maintained in culture for 140 passages without obvious signs of losing its self-renewal or differentiation capacity.

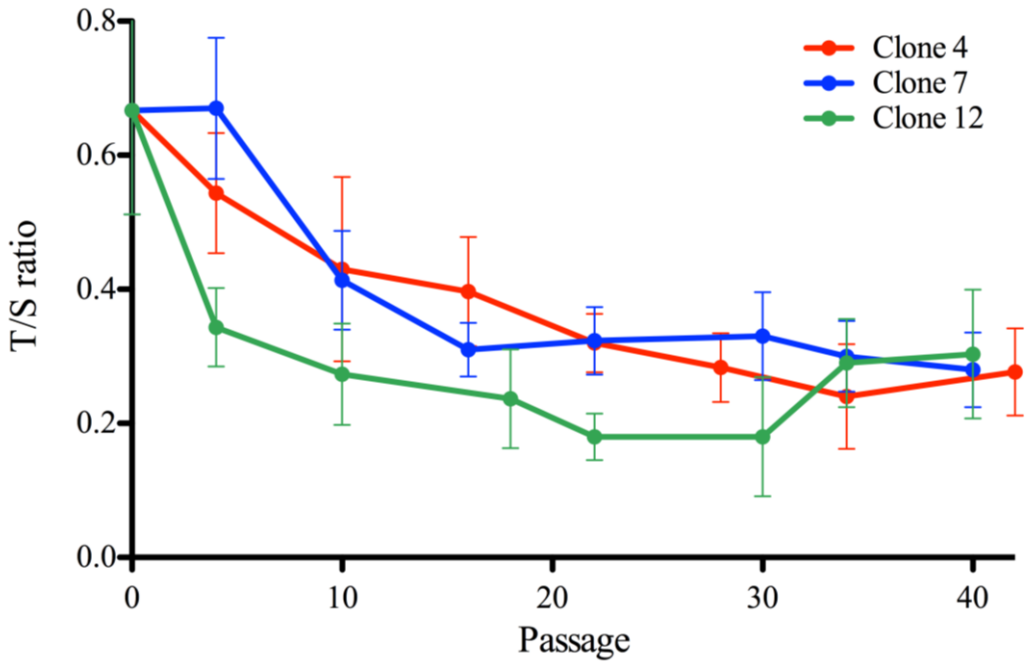

Figure 4.22 – Quantitative PCR for telomere length in *DKC1*[A353V] iPSC clones. Telomere lengths represented as a T/S ratio. Telomere shortening was observed in iPSCs during the first passages compared to parental fibroblasts (time point 0). Telomere length stabilized (c4 and c7) or slightly elongated (c12) at later passages.

To confirm the qPCR results, Southern blot analysis for telomere length was performed in seven selected samples previously analyzed by qPCR. Samples with either very high or very low T/S ratios of each clone were chosen because of potential inaccurate measurement of telomere length. The samples selected were: c4 p34, c7 p10, c7 p40, c12 p10, c12 p22, and c12 p30, and the parental fibroblasts (Figure 4.23). TRF lengths analyzed by Southern blot

were (in kilobases): c4 p34 = 3.9, c7 p10 = 6.1, c7 p40 = 5.6, c12 p10 = 5.2, c12 p22 = 3.8, c12 p30 = 3.8, and Fib p7 = 11.7.

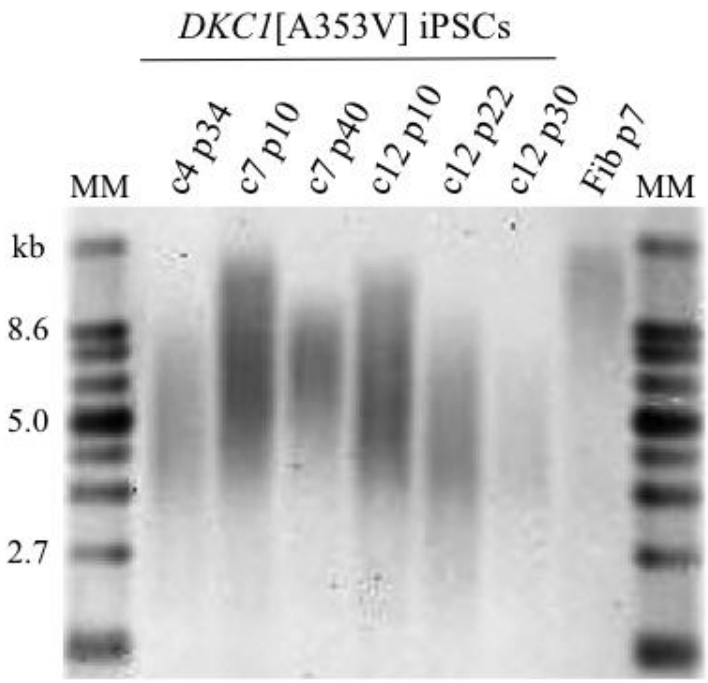

Figure 4.23 – Southern hybridization for telomere length in *DKC1*[A353V] iPSC clones and parental fibroblasts. Telomere lengths by Southern blot using genomic DNA from *DKC1*[A353V] fibroblasts (Fib p7) and iPSC clones 4, 7, and 12 at indicated passages (p). MM: molecular marker; kb: kilobases.

A strong positive linear relationship was found between qPCR and Southern blot measurements. The linear regression correlation coefficient (r^2 value) was 0.95 (Figure 4.24).

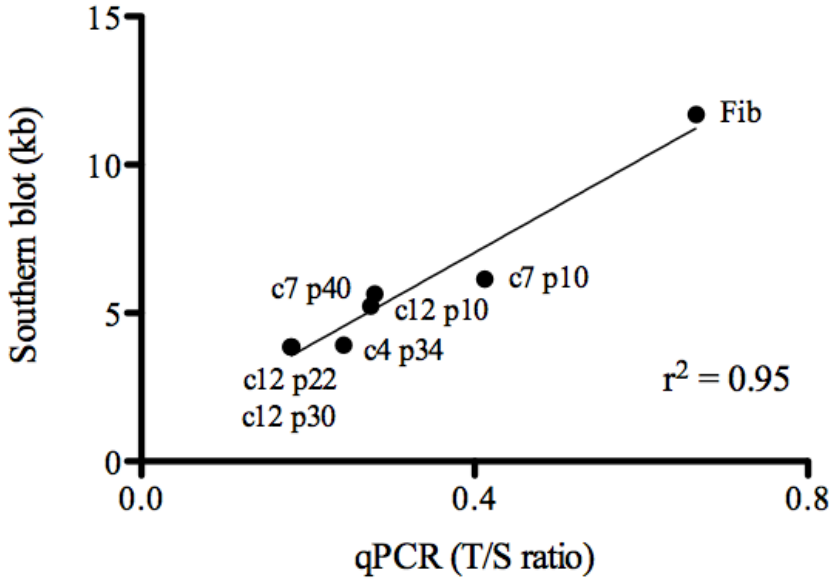

Figure 4.24 – Correlation between qPCR and Southern blot results. Linear regression was applied in telomere length results from qPCR (given as T/S ratio) and Southern blot (kilobases) from seven samples. Correlation coefficient (r^2 value) was 0.95.

4.4.2. *DKC1*[A353V] iPSC clones display telomerase activity

Telomerase activity in the iPSC clones was determined by the TRAP assay at early, late, and very late passages (Figure 4.25). The telomerase activity of the *DKC1*[A353V] iPSC c4 was assessed at p9, p16, p26, p34, p67, p81, p102, and p116 (Figure 4.25-A). Clone 7 was analyzed at p9, p10, p16, p22, and p34 (Figure 4.25-B), and the c12 was analyzed at p8, p10, and p30 (Figure 4.25-C). The telomerase activities of the parental fibroblasts and H1 hESCs (positive control) were also measured. The activity was normalized to HeLa cells. Expectedly, fibroblasts showed almost undetectable telomerase activity, whereas high activity was measured in H1. Telomerase is reactivated in the induction of pluripotency and is the major mechanism responsible for elongating telomeres in iPSCs. The *DKC1*[A353V] iPSC clones reestablished telomerase activity following the reprograming, though variation was observed. However, higher activity was observed at time points with telomere stabilization or elongation, apparently at later passages.

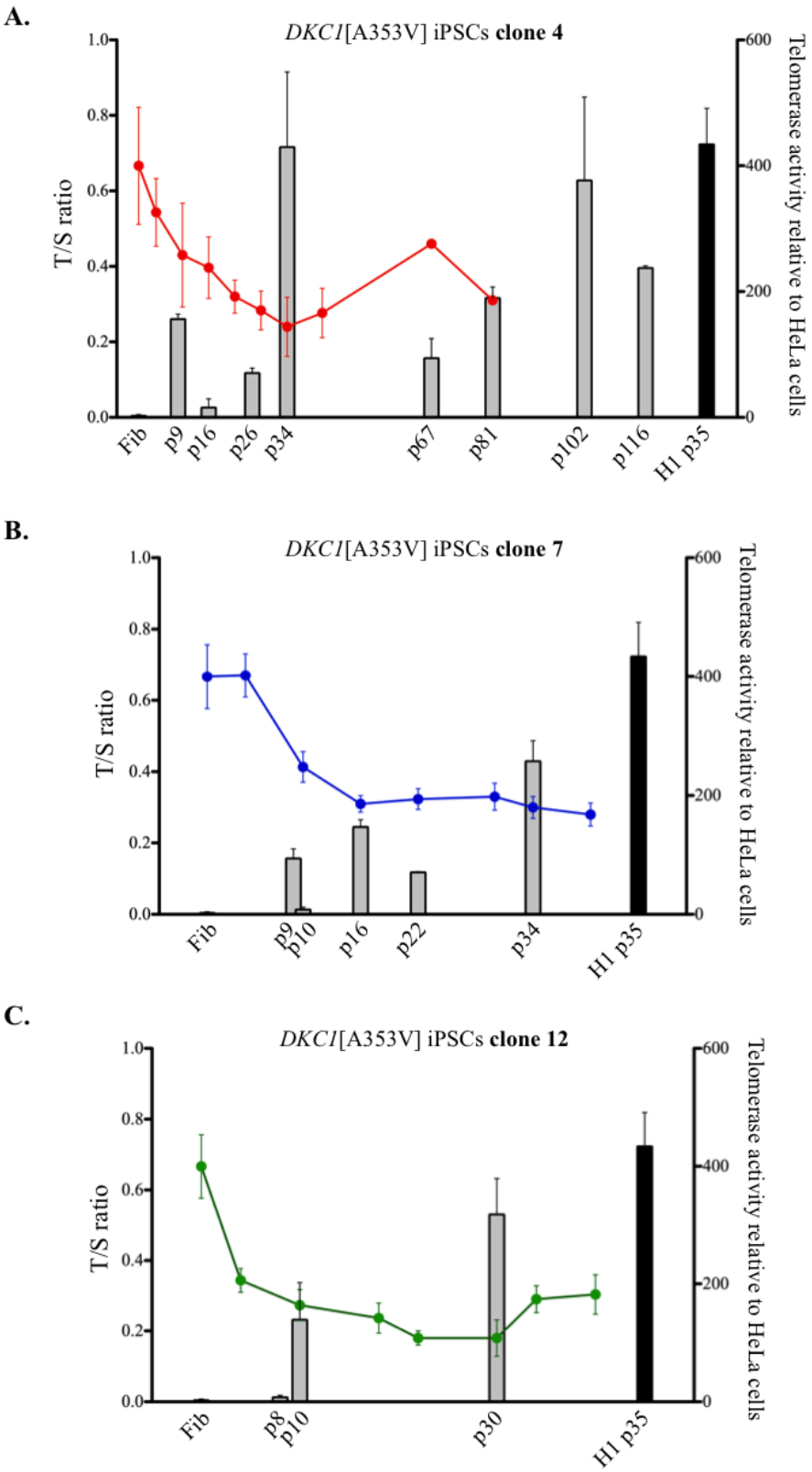

Figure 4.25 – Dynamics of telomerase activity and telomere length in the *DKC1*[A353V] iPSC clones 4, 7, and 12 maintained in long-term culture. The telomerase activity of iPSCs (grey bars) and H1 hESCs (black bars) was measured and normalized to the activity of HeLa cells. Data represent the average and standard deviation (SD) of two independent experiments. Telomere length previously measured by qPCR (T/S ratio) was plotted along with telomerase activity. Each dot (connected with colored lines) represents the average and SD of three independent qPCR assays, at a specific passage of: (**A**) clone 4, red line; (**B**) clone 7, blue line; (**C**) clone 12, green line. Passage 0 represents the measurement of parental fibroblasts (p7) immediately before reprogramming.

4.4.3. *DKC1*[A353V] iPSC clones restore *TERT*, *TERC*, and *DKC1* expression

Expression of telomerase complex members *TERT*, *TERC*, and *DKC1* was investigated by RT-qPCR in *DKC1*-deficient iPSCs to investigate potential compensatory mechanisms for telomere maintenance in these cells. Firstly, the quality of the RNA samples was analyzed using the Bioanalyzer, which generates an RNA Integrity Number (RIN) ranging from degraded (RIN = 2) to intact (RIN = 10). RIN values were greater than 9.2 (Figure 4.26).

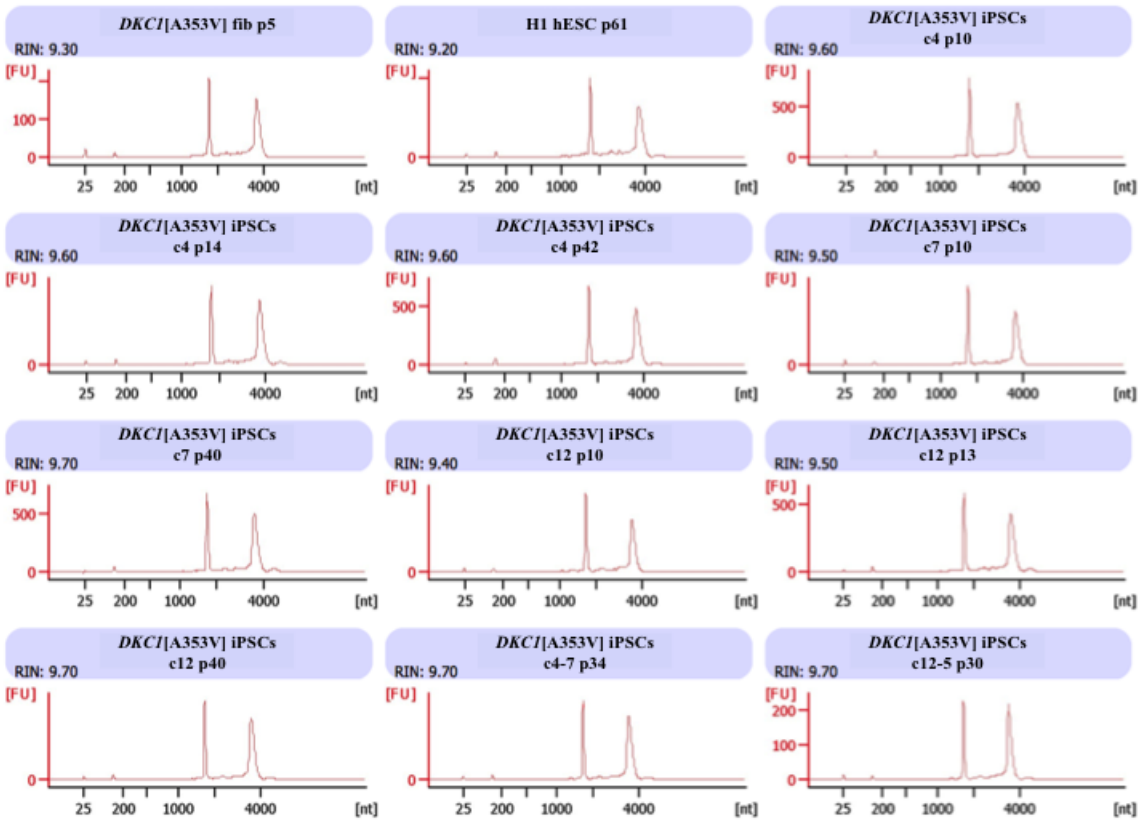

Figure 4.26 – Evaluation of the integrity of RNA samples from *DKC1*[A353V] iPSC clones prior to RT-qPCR. The graphs represent electropherograms for each RNA sample analyzed. The two peaks represent the 18S and 28S subunits of ribosomal RNA. The software generates an RNA Integrity Number (RIN) for each sample. RNA samples displaying RIN ≥ 7 are considered integrate.

Expression levels of *TERT*, *TERC*, and *DKC1* in *DKC1*[A353V] iPSC clones were normalized to H1 (Figure 4.27). All iPSC clones had marked increases in the mRNA expression levels of the three genes compared to parental fibroblasts. The *TERT* expression levels were undetectable in the parental fibroblasts, and reestablished after reprogramming, achieving, on average, 60% of the expression levels observed in H1. *TERT* expression varied

between clones and passages (coefficient of variance [CV] of 48%). iPSC c4 and c12 displayed a two-fold increase in *TERT* expression at late passages (c4 p42, c12 p40) compared to early passages (c4 p10, c12 p10). Clone 7 did not display differences between p10 and p40. The cre-excised clone 12-5 at p30 displayed *TERT* level similar to H1. *TERC* expression was fairly stable among different clones and passages (CV = 17%). Relative to parental fibroblasts, *TERC* levels increased four-fold in the reprogrammed cells, but the expression levels were still lower than the level observed in H1 (on average, 42% of the *TERC* level in H1). *DKC1* expression was increased between three to seven-fold in the reprogrammed cells compared to the parental fibroblasts. Compared to H1, *DKC1*[A353V] iPSCs exhibit an up to three-fold increase of *DKC1* expression (c7 p40). Variation was observed between clones and passages (CV = 31%).

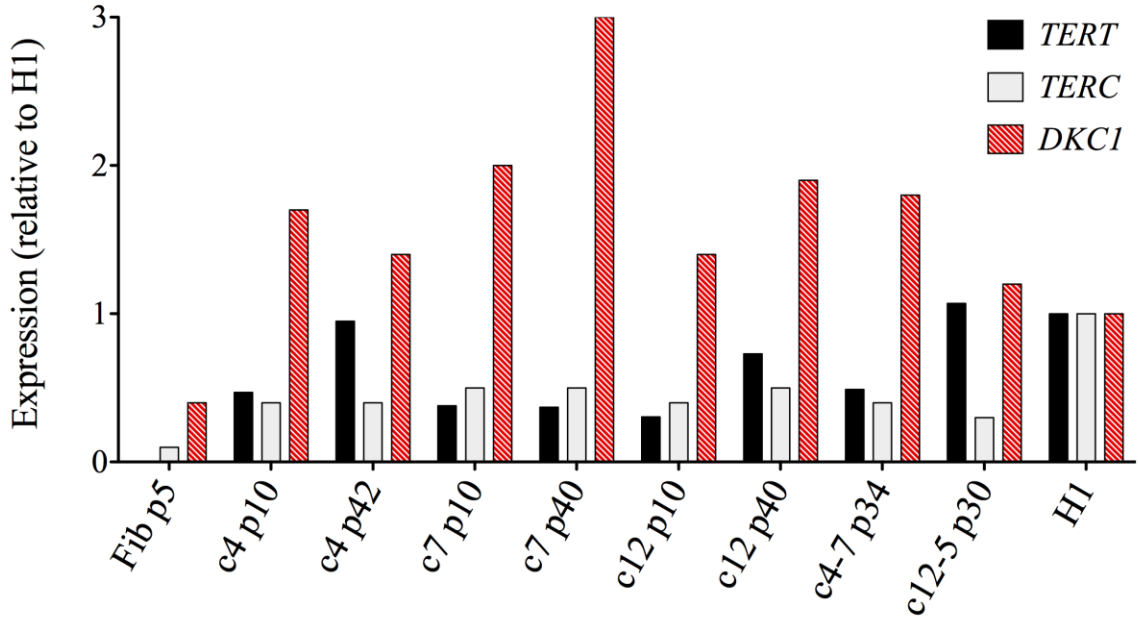

Figure 4.27 – Expression levels of *TERT*, *TERC*, and *DKC1* in *DKC1*[A353V] iPSC clones. The expression levels were assessed by RT-qPCR at different passages (p) in the clones (c) 4, 7, and 12, in the transgene-free clones 4-7 and 12-5, and in the parental fibroblasts (Fib). Expression levels were normalized to *GAPDH* and results shown are normalized to H1 hESCs.

4.5. Absence of copy number variations in the *DKC1*[A353V] iPSC clones maintained in long-term culture

Prolonged *in vitro* culture of ESCs and iPSCs can result in chromosomal abnormalities that may confer a selective advantage and influence telomere maintenance (Winkler *et al*., 2013; Hong *et al*., 2014). To exclude potential chromosomal alterations in the *DKC1*[A353V] iPSC clones, next generation cytogenetics was performed using the Affymetrix CytoScan HD Arrays. The three *DKC1*[A353V] clones were analyzed in long-term culture (c4 p42, c7 p34, and c12 p40). The Figure 4.28 exemplifies results showing the chromosome 11 of the three clones. No gain or loss of DNA copy number variants was observed in the genome of the clones compared to the Database of Genomic Variants for the human population. However, a deletion of 3 exons (17 to 19) of the *DLG2* gene (chromosome 11), was detected in c7 p34 after adjusting the filter of copy number variants for >200 kbp (Figure 4.28-B). This filter is more restrictive, and is not applied in regular analysis for pathological lesions according to previous studies. Since this deletion was observed in clone 7, the transgene-free version of the clone (c7-4) was excluded of hematopoietic differentiation experiments, as it was not clear whether this alteration could play a role in the differentiation.

A.

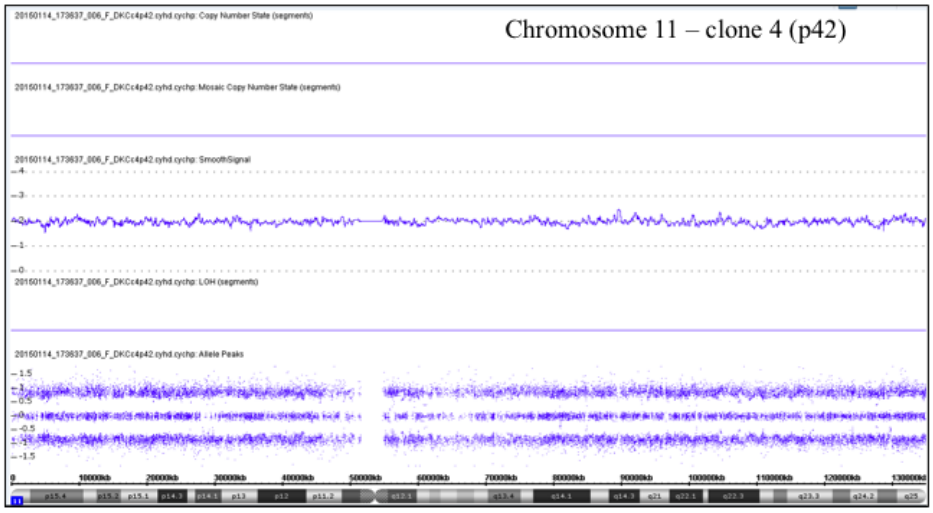

B.

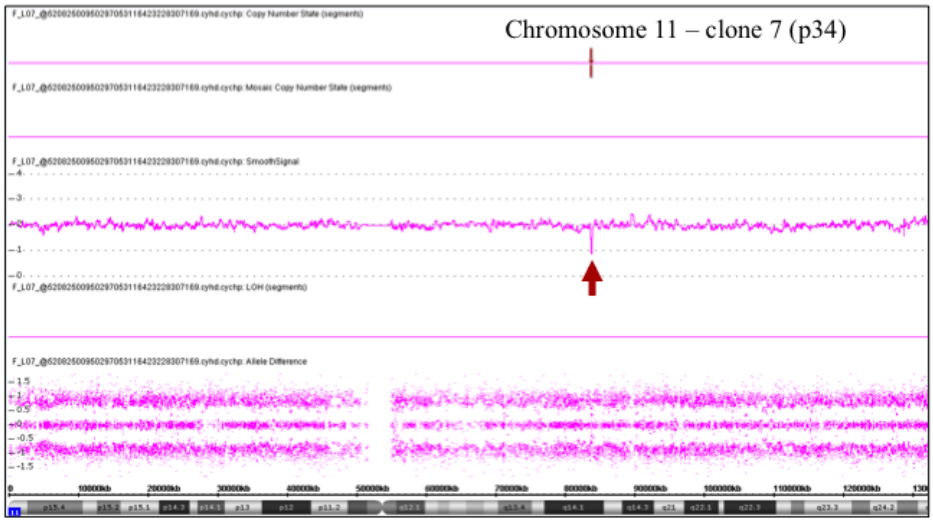

C.

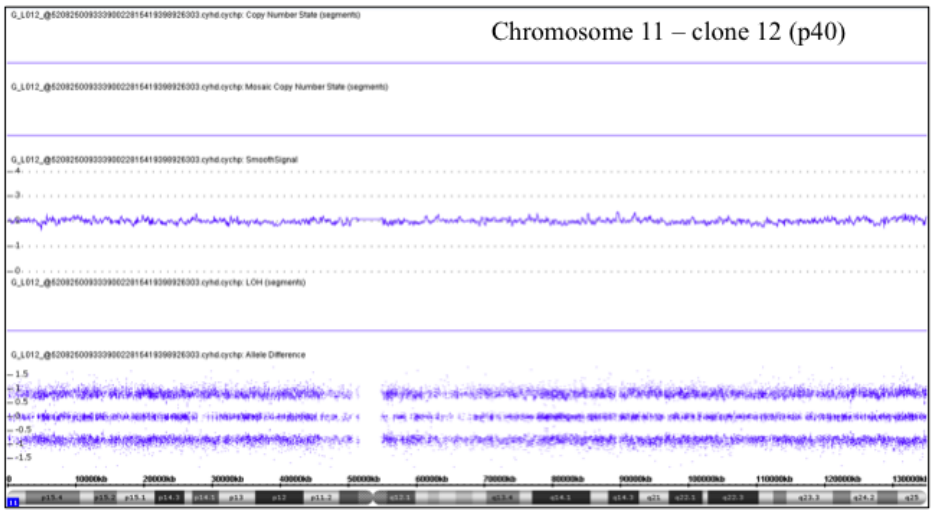

Figure 4.28 – SNP array analysis on *DKC1*[A353V] iPSC clones. Example of screening for copy number variants of chromosome 11 in *DKC1*[A353V] iPSCs (**A**) clone 4, (**B**) clone 7 with a deleted region indicated by the red arrow, and (**C**) clone 12. Clones 4 and 12 did not display copy number variants.

4.6. Absence of alternative lengthening of telomeres in the *DKC1*[A353V] iPSC clones

4.6.1. DNA C-circles are absent in the *DKC1*[A353V] iPSC clones

Due to the unexpected pattern of telomere length stabilization in the *DKC1*[A353V] iPSC clones, two approaches were applied to investigate Alternative Lengthening of Telomeres (ALT): DNA C-circles and ALT-associated promyelocytic leukemia bodies (APBs). The accumulation of DNA C-circles represents a quantifiable marker for ALT activity. The *DKC1*[A353V] iPSC c4, c7, and c12 were assessed at different passages, according to T/S values observed in the qPCR results for telomere length (Figure 4.22). Passages were selected for each clone in moments of supposed telomere shortening (c4 p18; c7 p34, p42; c12 p10), or telomere stabilization (c4 p54; c7 p22; c12 p40). In addition, the parental fibroblasts, one control iPSC line, and one cre-excised clone (c4-7 at p24) were analyzed. No accumulation of DNA C-circles was detected in the samples evaluated (Figure 4.29).

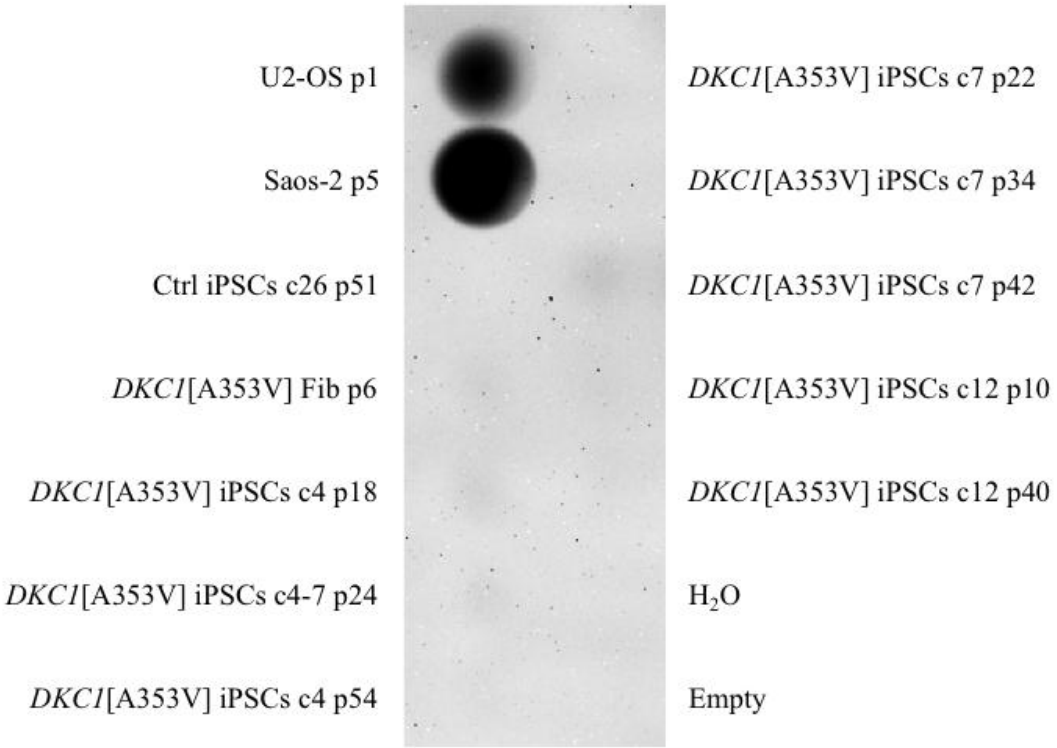

Figure 4.29 – Absence of DNA C-circles in *DKC1*[A353V] iPSC clones. Dot blot of C-circle assay performed on genomic DNA from *DKC1*[A353V] fibroblasts (Fib p6) and iPSC clones 4, 7, and 12 at indicated passages (p), as well as iPSCs from control (Ctrl iPSC clone 26). The transgene-free clone 4-7 at p24 was also evaluated. Genomic DNA from the ALT-positive cell lines U2-OS and Saos-2 was used as positive control.

4.6.2. No co-localization of PML protein and telomeres in the *DKC1*[A353V] iPSC clones

The APB assay was carried out in order to check whether the PML proteins (the putative platforms for homologous recombination of telomeres) were co-localizing with telomeric DNA in the cellular nuclei. The assay was performed on *DKC1*-mutant iPSC clones at different passages. Clone 4 was investigated in one early and one very late passage (p11 and p124, respectively). Clone 7 was investigated at p13. Clone 12 was investigated in an early passage (p15), and in a late passage of its transgene-free version (c12-5 at p34). The parental fibroblasts, the iPSCs control (c26 p53), and H1 hESCs were also investigated for APBs. No co-localization was observed in the *DKC1*-mutant iPSCs either in early passages (c4 p11, c7 p13, c12 p15) or after long-term culture (c4 p124). Fibroblasts, transgene-free c12-5, iPSCs control, and H1 hESCs were all negative for APBs. VA13 cell line was set as positive control (Figure 4.30).

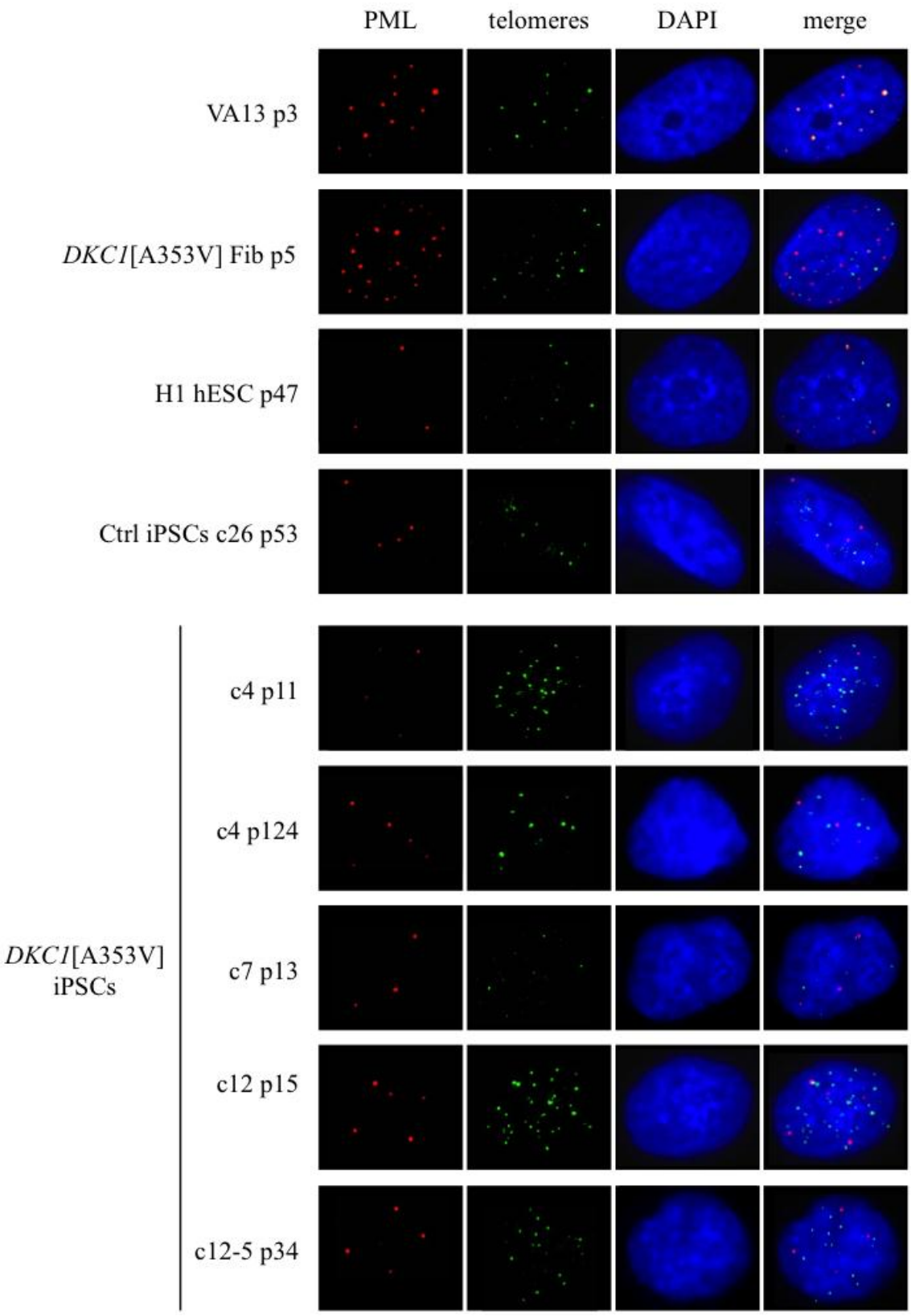

Figure 4.30 – PML bodies did not co-localize with telomeres in *DKC1*[A353V] iPSC clones. Immunofluorescence of *DKC1*[A353V] fibroblasts (Fib p5) and iPSC clones 4, 7, and 12 at indicated passages (p), as well as iPSCs from control (Ctrl iPSC clone 26), and H1 hESCs. The transgene-free clone 12-5 was also evaluated. PML bodies were stained with anti-PML antibody (red) and telomeres were labeled with FITC-conjugated PNA probe (green). Interphase nuclei were counterstained with DAPI (blue). Co-localization of PML bodies and telomeres was detected only in VA13 cells (positive control).

4.7. Increased capacity of generating hematopoietic progenitors in the *DKC1*[A353V] iPSC clones

Bone marrow failure is a hallmark of DC phenotype. Thus, Hematopoietic Stem Cell (HSC) differentiation was carried out in the *DKC1*-mutant clones in an attempt to assess the capacity of these pluripotent cells in generating hematopoietic progenitors. The differentiation was performed on *DKC1*[A353V] c4-7 at p28 and c12-5 at p29, as well as on H1 hESCs and iPSC controls (c26 p47, c26-3 p56, and iPSCs c7 p16: a PBMCs derived control line). The HSC formation was induced by exposing the PSCs-derived EBs to hematopoietic cytokines over a period of 13 days. Then, the EBs were dissociated, and single cells were seeded on methylcellulose, a semi-solid culture medium containing a cytokine cocktail that favors the differentiation of hematopoietic progenitors toward myeloid lineages (including erythroid and megakaryocyte progenitors). After 14 days of culture in the methylcellulose, the hematopoietic colony-forming units (CFUs) were identified and counted. Although no difference was observed between control and *DKC1*-mutant iPSCs in the formation and morphology of EBs during differentiation (Figure 4.31), an increased capacity on generating hematopoietic progenitors in the *DKC1*-mutant iPSCs (c4-7 p28, c12-5 p29) was observed, as demonstrated by the number of CFUs (Figure 4.32). Moreover, the colonies were bigger in these *DKC1*-mutant iPSCs in comparison to the CFUs generated from iPSCs controls (Figure 4.33-A). The cytological analysis of CFUs from *DKC1*-mutant clone 4-7 confirmed the generation of hematopoietic lineages (Figure 4.33-B).

In order to test whether later passages could exhibit different patterns of HSC generation, the c12-5 at p35, and the clone 4 maintained in long-term culture (p114) were differentiated. The differentiation capacity was reduced in c12-5 in the later passage when compared to c12-5 at p29 (Figure 4.32). The c4 at p114 indicated differentiation capacity even for a *DKC1*-mutant iPSC line in very late passage. However, reduction in the differentiation capacity of this clone was observed when compared to earlier passages (c4-7 p28, and c12-5 p29, p35; Figure 4.32). These findings indicate that the *DKC1*-mutant iPSC clones exhibited a superior HSC differentiation capacity in earlier passages compared to late passages. Moreover, the *DKC1*-mutant clones at early passages displayed increased ability to generate hematopoietic progenitors compared to the PSCs controls differentiated in the assays.

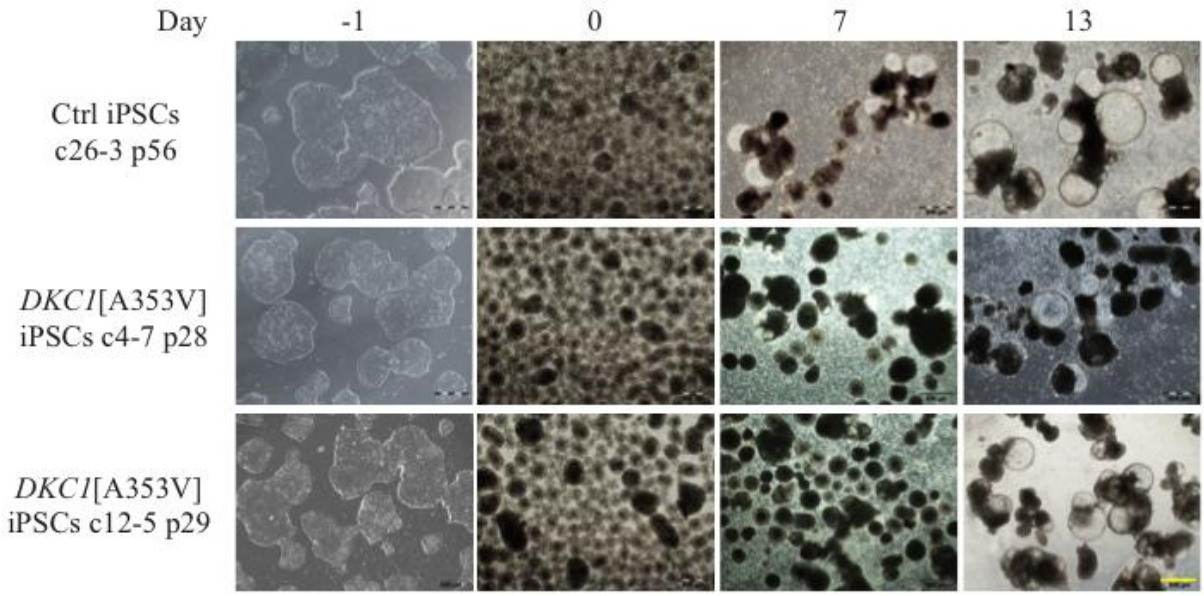

Figure 4.31 – Morphological changes during the hematopoietic differentiation process of the *DKC1*-mutant and control iPSCs. The iPSCs (control and *DKC1*-mutants) were shown during the differentiation process, from iPSCs colonies in the undifferentiated state (on day –1), EBs on day 0, to differentiated EBs with cystic structures on days 7 and 13. Both iPSCs mutants and control exhibited no morphological differences that could be detected under the inverted microscope during the differentiation. Scale bar = 500 μm.

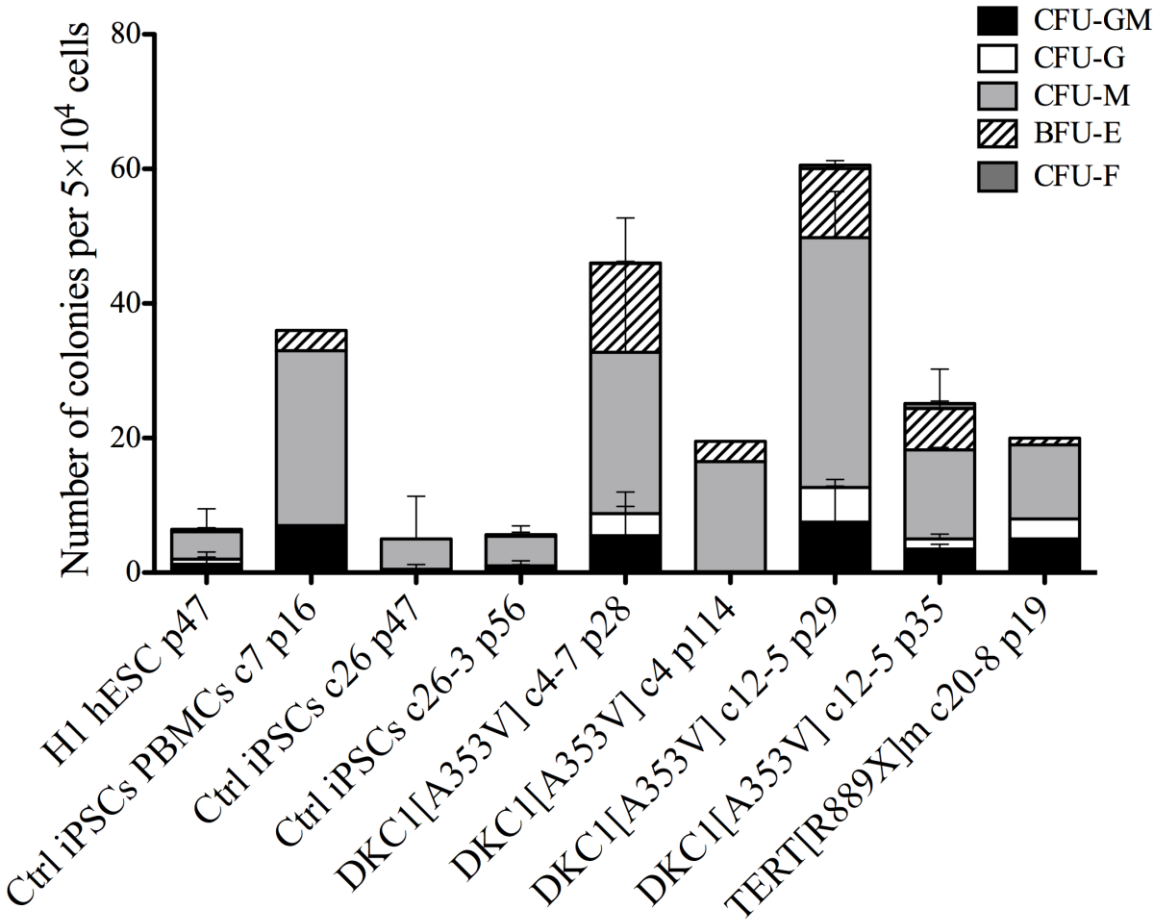

Figure 4.32 – Colony-forming units (CFU) counts from control and mutant iPSCs after hematopoietic stem cell differentiation. Qualitative and quantitative analysis of hematopoietic colonies derived from controls (H1 hESC, iPSCs generated from peripheral blood mononuclear cells [PBMCs], and from fibroblasts [c26 and c26-3]) as well as clones (c) of *DKC1*- and *TERT*-mutant iPSCs at distinct passages (p). CFU analysis showed elevated capacity of *DKC1*-mutant iPSCs in generating myeloid lineages (c4-7 p28 and c12-5 p29). Counts represent average of two independent experiments. CFU-GM, CFU-granulocyte, macrophage; CFU-G, CFU-granulocyte; CFU-M, CFU-macrophage; BFU-E, burst forming unit erythroid; CFU-F, CFU-fibroblast. Colonies of the types CFU-E (CFU-erythroid), and CFU-GEMM (CFU-granulocyte, erythrocyte, monocyte, megakaryocyte) were not observed in the assays.

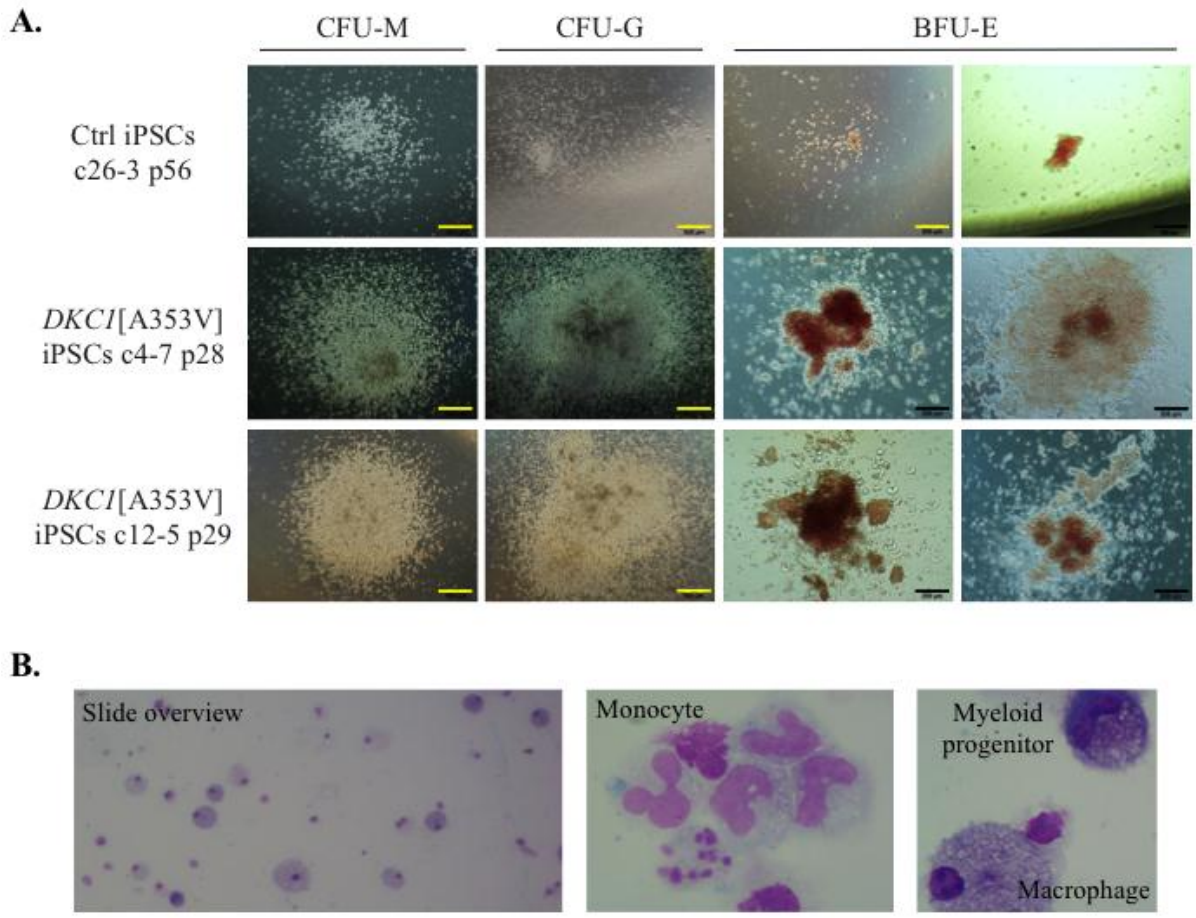

Figure 4.33 – Morphology of hematopoietic cells and colonies from *DKC1*-mutant iPSCs induced to hematopoietic stem cell differentiation. (**A**) Morphology of CFUs generated from iPSCs control and *DKC1*-mutant clones 4-7 and 12-5, visualized under stereomicroscope. CFU-G, CFU-granulocyte; CFU-M, CFU-macrophage; BFU-E, burst forming unit erythroid. Scale bars: yellow = 500 µm, black = 200 µm. (**B**) Cytological analysis of CFUs from HSC differentiation of *DKC1*[A353V] iPSCs c4-7 after cytospin and Wright's staining.

5. DISCUSSION

5. Discussion

In the present study, skin fibroblasts from a DC patient carrying a *DKC1* A353V gene mutation were successfully reprogramed into the pluripotent state. Telomere dynamics was investigated during passaging and telomere erosion was detected in the first passages after reprogramming; telomere length stabilization was achieved after passage 20. Telomerase activity was detected after reprogramming, especially at late passages. Hematopoietic differentiation was carried out in two *DKC1*-mutant iPSC clones, displaying increased capacity to generate hematopoietic lineages.

For adequate use of iPSCs to model disease, careful characterization is required to ensure the two properties that make iPSCs similar to ESCs: pluripotency and self-renewal. Carpenter *et al*. (2003) reviewed the data available for 26 hESC lines derived from multiple laboratories and demonstrated that these cell lines shared common features, including similar morphology (cells grew as tightly compacted colonies), similar expression profiles of surface markers (SSEA4, TRA-1-60, and TRA-1-81), and pluripotency markers (OCT4), as well as high levels of telomerase expression. Other defining feature of the hESC lines highlighted by the authors was the ability to differentiate into derivatives of all three germ lineages both *in vivo* (generation of teratomas when inoculated in immunodeficient mice) and *in vitro* (formation of EBs). Thus, iPSCs must fulfill the same criteria required for ESC characterization (reviewed by Asprer and Lakshmipathy, 2015):

- Morphology, must resemble hESCs (Takahashi *et al*., 2007);
- Expression of self-renewal and pluripotency markers (Adewumi *et al*., 2007), along with ability to differentiate into the three germ lineages (Itskovitz-Eldor *et al*., 2000; Muller *et al*., 2010): together, these features ensure the functional pluripotency of the iPSCs;
- Normal karyotype: genetic abnormalities may have been acquired during reprogramming, which may lead to alterations in cell behavior (Martins-Taylor *et al*., 2011; Mayshar *et al*., 2010).

The three *DKC1*-mutant iPSC clones generated in the present study fulfilled all the criteria described above. The iPSCs resembled ESCs since the arising of the colonies in the reprogramming experiment (Figure 4.7). The three iPSC clones selected for expansion maintained this morphology even after several rounds of cell passaging (Figure 4.18). Clone 4, maintained in long-term culture, not only kept morphology (Figure 4.19), but also stained

positive for alkaline phosphatase (Figure 4.20), a cell surface marker that characterizes undifferentiated ESCs (Thomson *et al*., 1998). All the three *DKC1*-mutant iPSC clones stained positive for pluripotency markers before (c4, c7, c12, Figure 4.9) and after transgene removal (c4-7, c7-4, c12-5, Figure 4.12).

In vitro differentiation of the transgene-free clones 4-7, 7-4, and 12-5 was performed. All three clones formed EBs that expressed differentiation markers similarly to EBs derived from H1 ESCs. *In vivo* differentiation (teratoma assay) of the transgene-free clones 4-7 and 12-5 was performed, and a tumor resembling teratoma was collected from one mouse inoculated with cells from the clone 4-7, whereas the two mice inoculated with the clone 12-5 developed cystic teratomas. Unfortunately, at the time of sending this thesis to press, the histopathological analysis was not fully completed and the results could not be added as part of the thesis. However, the EB formation assay was sufficient to demonstrate the ability of the three clones to differentiate into the endoderm, mesoderm, and ectoderm lineages.

No chromosomal abnormality was observed during reprogramming of the three clones, as demonstrated by standard G-banding technique (Figure 4.16). Several studies have described the acquisition of copy number variations in iPSCs due to time in culture, or even during reprogramming (Hussein *et al*., 2011; Laurent *et al*., 2011; Martins-Taylor *et al*., 2011). No copy number variation, deletions, or insertions were detected in clones 4, 7, and 12 at late passages in the present study (Figure 4.28).

The results presented here are sufficient to conclude that the *DKC1*-mutant fibroblasts derived from a DC patient were successfully reprogrammed to the pluripotent state, retained the mutation from the parental cells, and did not acquire cytogenetic alterations or copy number variations due to the reprogramming process or the time in culture.

Induced PSCs are not a stable and homogeneous clonal population in culture, and factors as culture conditions or stochastic events may yield variation in the experimental results. Winkler *et al*. (2013) derived multiple clones from each starting patient sample, and observed significant heterogeneity in telomere dynamics among individual iPSC clones derived from the same patient, as well as among clones from different patients with identical mutations. Particularly, the acquisition of a chromosomal abnormality was detected in one clone displaying major discrepancies. In agreement with these findings, Mills *et al*. (2013) derived and analyzed three independent iPSC clones from fibroblasts of three different normal subjects. The authors performed gene expression profiling and hematopoietic differentiation assays and found that clones from the same subject were generally more similar among them

than clones from different subjects. However, one clone displayed different proliferation rates and hematopoietic potential compared to other clones from the same individual. The differences were associated with the acquisition of several copy number variations (CNVs) during reprogramming. Together, these findings emphasize the risk of relying on single mutant clones and single control clones in any assay that uses iPSCs (Chang *et al*., 2008; Jung *et al*., 2015). In the present study, three independent *DKC1*-mutant clones (4, 7, and 12) were used for telomere dynamics experiments, and two clones (4-7 and 12-5) were used for hematopoietic differentiation. The reprogramming transgenes did not influence the expression of telomerase genes (Winkler *et al*. 2013), thus clones before transgene removal were used in telomere and telomerase dynamics experiments. Since there is no evidence that transgenes do not influence hematopoietic differentiation, this assay also was performed with the transgene-free clones. Clone 7-4 was excluded of differentiation experiments, since a deletion of 3 exons in the *DLG2* gene was detected in the clone 7, from which clone 7-4 was derived (Figure 4.28).

The *DKC1* A353V gene mutation, carried by the patient studied, is the most common lesion found in humans with X-linked DC (approximately 40% of cases and often as a *de novo* mutation) (Knight *et al*., 1999; Vulliamy *et al*., 2006) – Figure 4.2. It represents an example of a CpG > TpG change that is known to occur at high frequency as a result of the deamination of the methylated cytosine (Knight *et al*., 1999). The A353V substitution is responsible for affecting the dyskerin region localized in the PUA RNA-binding domain, the putative site for interaction with TERC. In mouse ESCs carrying the same lesion in *Dkc1*, cells display severe destabilization of mTerc, reduction in telomerase activity, and significant continuous telomere loss in *in vitro* cell culture (Mochizuki *et al*., 2004). Conversely, the *DKC1*-mutant iPSCs derived in the present study (also referred as *DKC1*[A353V] iPSCs) exhibited telomere length stability and telomerase activity similar to levels detected in H1 hESCs, especially at late passages.

Three other groups have reprogrammed *DKC1*-mutant iPSCs (Agarwal *et al*., 2010; Batista *et al*., 2011; Gu *et al*., 2015). Different results were described in telomere dynamics and telomerase activity, even when the same mutation, or the same initial population of somatic cells was reprogrammed. Table 5.1 summarizes the main findings.

Table 5.1 – Overview of current studies describing reprogramming of *DKC1*-mutant fibroblasts.

	Agarwal *et al.* (2010)	**Batista *et al.* (2011)**	**Gu *et al.* (2015)**	**Donaires *et al.***
DKC1 mutations	• A386T • del37L*	• L54V • del37L*	• A353V • Q31E • del37L*	• A353V
Reprogramming method	Retroviruses of *Oct4*, *Sox2*, *Klf4*, and *c-myc*	• L54V: lentiviral (STEMCCA); hypoxia • del37L: retroviral; hypoxia	lentiviral (STEMCCA)	lentiviral (STEMCCA); normoxia
Reprogramming efficiency	0.002%	• L54V: 0.002% • del37L: 0.04%***	Not shown	0.01%
Telomere length of parental fibroblasts	Not clearly described	• L54V: bellow 1st percentile (PBMCs)** • del37L: not clearly described	• A353V: very short; bellow 1st percentile (PBMCs)** • Q31E: short; at 1st percentile (PBMCs)** • del37L: not shown	Bellow 10th percentile (PBMCs)**
Telomere length after reprogramming compared to parental fibroblasts	Shorter	Shorter	• A353V: significantly shorter • Q31E: similar • del37L: shorter	Shorter
Telomere length in the iPSCs achieved lengths of parental fibroblasts	Yes (around p20)	No	• A353V: no • Q31E: yes • del37L: no	No
Telomere maintenance of iPSCs over time	Elongation	Attrition	Not clearly described	Achieved a plateau
Long-term culture of iPSCs	Feasible	Impossible: iPSCs achieved senescence around p36	Not clearly described	Feasible (currently at p140)
Telomerase activity (TRAP assay) in the iPSCs	40% of wild-type iPSCs	5 to 15% of wild-type iPSCs	• A353V and del37L: 20% of wild-type iPSCs • Q31E: similar to wild-type iPSCs	• Clone 4: 4 to 100% of H1 • Clone 7: 1 to 60% of H1 • Clone 12: 1 to 74% of H1

* Same del37L fibroblasts; cells commercially available (GM01774, Coriell Cell Repository, Camden, NJ, USA);
** PBMCs: peripheral blood mononuclear cells; telomere measurements performed in patients peripheral blood at time of diagnosis. Patients' telomere lengths compared to curves of telomere length from healthy control subjects;
*** Fibroblasts were unable to be reprogrammed in normoxic condition (21% O_2).

Similar to the present study, Gu *et al*. (2015) reprogrammed fibroblasts carrying the *DKC1* A353V gene mutation using STEMCCA lentivirus. Reprogramming efficiency of their experiments was not provided. Here, reprogramming efficiency was 0.01%, five-fold higher than the efficiency described by Agarwal *et al*. (2010) and Batista *et al*. (2011). The reprogramming experiments were conducted in normoxic conditions, whereas Batista *et al*. (2011) were able to reprogram *DKC1*-muntat fibroblasts only in hypoxia. Low (5%) oxygen levels alter the intracellular redox state and enhance the generation of iPSCs (Yoshida *et al*., 2009). It promotes telomerase expression and telomere extension in human iPSCs, regardless of telomerase mutation status (Winkler *et al*., 2013).

In Agarwal's, Batista's, and Gu's studies, the same mutant fibroblasts (commercially available del37L fibroblasts) were reprogrammed. Telomere length of these fibroblasts was not provided. However, the three groups described telomere erosion during the first passages of iPSCs compared to parental fibroblasts. Telomere length of L54V fibroblasts (Batista *et al*., 2011) was short (below the first percentile), and derived iPSCs displayed telomere length even shorter. Q31E fibroblasts (Gu *et al*., 2015) displayed short telomeres (at the first percentile), and similar telomere length was observed in the Q31E iPSCs.

Telomere length of A353V fibroblasts in Gu's study was described as very short (below the first percentile), the shortest in comparison with telomeres of the other patients in the study. Telomere lengths of the derived iPSCs were significantly shorter than the parental fibroblasts; these cells displayed the most severe effect on telomere maintenance compared to the other derived iPSCs (Q31E and del37L). In the present study, fibroblasts carrying the same mutation displayed telomere length below the tenth percentile, which is short, though not critically short (below the first percentile). Although telomere erosion was observed in the first passages of iPSCs, telomere lengths stabilized at passage 20. Together, these findings suggest that reprogramming efficiency and telomere length of the derived iPSCs may be related to the telomere length of the fibroblasts prior to reprogramming. Fibroblasts that are wild-type for mutations in telomere pathways are efficiently reprogrammable even when telomeres are critically short, since reprogramming activates telomerase (Lapasset *et al*., 2011). However, reactivation of impaired telomerase in cells deficient for telomerase-related genes is unable to efficiently elongate telomeres, thus reflecting poor reprogramming efficiency. In murine cells, telomerase is reactivated approximately ten days after reprogramming is initiated (Stadtfeld *et al*. 2008). Thus, the reactivation of telomerase is a late event during reprogramming, which may explain the telomere attrition observed in the first passages of iPSCs in the four studies. The late activation of telomerase may not recover

telomere length in time when somatic cells display damaged telomeres along with dysfunctional telomerase, such as cells from DC patients.

Telomere maintenance of iPSCs over time was the most discrepant aspect of these studies. In Batista's work, telomeres of the *DKC1*-mutant iPSCs continued to shorten after several rounds of cell division leading to senescence. Conversely, Agarwal *et al*. observed that their reprogrammed cells overcame a critical limitation in TERC levels to restore telomere maintenance and self-renewal. Here, the three clones exhibited a pattern of telomere stabilization over time. Telomere length behavior in the clones was consistent with a possible late activation of telomere-maintenance mechanisms. Thus, the known mechanisms responsible for telomere maintenance were investigated: ALT and telomerase.

Henson *et al*. (2009) demonstrated that partially single-stranded telomeric $(CCCTAA)_n$ DNA circles (C-circles) represent specific markers for ALT activity, and developed an assay to measure these DNA circles. The assay was performed in the three iPSC clones at different passages, including the ones with apparent telomere shortening, or stabilization, in which the putative activation of ALT mechanisms might be responsible for this phenomenon in the absence of normal dyskerin. No DNA C-circles was detected (Figure 4.29). The localization of telomeres at the PML bodies (the so-called APBs) is another hallmark of ALT. PML bodies are the putative nuclear platforms for telomere recombination (Yeager *et al*., 1999). No APBs were detected when screening the three *DKC1*-mutant iPSC clones at different passages (Figure 4.30). The absence of both DNA C-circles and APBs suggests that the pattern of telomere length stabilization in the *DKC1*-mutant iPSC clones is likely ALT-independent and thus telomerase-mediated.

Human ESCs bypass telomere attrition and exhibit unlimited capacity of division by highly expressing telomerase (Thomson *et al*., 1998). Reprogramming stimulates *TERT* through direct or indirect action of both endogenous and exogenous *MYC* and *KLF4* transcription factors (Takahashi *et al*., 2007; Wu *et al*., 1999). The *TERC* promoter is a transcriptional target of *NANOG*, one of the genes overexpressed in the pluripotent state, which culminates in *TERC* up-regulation (Agarwal *et al*., 2010). Thus, telomerase appears to be the major mechanism responsible telomere elongation in the induction of pluripotency (Winkler *et al*. 2013), which extends telomeres to lengths that exceed the parental somatic cells (Agarwal *et al*., 2010; Batista *et al*., 2011). However, in *DKC1*-mutant iPSCs, this mechanism is unlikely, due to the intrinsic mutation in the dyskerin region responsible for TERC binding, resulting in destabilization of the telomerase holoenzyme, which is the molecular basis for disease development.

Telomerase activity was assessed in the three *DKC1*[A353V] iPSC clones along several passages. Generally, higher telomerase activity was observed at time points followed by telomere elongation, for instance c4 p34 (Figure 4.25-A), c7 p16 (Figure 4.25-B), and c12 p30 (Figure 4.25-C), and reduced levels of telomerase activity were associated with shorter telomeres in further passages, as evidenced in c4 p16, p26, and p67 (Figure 4.25-A), c7 p10 (Figure 4.25-B), and c12 p8, and p10 (Figure 4.25-C). However, telomerase activity did not directly correlate with telomere length.

Telomere length and telomerase activity were assessed in H9 hESCs and in two clonal cell lines isolated from H9: H9.1 and H9.2 (Amit *et al*., 2000). Similar to that observed here and in other telomerase-positive cell lines, the changes in telomere length did not directly correlated with telomerase activity. In agreement with our observations, the authors detected telomere length fluctuations from passage to passage (ranging from 8 to 12 kb) in each clone, but the length was generally stable to a level that bypassed senescence. Amit *et al*. also observed that H9 displayed telomere shortening with increased passaging, which did not affect the proliferation rate of the hESC line. Similarly, Yang *et al*. (1999) demonstrated that immortalized endothelial cells expressed telomerase and continued to proliferate, though displaying telomere shortening that was eventually stabilized.

The three *DKC1*[A353V] iPSC clones derived in the present study displayed higher telomerase activity compared to *DKC1*-mutant iPSCs from the other three studies (Table 5.1). Clone 4 has exhibited telomerase activity levels similar to H1 hESCs at passages 34 and 102 (Figure 4.25-A). Agarwal *et al*. (2010) observed that their two *DKC1*-mutant iPSC lines exhibited 40% of telomerase activity of wild-type iPSCs. Batista *et al*. (2011) observed severe reduction of telomerase activity in the two *DKC1*-mutant iPSC lines, ranging from 5 to 15% of wild-type iPSCs. Gu *et al*. (2015) observed about 20% of telomerase activity in the *DKC1*-mutant iPSCs (carrying either A353V or del37L) compared to wild-type iPSCs. Since Agarwal *et al*. and us reported telomere elongation or maintenance in the mutant iPSCs, whereas Batista *et al*. and Gu *et al*. reported telomere attrition, the explanation for this apparent paradox may rely on the capacity of the mutant iPSCs in maintaining telomerase activity. However, functional dyskerin is necessary for the active telomerase enzyme complex (Cohen *et al*., 2007). The results presented here suggest that late-passage *DKC1*-mutant iPSCs were able to overcome telomerase deficiency caused by the *DKC1* mutation and maintain telomere lengths. Based on our findings that point to telomerase as the responsible for telomere length stability, this phenomenon may have at least two potential explanations. First, mutant iPSCs may display very high telomerase complex gene

expression, which counter the short half-life of the telomerase holoenzyme due to the deficient dyskerin. Alternatively, additional mechanisms that replace dyskerin in its function to stabilize the complex may be activated.

In order to address these hypotheses, *TERT*, *TERC*, and *DKC1* expression levels were investigated in the three *DKC1*-mutant iPSC clones. *TERT* levels were absent in parental fibroblasts and recapitulated in the iPSCs (Figure 4.27). Previous studies have demonstrated that ectopic expression of *TERT* is enough for elongating telomeres through telomerase and extending replicative life span in normal human cells (Bodnar *et al*., 1998; Vaziri *et al*., 1998). However, in *DKC1*-mutant fibroblasts, both *TERT* and *TERC* are required for elongating telomeres, whereas reduced *TERC* levels impair telomerase activity (Wong and Collins, 2006). Overexpression of *TERC* may overcome limitations in telomere maintenance in *DKC1*-mutant iPSCs (Agarwal *et al*. 2010). In the *DKC1*-mutant iPSC clones derived in the present study, *TERC* expression was four-fold increased compared to parental fibroblasts. Together, these observations may demonstrate that the *DKC1*-mutant fibroblasts recapitulate telomerase activity following reprogramming through up-regulation of both *TERT* and *TERC*. Thus, in accordance with Agarwal *et al*. (2010), the *DKC1*-mutant iPSCs may stabilize telomeres in a telomerase-dependent mechanism, despite the mutation in *DKC1*. However, it is still unclear whether other mechanisms apart of telomerase were involved in the telomere maintenance observed in the *DKC1*-mutant clones. Expression levels of *TERT* and *TERC* displayed variation along passages, but no significant correlation was verified between the levels of these genes and telomerase activity. In agreement with these findings, Winkler *et al*. (2013) also observed heterogeneity in *TERT* and *TERC* expression in telomerase-mutant iPSC clones at different passages, also demonstrating that telomerase activity did not directly correlate with either *TERT* or *TERC* mRNA.

As *TERT* and *TERC*, the levels of *DKC1* are increased in iPSCs compared to fibroblasts, which likely play an important role in the elevated telomerase enzymatic activity and efficiency of telomere elongation after reprogramming (Batista and Artandi, 2013). However, *TERT* and *TERC* expression was lower in mutant-iPSCs in comparison to H1 hESCs, indicating that the expression of these telomerase components does not counter the shorter holoenzyme half-life imposed by the mutation (Figure 4.27). Similarly, increased expression of *DKC1* was observed in all three clones at different passages, even three-fold increased when compared to H1 hESCs and seven-fold increased when compared to parental fibroblasts (c7 p40, Figure 4.27). However, despite up-regulation of *DKC1*, the dyskerin point mutations in iPSCs markedly compromise the amount of TERC incorporated into active

telomerase holoenzyme (Batista *et al*., 2011). However, even a hypomorphic telomerase impaired by mutations offers advantages in contrast to cells with complete abolishment of this enzyme (Batista and Artandi, 2013). Thus, the overexpression of mutant *DKC1* in the iPSCs may overcome the limitations imposed by the deficient protein. High levels of deficient dyskerin may contribute for assembling sufficient telomerase that avoids telomere attrition in the *DKC1*-mutant iPSC clones. Gu *et al*. (2015) demonstrated that both wild-type and mutant dyskerin proteins (including A353V) were located predominantly in the iPSCs nucleoli, as expected. Thus, even mutant dyskerin may present diminished function, but still superior than total abolishment of this protein.

Finally, additional mechanisms may compensate for dyskerin deficiency. RNA sequencing (also called whole transcriptome shotgun sequencing) is warranted to address this hypothesis. The comparison between transcriptomes before and after telomere stabilization may clarify whether telomerase and/or other proteins and pathways are involved in the telomere length stabilization in the *DKC1*-mutant iPSCs.

The differentiation of iPSCs has been extensively described as a powerful disease-modeling system, and also is a promise as source of cells for autologous transplant (Nishikawa *et al*., 2008). In the present study, transgene-free *DKC1*-mutant iPSCs were derived and differentiated toward hematopoietic lineages. Both *DKC1*[A353V] clones (4-7 and 12-5) at similar passages (p28 and p29, respectively) displayed increased counts of hematopoietic lineages compared to controls (Figure 4.32). Four controls were included in the experiments. However, four issues should be considered when interpreting the differentiation results.

First, the efficiency of H1 hematopoietic differentiation presented here was lower than anticipated by previous studies. In independent EB formation experiments, the average hematopoietic differentiation output was found to be approximately 50 colonies per 1×10^5 iPSCs plated (reviewed in Kardel and Eaves, 2012). However, these previous studies used different media, cytokines cocktails, and experimental time lengths than ours, making comparisons among studies difficult.

Second, Ctrl iPSCs c26 and c26-3 were derived from fibroblasts using reprogramming methods similar to the ones used for deriving the *DKC1*-mutant iPSCs. Ctrl iPSCs c26-3 is the transgene-free version of c26, thus representing the closest control (in terms of method) of the *DKC1*-mutant iPSCs. The differentiation of both c26 and c26-3 yielded similar numbers of hematopoietic colonies, suggesting that the presence of the reprogramming

transgenes did not influence hematopoietic differentiation in the controls. However, the differentiation efficiency was lower than anticipated by Winkler *et al*. (2013). The authors performed hematopoietic differentiation in an iPSC line derived from the same parental fibroblasts (CTRL-1), which resulted in approximately 47 colonies per 5×10^4 cells plated. Again, differentiation results between studies are not directly comparable, which makes this observation inconclusive. On the other hand, the same *TERT*-mutant iPSC line differentiated in the Winkler's study (*TERT*[R889X]m c20-8) resulted in similar number of hematopoietic colonies compared to the present study (approximately 20 colonies per 5×10^4 cells plated in both studies). In Winkler's study, this iPSC line presented impaired differentiation; here, the differentiation capacity was increased in comparison to H1, Ctrl iPSCs c26, and c26-3, and impaired in comparison to control iPSCs PBMCs. These observations may imply that H1, Ctrl iPSCs c26, and c26-3 yielded poor differentiation efficiencies.

Third, H1, Ctrl iPSCs c26, and c26-3 were used at late passages. However, Kotini *et al*. (2015) demonstrated that increasing passage number did not alter the differentiation potential of control PSC lines. Thus, a plausible reason to avoid the use of PSCs at late passages is the increased probability of these cells to acquire genetic abnormalities due to long-term culture. In the present study, it was speculated that there is a low probability that these three controls have acquired genetic abnormalities. These PSCs did not display abnormal behavior in culture, such as variation in proliferation rates or increased spontaneous differentiation, as experienced by Mills *et al*. (2013) and Winkler *et al*. (2013) in their abnormal clones. However, karyotyping is ongoing in these three PSCs lines in order to verify their cytogenetic integrity.

Finally, control iPSCs PBMCs was derived from a different source of somatic cells (PBMCs) and using a different reprogramming method (non-integrating episomal vectors). Methylation analysis has evidenced that iPSCs may retain an epigenetic memory of their somatic cell of origin, which could result in a bias in their differentiation potential (Kim *et al*., 2011). This control was derived from PBMCs and the epigenetic memory may favor its hematopoietic differentiation. However, the number of hematopoietic colonies in this control was decreased in comparison to *DKC1*-mutant clones 4-7 and 12-5 (at p28 and p29). Thus, even considering the issues in the differentiation of H1, Ctrl iPSCs c26, and c26-3, the Ctrl iPSCs PBMCs provides evidence that *DKC1*-mutant clones 4-7 (p28) and 12-5 (p29) displayed increased capacity in generating hematopoietic colonies.

Winkler *et al*. (2013) derived and differentiated iPSCs from four patients with AA or reduced bone marrow cellularity and heterozygous mutations in either *TERT* or *TERC*. The

hematopoietic differentiation was significantly decreased in the telomerase-mutant iPSCs in comparison to iPSCs generated from healthy subjects. The *TERT*-mutant iPSCs matched patients' clinical features, strictly reflecting the different severities of the hematopoietic phenotypes. This observation was clearly demonstrated in the differentiation of a sibling pair carrying the same *TERT* mutation (R889X), but featuring distinct clinical manifestations. The production of hematopoietic colonies following differentiation of the sibling presenting severe cytopenias was, on average, twenty-fold decreased when compared to the other sibling whose clinical presentation was minimally decreased marrow cellularity. In agreement with Winkler's study, Batista *et al*. (2011) demonstrated that the magnitude of the telomere maintenance defect in iPSCs is correlated with the clinical severity found in DC patients.

The DC patient carrying the *DKC1* lesion presented in this study has developed BMF and died one year after the isolation of his fibroblasts, by age of 4 due to a brain hemorrhage. In contrast to Winkler *et al*. and Batista *et al*., the *DKC1*-mutant iPSCs derived here displayed elevated capacity to generate hematopoietic progenitors (c4-7 p28, c12-5 p29) compared to controls. Given the severity of the clinical presentation of the DC patient, these findings gave rise to two hypotheses: (1) the elevated capacity in producing hematopoietic progenitors in the *DKC1*-mutant iPSC clones may reflect the hematopoietic stem cell exhaustion *in vivo* due to diminished self-renewal; and (2) the unexpected pattern of telomere length stabilization over time may explain the unexpected increasing in the production of hematopoietic colonies in the *DKC1*-mutant iPSC clones.

HSCs can undergo extensive proliferation and expansion in response to stress, whereas under normal conditions, these cells avoid premature exhaustion and preserve their capability for long-term and multi-lineage differentiation standing most of the time in a quiescent state (Singh *et al*., 2014). The telomere lengths in HSCs from human fetal liver and umbilical cord blood are approximately four kilobases longer than HSCs from adult bone marrow, suggesting that the HSCs have a finite replicative potential that may range from 100 to 5,000 population doublings, thus decreasing through aging (Lansdorp *et al*., 1994; Lansdorp *et al*., 1995; Vaziri *et al*., 1994). The differentiation of *DKC1*[A353V] clones 4-7 and 12-5 at earlier passages (p28 and p29) resulted in an increased number of hematopoietic colonies compared to late passages: clone 12-5 at passage 35, and clone 4 at passage 114 (Figure 4.32). However, telomeres play an essential role in signaling cell cycle progression and cell division in human HSCs (Baerlocher *et al*., 2003). Telomere stabilization observed in the *DKC1*-mutant iPSCs over time suggests that critical telomere length did not represent a cofactor in these cells. DC is considered a telomere and stem cell dysfunction (Kirwan and Dokal, 2009).

Thus, the stem cell dysfunction that leads to DC may be reversible in a system in which telomeres are stabilized to levels that guarantee self-renewal.

The increased differentiation potential in the *DKC1*-mutant iPSCs may be a consequence of telomere length stabilization and telomerase activity. HSCs from telomerase knockout mice exhibit impaired self-renewal through transplantation (Allsopp *et al*., 2003). When stimulated in culture, these HSCs undergo apoptosis (Rossi *et al*., 2007), indicating that functional telomerase and telomere maintenance are required for efficient HSC self-renewal and survival. In human HSCs, Morrison *et al*. (1996) adapted the telomerase activity assay for single cells of the HSC system at four stages of differentiation and demonstrated that the frequency of cells presenting telomerase activity was proportional to the frequency of cells inferred to have self-renewal potential in each differentiation stage. These findings suggest that the self-renewal potential of HSCs may be dependent on the level of telomerase activity. Thus, permanent or even transient activation of telomerase might enhance the self-renewal of HSCs (Elwood, 2004). Given the importance of telomerase in HSCs, the reestablishment of this enzyme in the *DKC1*[A353V] iPSC clones might have conferred an elevated capacity of hematopoietic differentiation, even in a clone that was maintained in long-term culture (c4 p114).

Understanding the complete mechanisms behind telomere maintenance and stem cell self-renewal observed in the *DKC1*-mutant model presented here may imply the development of more effective therapies for telomeropathies, such as DC. Also, the comprehensive understanding of the mechanisms whereby the *DKC1*-mutant iPSCs increase their hematopoietic differentiation potential may serve to develop therapies that either reverse or attenuate the effects of the mutations in the diseases.

6. CONCLUSION

6. Conclusion

In the present study, fibroblasts from a DC patient harboring a *DKC1* mutation were successfully reprogrammed to the pluripotent state. A comprehensive investigation of telomere dynamics was conducted in three patient-derived iPSCs clones over time. These cells were able to stabilize telomeres and displayed telomerase activity especially at late passages. The effects of dysfunctional dyskerin were investigated in hematopoiesis through differentiation of two *DKC1*-mutant iPSC clones, which displayed increased capacity to generate hematopoietic lineages. The developed model might be useful for further molecular studies on telomere biology and represent a platform for screening molecules that may serve for the treatment of telomeropathies, such as DC.

REFERENCES

References

Adewumi, O., Aflatoonian, B., Ahrlund-Richter, L., Amit, M., Andrews, P. W., Beighton, G., Bello, P. A., Benvenisty, N., Berry, L. S., Bevan, S., Blum, B., Brooking, J., Chen, K. G., Choo, A. B., Churchill, G. A., Corbel, M., Damjanov, I., Draper, J. S., Dvorak, P., Emanuelsson, K., Fleck, R. A., Ford, A., Gertow, K., Gertsenstein, M., Gokhale, P. J., Hamilton, R. S., Hampl, A., Healy, L. E., Hovatta, O., Hyllner, J., Imreh, M. P., Itskovitz-Eldor, J., Jackson, J., Johnson, J. L., Jones, M., Kee, K., King, B. L., Knowles, B. B., Lako, M., Lebrin, F., Mallon, B. S., Manning, D., Mayshar, Y., McKay, R. D., Michalska, A. E., Mikkola, M., Mileikovsky, M., Minger, S. L., Moore, H. D., Mummery, C. L., Nagy, A., Nakatsuji, N., O'Brien, C. M., Oh, S. K., Olsson, C., Otonkoski, T., Park, K. Y., Passier, R., Patel, H., Patel, M., Pedersen, R., Pera, M. F., Piekarczyk, M. S., Pera, R. A., Reubinoff, B. E., Robins, A. J., Rossant, J., Rugg-Gunn, P., Schulz, T. C., Semb, H., Sherrer, E. S., Siemen, H., Stacey, G. N., Stojkovic, M., Suemori, H., Szatkiewicz, J., Turetsky, T., Tuuri, T., van den Brink, S., Vintersten, K., Vuoristo, S., Ward, D., Weaver, T. A., Young, L. A., Zhang, W., and Initiative, I. S. C. (2007). Characterization of human embryonic stem cell lines by the International Stem Cell Initiative. *Nat Biotechnol* 25, 803-16.

Agarwal, S., and Daley, G. Q. (2011). Telomere dynamics in dyskeratosis congenita: the long and the short of iPS. *Cell Res* 21, 1157-60.

Agarwal, S., Loh, Y. H., McLoughlin, E. M., Huang, J., Park, I. H., Miller, J. D., Huo, H., Okuka, M., Dos Reis, R. M., Loewer, S., Ng, H. H., Keefe, D. L., Goldman, F. D., Klingelhutz, A. J., Liu, L., and Daley, G. Q. (2010). Telomere elongation in induced pluripotent stem cells from dyskeratosis congenita patients. *Nature* 464, 292-6.

Allsopp, R. C., Morin, G. B., DePinho, R., Harley, C. B., and Weissman, I. L. (2003). Telomerase is required to slow telomere shortening and extend replicative lifespan of HSCs during serial transplantation. *Blood* 102, 517-20.

Amit, M., Carpenter, M. K., Inokuma, M. S., Chiu, C. P., Harris, C. P., Waknitz, M. A., Itskovitz-Eldor, J., and Thomson, J. A. (2000). Clonally derived human embryonic stem cell lines maintain pluripotency and proliferative potential for prolonged periods of culture. *Dev Biol* 227, 271-8.

Apostolou, E., and Hochedlinger, K. (2011). Stem cells: iPS cells under attack. *Nature* 474, 165-6.

Armanios, M. Y., Chen, J. J., Cogan, J. D., Alder, J. K., Ingersoll, R. G., Markin, C., Lawson, W. E., Xie, M., Vulto, I., Phillips, J. A., Lansdorp, P. M., Greider, C. W., and Loyd, J. E. (2007). Telomerase mutations in families with idiopathic pulmonary fibrosis. *N Engl J Med* 356, 1317-26.

Asprer, J. S., and Lakshmipathy, U. (2015). Current methods and challenges in the comprehensive characterization of human pluripotent stem cells. *Stem Cell Rev* 11, 357-72.

Baerlocher, G. M., Roth, A., and Lansdorp, P. M. (2003). Telomeres in hematopoietic stem cells. *Ann N Y Acad Sci* 996, 44-8.

Ball, S. E., Gibson, F. M., Rizzo, S., Tooze, J. A., Marsh, J. C., and Gordon-Smith, E. C. (1998). Progressive telomere shortening in aplastic anemia. *Blood* 91, 3582-92.

Batista, L. F., and Artandi, S. E. (2013). Understanding telomere diseases through analysis of patient-derived iPS cells. *Curr Opin Genet Dev* 23, 526-33.

Batista, L. F., Pech, M. F., Zhong, F. L., Nguyen, H. N., Xie, K. T., Zaug, A. J., Crary, S. M., Choi, J., Sebastiano, V., Cherry, A., Giri, N., Wernig, M., Alter, B. P., Cech, T. R., Savage, S. A., Reijo Pera, R. A., and Artandi, S. E. (2011). Telomere shortening and loss of self-renewal in dyskeratosis congenita induced pluripotent stem cells. *Nature* 474, 399-402.

Bodnar, A. G., Ouellette, M., Frolkis, M., Holt, S. E., Chiu, C. P., Morin, G. B., Harley, C. B., Shay, J. W., Lichtsteiner, S., and Wright, W. E. (1998). Extension of life-span by introduction of telomerase into normal human cells. *Science* 279, 349-52.

Bongso, A., Fong, C. Y., Ng, S. C., and Ratnam, S. (1994). Isolation and culture of inner cell mass cells from human blastocysts. *Hum Reprod* 9, 2110-7.

Broccoli, D., Young, J. W., and de Lange, T. (1995). Telomerase activity in normal and malignant hematopoietic cells. *Proc Natl Acad Sci U S A* 92, 9082-6.

Brümmendorf, T. H., Maciejewski, J. P., Mak, J., Young, N. S., and Lansdorp, P. M. (2001). Telomere length in leukocyte subpopulations of patients with aplastic anemia. *Blood* 97, 895-900.

Calado, R. T., Brudno, J., Mehta, P., Kovacs, J. J., Wu, C., Zago, M. A., Chanock, S. J., Boyer, T. D., and Young, N. S. (2011). Constitutional telomerase mutations are genetic risk factors for cirrhosis. *Hepatology* 53, 1600-7.

Calado, R. T., and Dumitriu, B. (2013). Telomere dynamics in mice and humans. *Semin Hematol* 50, 165-74.

Calado, R. T., Regal, J. A., Kleiner, D. E., Schrump, D. S., Peterson, N. R., Pons, V., Chanock, S. J., Lansdorp, P. M., and Young, N. S. (2009). A spectrum of severe familial liver disorders associate with telomerase mutations. *PLoS One* 4, e7926.

Calado, R. T., and Young, N. S. (2008). Telomere maintenance and human bone marrow failure. *Blood* 111, 4446-55.

Calado, R. T., and Young, N. S. (2009). Telomere diseases. *N Engl J Med* 361, 2353-65.

Callicott, R. J., and Womack, J. E. (2006). Real-time PCR assay for measurement of mouse telomeres. *Comp Med* 56, 17-22.

Carpenter, M. K., Rosler, E., and Rao, M. S. (2003). Characterization and differentiation of human embryonic stem cells. *Cloning Stem Cells* 5, 79-88.

Cawthon, R. M. (2009). Telomere length measurement by a novel monochrome multiplex quantitative PCR method. *Nucleic Acids Res* 37, e21.

Cesare, A. J., and Griffith, J. D. (2004). Telomeric DNA in ALT cells is characterized by free telomeric circles and heterogeneous t-loops. *Mol Cell Biol* 24, 9948-57.

Chadwick, K., Wang, L., Li, L., Menendez, P., Murdoch, B., Rouleau, A., and Bhatia, M. (2003). Cytokines and BMP-4 promote hematopoietic differentiation of human embryonic stem cells. *Blood* 102, 906-15.

Chang, K. H., Nelson, A. M., Fields, P. A., Hesson, J. L., Ulyanova, T., Cao, H., Nakamoto, B., Ware, C. B., and Papayannopoulou, T. (2008). Diverse hematopoietic potentials of five human embryonic stem cell lines. *Exp Cell Res* 314, 2930-40.

Cong, Y. S., Wright, W. E., and Shay, J. W. (2002). Human telomerase and its regulation. *Microbiol Mol Biol Rev* 66, 407-25, table of contents.

Dang, S. M., Kyba, M., Perlingeiro, R., Daley, G. Q., and Zandstra, P. W. (2002). Efficiency of embryoid body formation and hematopoietic development from embryonic stem cells in different culture systems. *Biotechnol Bioeng* 78, 442-53.

de Lange, T. (1992). Human telomeres are attached to the nuclear matrix. *EMBO J* 11, 717-24.

de Lange, T. (2005). Shelterin: the protein complex that shapes and safeguards human telomeres. *Genes Dev* 19, 2100-10.

Dokal, I. (1999). Dyskeratosis congenita. *Br J Haematol* 105 Suppl 1, 11-5.

Dokal, I. (2000). Dyskeratosis congenita in all its forms. *Br J Haematol* 110, 768-79.

Dokal, I., Vulliamy, T., Mason, P., and Bessler, M. (2011). Clinical utility gene card for: dyskeratosis congenita. *Eur J Hum Genet* 19.

Elwood, N. (2004). Telomere biology of human hematopoietic stem cells. *Cancer Control* 11, 77-85.

Evans, M. J., and Kaufman, M. H. (1981). Establishment in culture of pluripotential cells from mouse embryos. *Nature* 292, 154-6.

Fogarty, P. F., Yamaguchi, H., Wiestner, A., Baerlocher, G. M., Sloand, E., Zeng, W. S., Read, E. J., Lansdorp, P. M., and Young, N. S. (2003). Late presentation of dyskeratosis congenita as apparently acquired aplastic anaemia due to mutations in telomerase RNA. *Lancet* 362, 1628-30.

Greider, C. W., and Blackburn, E. H. (1985). Identification of a specific telomere terminal transferase activity in Tetrahymena extracts. *Cell* 43, 405-13.

Gu, B. W., Apicella, M., Mills, J., Fan, J. M., Reeves, D. A., French, D., Podsakoff, G. M., Bessler, M., and Mason, P. J. (2015). Impaired Telomere Maintenance and Decreased Canonical WNT Signaling but Normal Ribosome Biogenesis in Induced Pluripotent Stem Cells from X-Linked Dyskeratosis Congenita Patients. *PLoS One* 10, e0127414.

GURDON, J. B. (1962). Adult frogs derived from the nuclei of single somatic cells. *Dev Biol* 4, 256-73.

Harley, C. B., Futcher, A. B., and Greider, C. W. (1990). Telomeres shorten during ageing of human fibroblasts. *Nature* 345, 458-60.

Hartmann, D., Srivastava, U., Thaler, M., Kleinhans, K. N., N'kontchou, G., Scheffold, A., Bauer, K., Kratzer, R. F., Kloos, N., Katz, S. F., Song, Z., Begus-Nahrmann, Y., Kleger, A., von Figura, G., Strnad, P., Lechel, A., Günes, C., Potthoff, A., Deterding, K., Wedemeyer, H., Ju, Z., Song, G., Xiao, F., Gillen, S., Schrezenmeier, H., Mertens, T., Ziol, M., Friess, H., Jarek, M., Manns, M. P., Beaugrand, M., and Rudolph, K. L. (2011). Telomerase gene mutations are associated with cirrhosis formation. *Hepatology* 53, 1608-17.

Hayflick, L. (1965). The limited in vitro lifetime of human diploid cell strains. *Exp Cell Res* 37, 614-36.

Heiss, N. S., Knight, S. W., Vulliamy, T. J., Klauck, S. M., Wiemann, S., Mason, P. J., Poustka, A., and Dokal, I. (1998). X-linked dyskeratosis congenita is caused by mutations in a highly conserved gene with putative nucleolar functions. *Nat Genet* 19, 32-8.

Henson, J. D., Cao, Y., Huschtscha, L. I., Chang, A. C., Au, A. Y., Pickett, H. A., and Reddel, R. R. (2009). DNA C-circles are specific and quantifiable markers of alternative-lengthening-of-telomeres activity. *Nat Biotechnol* 27, 1181-5.

Herbig, U., Jobling, W. A., Chen, B. P., Chen, D. J., and Sedivy, J. M. (2004). Telomere shortening triggers senescence of human cells through a pathway involving ATM, p53, and p21(CIP1), but not p16(INK4a). *Mol Cell* 14, 501-13.

Hong, S. G., Winkler, T., Wu, C., Guo, V., Pittaluga, S., Nicolae, A., Donahue, R. E., Metzger, M. E., Price, S. D., Uchida, N., Kuznetsov, S. A., Kilts, T., Li, L., Robey, P. G., and Dunbar, C. E. (2014). Path to the clinic: assessment of iPSC-based cell therapies in vivo in a nonhuman primate model. *Cell Rep* 7, 1298-309.

Hussein, S. M., Batada, N. N., Vuoristo, S., Ching, R. W., Autio, R., Närvä, E., Ng, S., Sourour, M., Hämäläinen, R., Olsson, C., Lundin, K., Mikkola, M., Trokovic, R., Peitz, M., Brüstle, O., Bazett-Jones, D. P., Alitalo, K., Lahesmaa, R., Nagy, A., and Otonkoski, T. (2011). Copy number variation and selection during reprogramming to pluripotency. *Nature* 471, 58-62.

Itskovitz-Eldor, J., Schuldiner, M., Karsenti, D., Eden, A., Yanuka, O., Amit, M., Soreq, H., and Benvenisty, N. (2000). Differentiation of human embryonic stem cells into embryoid bodies compromising the three embryonic germ layers. *Mol Med* 6, 88-95.

Jung, M., Dunbar, C. E., and Winkler, T. (2015). Modeling Human Bone Marrow Failure Syndromes Using Pluripotent Stem Cells and Genome Engineering. *Mol Ther*.

Kardel, M. D., and Eaves, C. J. (2012). Modeling human hematopoietic cell development from pluripotent stem cells. *Exp Hematol* 40, 601-11.

Keller, G., Kennedy, M., Papayannopoulou, T., and Wiles, M. V. (1993). Hematopoietic commitment during embryonic stem cell differentiation in culture. *Mol Cell Biol* 13, 473-86.

Keller, G. M. (1995). In vitro differentiation of embryonic stem cells. *Curr Opin Cell Biol* 7, 862-9.

Kim, K., Zhao, R., Doi, A., Ng, K., Unternaehrer, J., Cahan, P., Huo, H., Loh, Y. H., Aryee, M. J., Lensch, M. W., Li, H., Collins, J. J., Feinberg, A. P., and Daley, G. Q. (2011). Donor cell type can influence the epigenome and differentiation potential of human induced pluripotent stem cells. *Nat Biotechnol* 29, 1117-9.

Kirwan, M., and Dokal, I. (2008). Dyskeratosis congenita: a genetic disorder of many faces. *Clin Genet* 73, 103-12.

Kirwan, M., and Dokal, I. (2009). Dyskeratosis congenita, stem cells and telomeres. *Biochim Biophys Acta* 1792, 371-9.

Knight, S. W., Heiss, N. S., Vulliamy, T. J., Greschner, S., Stavrides, G., Pai, G. S., Lestringant, G., Varma, N., Mason, P. J., Dokal, I., and Poustka, A. (1999). X-linked dyskeratosis congenita is predominantly caused by missense mutations in the DKC1 gene. *Am J Hum Genet* 65, 50-8.

Kotini, A. G., Chang, C. J., Boussaad, I., Delrow, J. J., Dolezal, E. K., Nagulapally, A. B., Perna, F., Fishbein, G. A., Klimek, V. M., Hawkins, R. D., Huangfu, D., Murry, C. E., Graubert, T., Nimer, S. D., and Papapetrou, E. P. (2015). Functional analysis of a chromosomal deletion associated with myelodysplastic syndromes using isogenic human induced pluripotent stem cells. *Nat Biotechnol* 33, 646-55.

Lansdorp, P. M. (1995). Telomere length and proliferation potential of hematopoietic stem cells. *J Cell Sci* 108 (Pt 1), 1-6.

Lansdorp, P. M., Dragowska, W., Thomas, T. E., Little, M. T., and Mayani, H. (1994). Age-related decline in proliferative potential of purified stem cell candidates. *Blood Cells* 20, 376-80; discussion 380-1.

Lapasset, L., Milhavet, O., Prieur, A., Besnard, E., Babled, A., Aït-Hamou, N., Leschik, J., Pellestor, F., Ramirez, J. M., De Vos, J., Lehmann, S., and Lemaitre, J. M. (2011). Rejuvenating senescent and centenarian human cells by reprogramming through the pluripotent state. *Genes Dev* 25, 2248-53.

Laurent, L. C., Ulitsky, I., Slavin, I., Tran, H., Schork, A., Morey, R., Lynch, C., Harness, J. V., Lee, S., Barrero, M. J., Ku, S., Martynova, M., Semechkin, R., Galat, V., Gottesfeld, J., Izpisua Belmonte, J. C., Murry, C., Keirstead, H. S., Park, H. S., Schmidt, U., Laslett, A. L., Muller, F. J., Nievergelt, C. M., Shamir, R., and Loring, J. F. (2011). Dynamic changes in the copy number of pluripotency and cell proliferation genes in human ESCs and iPSCs during reprogramming and time in culture. *Cell Stem Cell* 8, 106-18.

Livak, K. J., and Schmittgen, T. D. (2001). Analysis of relative gene expression data using real-time quantitative PCR and the 2(-Delta Delta C(T)) Method. *Methods* 25, 402-8.

Londoño-Vallejo, J. A., Der-Sarkissian, H., Cazes, L., Bacchetti, S., and Reddel, R. R. (2004). Alternative lengthening of telomeres is characterized by high rates of telomeric exchange. *Cancer Res* 64, 2324-7.

Makarov, V. L., Hirose, Y., and Langmore, J. P. (1997). Long G tails at both ends of human chromosomes suggest a C strand degradation mechanism for telomere shortening. *Cell* 88, 657-66.

Marion, R. M., Strati, K., Li, H., Tejera, A., Schoeftner, S., Ortega, S., Serrano, M., and Blasco, M. A. (2009). Telomeres acquire embryonic stem cell characteristics in induced pluripotent stem cells. *Cell Stem Cell* 4, 141-54.

Martin, G. R. (1981). Isolation of a pluripotent cell line from early mouse embryos cultured in medium conditioned by teratocarcinoma stem cells. *Proc Natl Acad Sci U S A* 78, 7634-8.

Martins-Taylor, K., Nisler, B. S., Taapken, S. M., Compton, T., Crandall, L., Montgomery, K. D., Lalande, M., and Xu, R. H. (2011). Recurrent copy number variations in human induced pluripotent stem cells. *Nat Biotechnol* 29, 488-91.

McClintock, B. (1941). The Stability of Broken Ends of Chromosomes in Zea Mays. *Genetics* 26, 234-82.

Mills, J. A., Wang, K., Paluru, P., Ying, L., Lu, L., Galvão, A. M., Xu, D., Yao, Y., Sullivan, S. K., Sullivan, L. M., Mac, H., Omari, A., Jean, J. C., Shen, S., Gower, A., Spira, A., Mostoslavsky, G., Kotton, D. N., French, D. L., Weiss, M. J., and Gadue, P. (2013). Clonal genetic and hematopoietic heterogeneity among human-induced pluripotent stem cell lines. *Blood* 122, 2047-51.

Mitchell, J. R., Wood, E., and Collins, K. (1999). A telomerase component is defective in the human disease dyskeratosis congenita. *Nature* 402, 551-5.

Moyzis, R. K., Buckingham, J. M., Cram, L. S., Dani, M., Deaven, L. L., Jones, M. D., Meyne, J., Ratliff, R. L., and Wu, J. R. (1988). A highly conserved repetitive DNA sequence, (TTAGGG)n, present at the telomeres of human chromosomes. *Proc Natl Acad Sci U S A* 85, 6622-6.

Müller, F. J., Goldmann, J., Löser, P., and Loring, J. F. (2010). A call to standardize teratoma assays used to define human pluripotent cell lines. *Cell Stem Cell* 6, 412-4.

Muller, H. (1938). The remaking of chromosomes. *Collect*. *Net*, 13, pp. 181–198

Nabetani, A., and Ishikawa, F. (2009). Unusual telomeric DNAs in human telomerase-negative immortalized cells. *Mol Cell Biol* 29, 703-13.

Nakano, T., Kodama, H., and Honjo, T. (1996). In vitro development of primitive and definitive erythrocytes from different precursors. *Science* 272, 722-4.

Ng, E. S., Davis, R., Stanley, E. G., and Elefanty, A. G. (2008). A protocol describing the use of a recombinant protein-based, animal product-free medium (APEL) for human embryonic stem cell differentiation as spin embryoid bodies. *Nat Protoc* 3, 768-76.

Nishikawa, S., Goldstein, R. A., and Nierras, C. R. (2008). The promise of human induced pluripotent stem cells for research and therapy. *Nat Rev Mol Cell Biol* 9, 725-9.

Olovnikov, A. M. (1971). [Principle of marginotomy in template synthesis of polynucleotides]. *Dokl Akad Nauk SSSR* 201, 1496-9.

Orkin, S. H., and Zon, L. I. (2008). Hematopoiesis: an evolving paradigm for stem cell biology. *Cell* 132, 631-44.

Rossi, D. J., Bryder, D., Seita, J., Nussenzweig, A., Hoeijmakers, J., and Weissman, I. L. (2007). Deficiencies in DNA damage repair limit the function of haematopoietic stem cells with age. *Nature* 447, 725-9.

Shay, J. W., and Wright, W. E. (2000). Hayflick, his limit, and cellular ageing. *Nat Rev Mol Cell Biol* 1, 72-6.

Singh, K. P., Bennett, J. A., Casado, F. L., Walrath, J. L., Welle, S. L., and Gasiewicz, T. A. (2014). Loss of aryl hydrocarbon receptor promotes gene changes associated with premature hematopoietic stem cell exhaustion and development of a myeloproliferative disorder in aging mice. *Stem Cells Dev* 23, 95-106.

Somers, A., Jean, J. C., Sommer, C. A., Omari, A., Ford, C. C., Mills, J. A., Ying, L., Sommer, A. G., Jean, J. M., Smith, B. W., Lafyatis, R., Demierre, M. F., Weiss, D. J., French, D. L., Gadue, P., Murphy, G. J., Mostoslavsky, G., and Kotton, D. N. (2010). Generation of transgene-free lung disease-specific human induced pluripotent stem cells using a single excisable lentiviral stem cell cassette. *Stem Cells* 28, 1728-40.

Sommer, C. A., Stadtfeld, M., Murphy, G. J., Hochedlinger, K., Kotton, D. N., and Mostoslavsky, G. (2009). Induced pluripotent stem cell generation using a single lentiviral stem cell cassette. *Stem Cells* 27, 543-9.

Stadtfeld, M., Maherali, N., Breault, D. T., and Hochedlinger, K. (2008a). Defining molecular cornerstones during fibroblast to iPS cell reprogramming in mouse. *Cell Stem Cell* 2, 230-40.

Stadtfeld, M., Maherali, N., Breault, D. T., and Hochedlinger, K. (2008b). Defining molecular cornerstones during fibroblast to iPS cell reprogramming in mouse. *Cell Stem Cell* 2, 230-40.

Szostak, J. W., and Blackburn, E. H. (1982). Cloning yeast telomeres on linear plasmid vectors. *Cell* 29, 245-55.

Takahashi, K., Tanabe, K., Ohnuki, M., Narita, M., Ichisaka, T., Tomoda, K., and Yamanaka, S. (2007). Induction of pluripotent stem cells from adult human fibroblasts by defined factors. *Cell* 131, 861-72.

Takahashi, K., and Yamanaka, S. (2006). Induction of pluripotent stem cells from mouse embryonic and adult fibroblast cultures by defined factors. *Cell* 126, 663-76.

Thomson, J. A., Itskovitz-Eldor, J., Shapiro, S. S., Waknitz, M. A., Swiergiel, J. J., Marshall, V. S., and Jones, J. M. (1998). Embryonic stem cell lines derived from human blastocysts. *Science* 282, 1145-7.

Tsakiri, K. D., Cronkhite, J. T., Kuan, P. J., Xing, C., Raghu, G., Weissler, J. C., Rosenblatt, R. L., Shay, J. W., and Garcia, C. K. (2007). Adult-onset pulmonary fibrosis caused by mutations in telomerase. *Proc Natl Acad Sci U S A* 104, 7552-7.

Uringa, E. J., Youds, J. L., Lisaingo, K., Lansdorp, P. M., and Boulton, S. J. (2011). RTEL1: an essential helicase for telomere maintenance and the regulation of homologous recombination. *Nucleic Acids Res* 39, 1647-55.

Vaziri, H., and Benchimol, S. (1998a). Reconstitution of telomerase activity in normal human cells leads to elongation of telomeres and extended replicative life span. *Curr Biol* 8, 279-82.

Vaziri, H., and Benchimol, S. (1998b). Reconstitution of telomerase activity in normal human cells leads to elongation of telomeres and extended replicative life span. *Curr Biol* 8, 279-82.

Vaziri, H., Dragowska, W., Allsopp, R. C., Thomas, T. E., Harley, C. B., and Lansdorp, P. M. (1994). Evidence for a mitotic clock in human hematopoietic stem cells: loss of telomeric DNA with age. *Proc Natl Acad Sci U S A* 91, 9857-60.

Vulliamy, T. J., Marrone, A., Knight, S. W., Walne, A., Mason, P. J., and Dokal, I. (2006). Mutations in dyskeratosis congenita: their impact on telomere length and the diversity of clinical presentation. *Blood* 107, 2680-5.

Walne, A. J., Vulliamy, T., Kirwan, M., Plagnol, V., and Dokal, I. (2013). Constitutional mutations in RTEL1 cause severe dyskeratosis congenita. *Am J Hum Genet* 92, 448-53.

Wang, R. C., Smogorzewska, A., and de Lange, T. (2004). Homologous recombination generates T-loop-sized deletions at human telomeres. *Cell* 119, 355-68.

Winkler, T., Hong, S. G., Decker, J. E., Morgan, M. J., Wu, C., Hughes, W. M., Yang, Y., Wangsa, D., Padilla-Nash, H. M., Ried, T., Young, N. S., Dunbar, C. E., and Calado, R. T. (2013). Defective telomere elongation and hematopoiesis from telomerase-mutant aplastic anemia iPSCs. *J Clin Invest* 123, 1952-63.

Wong, J. M., and Collins, K. (2006). Telomerase RNA level limits telomere maintenance in X-linked dyskeratosis congenita. *Genes Dev* 20, 2848-58.

Yamaguchi, H., Calado, R. T., Ly, H., Kajigaya, S., Baerlocher, G. M., Chanock, S. J., Lansdorp, P. M., and Young, N. S. (2005). Mutations in TERT, the gene for telomerase reverse transcriptase, in aplastic anemia. *N Engl J Med* 352, 1413-24.

Yamanaka, S. (2007). Strategies and new developments in the generation of patient-specific pluripotent stem cells. *Cell Stem Cell* 1, 39-49.

Yamanaka, S., and Blau, H. M. (2010). Nuclear reprogramming to a pluripotent state by three approaches. *Nature* 465, 704-12.

Yang, J., Chang, E., Cherry, A. M., Bangs, C. D., Oei, Y., Bodnar, A., Bronstein, A., Chiu, C. P., and Herron, G. S. (1999). Human endothelial cell life extension by telomerase expression. *J Biol Chem* 274, 26141-8.

Yeager, T. R., Neumann, A. A., Englezou, A., Huschtscha, L. I., Noble, J. R., and Reddel, R. R. (1999). Telomerase-negative immortalized human cells contain a novel type of promyelocytic leukemia (PML) body. *Cancer Res* 59, 4175-9.

Yoshida, Y., Takahashi, K., Okita, K., Ichisaka, T., and Yamanaka, S. (2009). Hypoxia enhances the generation of induced pluripotent stem cells. *Cell Stem Cell* 5, 237-41.

Young, N. S., Scheinberg, P., and Calado, R. T. (2008). Aplastic anemia. *Curr Opin Hematol* 15, 162-8.

APPENDIX

Appendix

A.1. Brief introduction

Telomere attrition as a consequence of mutations in telomerase genes has been linked to human dysfunctions with broad clinical spectrum, the telomeropathies. Mutations in telomerase genes have been described in familial degenerative diseases as hematopoietic dysfunctions (Calado, 2009), aplastic anemia (Yamaguchi *et al*., 2003; Yamaguchi *et al*., 2005; Calado and Young, 2008), idiopatic pulmonary fibrosis (Armanios *et al*., 2007; Tsakiri *et al*., 2007; Mushiroda *et al*., 2008), myelodysplastic syndrome, and hepatic diseases (Calado and Young, 2009; Hartmann *et al*., 2011; Calado *et al*., 2011). Despite widely variable genetic penetrance in telomeropathies, a common characteristic that leads to the progressive failure of high proliferative tissues is restrict telomerase activity. These tissues require telomerase activity in their stem cell compartments to maintain proliferation rates.

In DC, although bone marrow failure is the most common cause of death, failure of other highly proliferative tissues is frequent, including the intestinal epithelium (Jonassaint *et al*., 2013). Moreover, tissues with remarkable regenerative capacity, such as the liver, may also be affected (Calado and Young, 2009). Given the broad range of organ systems involved in telomeropathies, such as DC, to investigate the development of these diseases in different tissues may provide important information.

The derivation of iPSCs from patients' somatic cells provides a powerful disease model, since these pluripotent cells can be differentiated in virtually any cell type. Several studies have focused on differentiation of pluripotent stem cells (iPSCs and ESCs) into hematopoietic stem cells (reviewed in Jung *et al*., 2015), hepatocytes (Hay *et al*., 2007; Basma *et al*., 2009; Sullivan *et al*., 2010; Greenhough *et al*., 2010; Medine *et al*., 2011), and, most recently, intestinal tissue (McCracken *et al*., 2011).

Besides the hematopoietic tissue, differentiation in other tissues was carried out in the *DKC1*[A353V] iPSCs derived in the present study. Differentiations in hepatocytes and intestinal tissue (usually affected in telomeropathies) were conducted. Moreover, a different protocol of hematopoietic differentiation was tested before establishing the methods described previously. Here information is provided regarding other experiments that were conducted in the present study, but that were not concluded in time to be added as part of the thesis.

A.2. Material and methods

A.2.1. Hematopoietic differentiation in adherent cell culture

Hematopoietic stem cell (HSC) differentiation was first performed in adherent cell cultures of iPSCs using a protocol adapted from the published protocols of Ng *et al*. (2008) and Chadwick *et al*. (2003). The company Stem Cell Technologies provided the protocol, which was adapted for iPSCs in feeder-independent platform, and using STEMdiff APEL (Albumin Polyvinyl alcohol Essential Lipids) medium as basal medium (Stem Cell Technologies). Instead of deriving EBs prior to differentiation, cells cultured in Matrigel (Corning) and mTeSR medium (Stem Cell Technologies) were submitted to differentiation in the adherent layer using STEMdiff APEL supplemented with a series of cytokines combinations. In order to induce iPSCs to the mesodermal germ layer, cells were exposed for four days to medium containing 30 ng/mL VEGF, 30 ng/mL BMP4, 40 ng/mL SCF, and 50 ng/mL Activin A (all R&D Systems). Then, to induce mesodermal cells to the hematopoietic lineages, cells were exposed for nine days to basal medium supplemented with 300 ng/mL SCF, 300 ng/mL Flt3L, 10 ng/mL IL-3, 10 ng/mL IL-6, 50 ng/mL G-CSF, and 25 ng/mL BMP4 (all R&D Systems).

The efficiency of HSC differentiation was checked through Fluorescence Activated Cell Sorting (FACS) analysis at different time points (days 0, 7, and 13) for the expression of the hematopoietic endothelial markers CD34 and CD45. Cells were harvested using 0.05% trypsin (Gibco), dissociated in single cells using cell strainer, washed twice with 1×PBS, and counted. Aliquots of 2×10^5 cells were prepared and stained with LIVE/DEAD Fixable Violet Dead Cell Stain Kit (Invitrogen) to check viability, followed by CD34 (PE) and CD45 (FITC) antibodies (BD) staining. Data was acquired on a LSR II Flow Cytometer System (BD) and analyzed using FlowJo software. Additionally, colony-forming cell (CFC) assay was performed on day 13. For this purpose, 1×10^5 cells were plated in 35 mm culture dishes in methylcellulose medium with recombinant cytokines (MethoCult H4435, Stem Cell Technologies) and incubated at 37°C for 14 days. Dishes were checked on day 14, and colonies, when present, were identified and counted under an inverted microscope according to the standard morphological criteria. The Figure A1 provides a schematic overview of the HSC differentiation procedure.

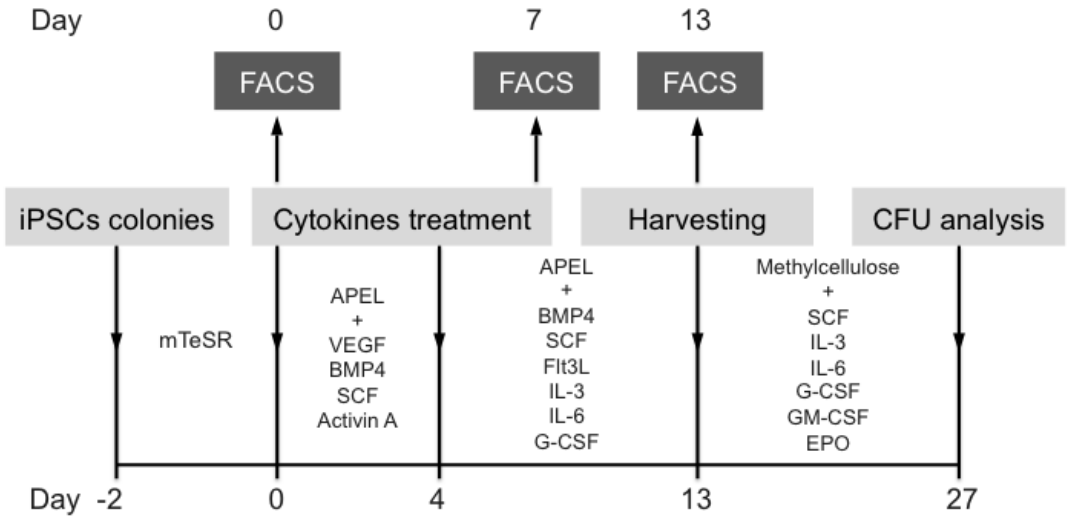

Figure A1 – Overview of the HSC differentiation in adherent iPSCs. First, iPSCs fully undifferentiated in feeder-independent cultures were passaged two days before starting cytokines treatment. Next, cells were guided to mesodermal differentiation with specific cytokines for three days (day 0 to 3). By day 4, medium was replaced with a different cytokines cocktail in order to promote maturation of the hematopoietic stem and progenitor cells. On day 13, the adherent differentiation tissue was harvested with trypsin, and cells were seeded in semi-solid medium (methylcellulose) containing cytokines. CFUs formed after 14 days in methylcellulose were classified and counted. The efficiency of the differentiation was accompanied by regular flow cytometry analyzes (FACS) on days 0, 7, and 13.

A.2.2. Hepatic differentiation

Two different protocols were tested to promote hepatic differentiation of PSCs. The first test was performed in collaboration with Dr. T. Jake Liang and his lab (Liver Diseases Branch, NIDDK, NIH, USA). Methods described by Basma *et al*. (2009) were adapted for iPSCs differentiation in adherent cell cultures. Cells cultured in Matrigel (BD) and mTeSR medium (Stem Cell Technologies) were first differentiated towards definitive endoderm (DE). For DE induction, cells were maintained for three days in RPMI 1640 medium supplemented with 2 mM L-glutamine (all Gibco), 100 ng/mL bFGF (Peprotech), 100 ng/mL Activin A (R&D Systems), and increasing amounts of HyClone FBS (Thermo Scientific): 0% (first day), 0.2% (second day), and 2% (third day). The efficiency of DE induction was assessed by immunofluorescence for SOX17 (R&D Systems) and FOXA2 (Santa Cruz Biotechnology). Hepatic specification was achieved after eight days of cell culture in DMEM/F12 (Gibco) containing 10% KSR, 1% NEAA, 1% L-glutamine (all Gibco), 1% DMSO (Sigma-Aldrich), and 100 ng/mL HGF (R&D Systems). Then, hepatoblasts maturation was achieved after three days in similar medium containing 10 µM

dexamethasone (Sigma-Aldrich) in place of DMSO and HGF. Finally, human hepatocytes, when derived, can be maintained for up to one week in L15 medium with 8.4% FBS, 1% L-glutamine, and 1% tryptose phosphate (all Life Technologies), 1 μM insulin, 10 μM hydrocortisone, and 10 μM dexamethasone (all Sigma-Aldrich). Hepatic specification efficiency was assessed by the percentage of alpha-fetoprotein (AFP)-positive cells using immunofluorescence. Moreover, the efficiency of final differentiation was assessed by the percentage of albumin-positive cells. Researchers of Dr. T. Jake Liang's lab performed these assays. The Figure A2 provides a schematic overview of the hepatic differentiation.

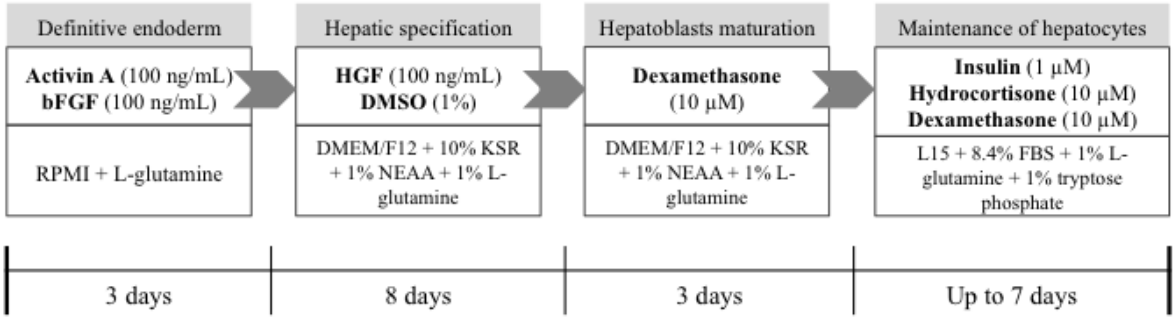

Figure A2 – First approach for hepatic differentiation of PSCs. First, iPSCs were guided to definitive endoderm differentiation with exposure to Activin A and bFGF. Hepatic specification was performed treating cells for eight days with medium containing HGF. The maturation of hepatoblasts was achieved through three days of treatment with medium containing dexamethasone. The hepatocytes, when derived, can be maintained in medium containing insulin, hydrocortisone, and dexamethasone for seven days.

The second test was performed in collaboration with Dr. Lygia da Veiga Pereira and her lab (National Laboratory of Embryonic Stem Cells, USP, Brazil). Hepatic differentiation was carried out according to methods described by Medine *et al*. (2011). First, fully undifferentiated PSCs were platted three days before starting differentiation. The colonies were guided to DE differentiation by supplementing RPMI 1640 medium (Gibco) with 1× B27 (Invitrogen), 100 ng/mL Activin A, and 50 ng/mL WNT3a (R&D Systems), and treating cells for three days with daily media change. Next, the generation of hepatoblasts was carried out using Knockout DMEM medium (Gibco) plus 20% KSR (Gibco), and 1% DMSO (Sigma-Aldrich), for 5 days, with media changing every 48 h. Then, hepatic maturation was achieved by culturing hepatoblasts for nine days in HepatoZYME medium (Gibco) supplemented with 10 ng/mL HGF, and 20 ng/mL Oncostatin M (R&D Systems), changing

media every 48 h. The Figure A3 provides a schematic overview of the second protocol used for hepatic differentiation.

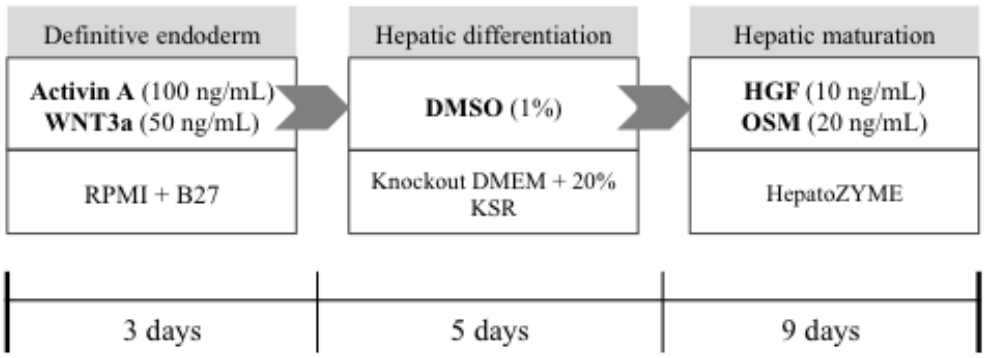

Figure A3 – Second approach for hepatic differentiation of PSCs. First, the PSCs were guided to definitive endoderm with Activin A and WNT3a. Hepatic differentiation was stimulated in medium containing DMSO. Then, hepatic maturation was achieved with HGF and OSM (adapted from Medine *et al*., 2011).

A.2.3. Intestinal tissue differentiation

Generation of intestinal tissue from PSCs was performed as described by McCracken *et al*. (2011). Fully undifferentiated PSCs were cultured until achieve high confluence (about 95%), in Matrigel (BD) and mTeSR medium (Stem Cell Technologies). First, cells were differentiated towards DE for three days in RPMI 1640 medium supplemented with 2 mM L-glutamine, 100 U/mL penicillin, 100 µg/mL streptomycin (all Gibco), 100 ng/mL Activin A (R&D Systems), and increasing amounts of HyClone FBS (Thermo Scientific): day 1 = 0%, day 2 = 0.2%, and day 3 = 2%. DE induction efficiency was assessed by immunocytochemistry of FOXA2 and SOX17 (as previously described in the section "3.2.10.b – Immunocytochemistry"). Primary and secondary antibodies were provided in Table S1. DE was differentiated into mid- and hindgut for four days in RPMI 1640 medium supplemented with 2 mM L-glutamine, 100 U/mL penicillin, 100 µg/mL streptomycin (all Gibco), 2% HyClone FBS (Thermo Scientific), 500 ng/mL FGF4, and 500 ng/mL WNT3a. Immunocytochemistry was carried out on the epithelial monolayers at the end of four days of mid- and hindgut induction using anti-CDX2 antibody (Table S1).

Table S1 – Antibodies for DE and epithelial markers.

Marker	Primary antibody	Secondary antibody
FOXA2	Rabbit Anti-FOXA2 (Abcam)	Donkey anti-rabbit Cy3 (Jackson ImmunoResearch)
SOX17	Goat anti-SOX17 (R&D Systems)	Donkey anti-Goat IgG H&L DyLight 488 (Abcam)
CDX2	Rabbit anti-CDX2 (Thermo Scientific)	Donkey anti-rabbit Cy3 (Jackson ImmunoResearch)

After 48 h of exposure to mid- and hindgut differentiation medium, free-floating structures (mid- and hindgut spheroids) that have budded from the adherent epithelium were collected and transferred to three-dimensional culture in Matrigel (Corning) containing 1× B27 supplement (Invitrogen), 500 ng/mL RSpondin1, 100 ng/mL Noggin, and 100 ng/mL EGF (all R&D Systems). The Matrigel drops containing the spheroids were maintained immersed in intestine growth medium composed of Advanced DMEM/F12, 2 mM L-glutamine, 100 U/mL penicillin, 100 µg/mL streptomycin, 15 mM HEPES buffer (all Gibco), 1× B27 supplement (Invitrogen), 500 ng/mL RSpondin1, 100 ng/mL Noggin, and 100 ng/mL EGF (all R&D Systems). Mid- and hindgut spheroids were grown into human intestinal organoids for 28 days and then split manually by cutting the organoids into halves using a sterile scalpel under stereomicroscope. Organoids collected on day 15 after transferring to 3D culture were fixed in 4% paraformaldehyde and sent to the NHLBI (NIH) pathology core facility for cutting and staining. A schematic overview of the intestinal tissue differentiation is provided in the Figure A4.

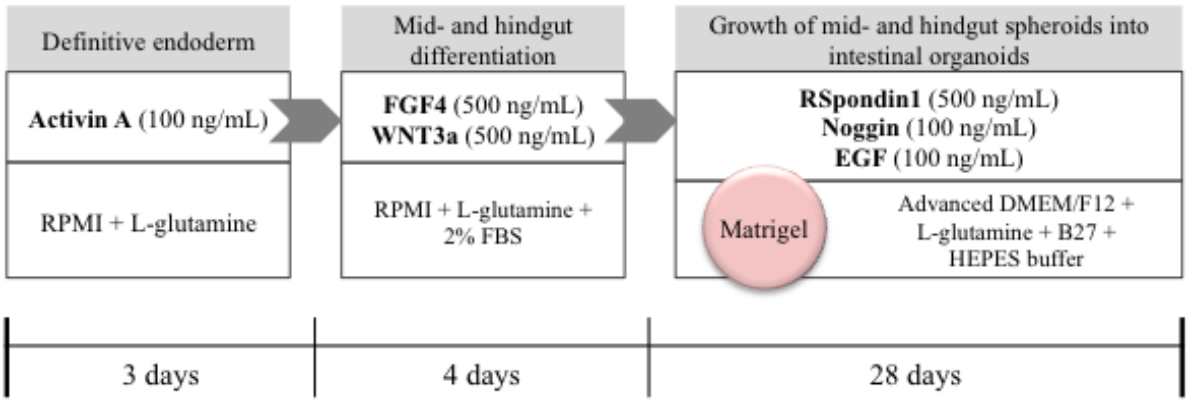

Figure A4 – Overview of intestinal tissue differentiation of PSCs. Cells at high confluence (about 95%) and fully undifferentiated were induced to definitive endoderm with Activin A for three days. The DE tissue was then differentiated into mid- and hindgut with FGF4 and WNT3a for four days. After 48 h of exposure to the medium with cytokines, rounded structures were budding from the adherent tissue and remained floating in the medium. These structures, called spheroids, were collected and transferred to a three-dimensional culture in Matrigel drops (supplemented with RSpondin1, Noggin, EGF). Matrigel drops were immersed into medium containing the same cocktail of cytokines, in which spheroids were grown to form more complex and differentiated structures, called intestinal organoids.

A.3. Results and discussion

A.3.1. Hematopoietic differentiation in adherent cell culture

Before establishing the HSC differentiation method through EBs formation (described in the section "3.2.18. Hematopoietic Stem Cell differentiation"), another method was tested. First, a pilot experiment was conducted encompassing the control iPSCs and *DKC1*[A353V] iPSCs c12. The percentage of $CD34^+$ cells on day 7 was higher in mutated than in control iPSCs (44.8% and 30.2%, respectively). However, in the end of differentiation (day 13), iPSCs control was more efficient in generating hematopoietic progenitors, as evidenced by percentage of CD34/CD45 double positive cells (3.11% in control against 0.03% in mutant) – Figure A5.

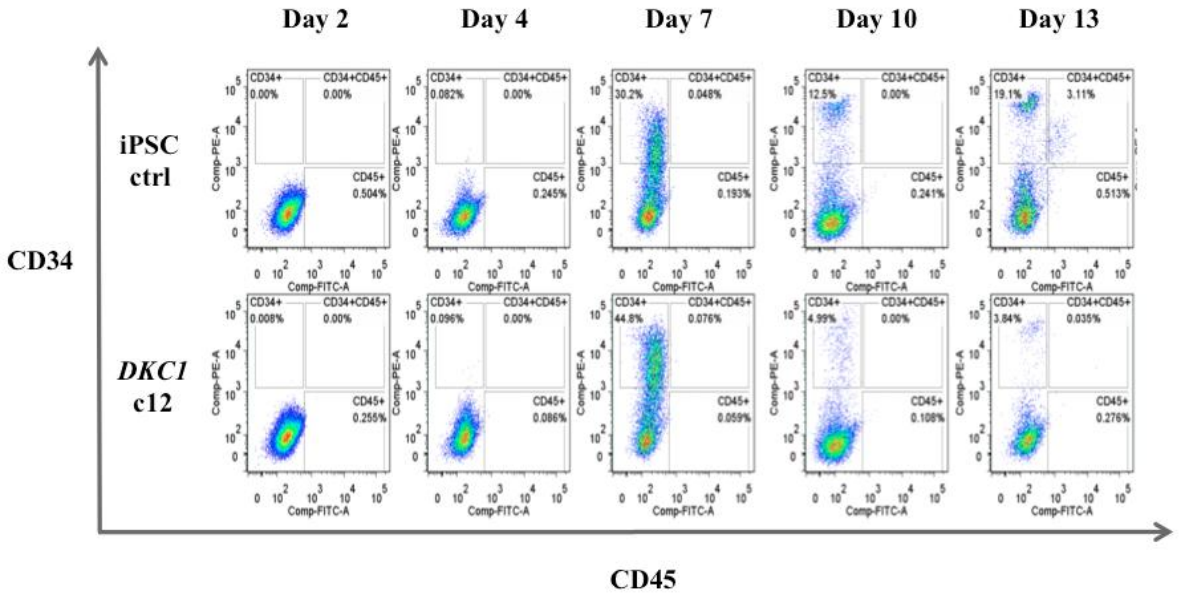

Figure A5 – FACS analysis of HSC differentiation of iPSCs control and *DKC1*[A353V] (c12) over time. Percentage of $CD34^+$ cells was increased in mutant iPSCs on day 7, but is not efficient as iPSCs control to give rise to $CD34^+/CD45^+$ hematopoietic progenitors (day 13).

The HSC differentiation experiment of *DKC1*[A353V] iPSCs c12 was repeated in different passages (p18 and p34). Again, a marked difference was observed on day 7: while percentage of $CD34^+$ cells was 0.25 in the control, percentage was 3.47 in c12 p18, and 7.82 in c12 p34 (data from FACS analysis not shown). Following the pilot experiments, HSC differentiation was carried out in two independent sets of experiments. First, the control iPSCs and two *DKC1*[A353V] iPSCs clones (c4-7 and c7-4) in the same passage (p26) were differentiated. In the second experiment, the iPSC control was differentiated along with *DKC1*[A353V] iPSCs c12-5 also in p26, as well as c4-7 in higher passage (p32). First experiment resulted in a poor differentiation towards hematopoietic progenitors even in the control (Figure A6). *DKC1*[A353V] iPSCs c4-7 and c7-4 (both p26) displayed impaired generation of hematopoietic progenitors (based on percentage of $CD34^+/CD45^+$ cells on day 13). Moreover, the pattern of higher percentage of $CD34^+$ cells in mutant iPSCs on day 7 was not observed. However, second experiment evidenced the same pattern observed in pilot experiments for c12, this time performed for c12-5 (Figure A7). Percentage of $CD34^+$ hemogenic endothelial cells observed on day 7 was 18.4% for c12-5 and 11.4% for control; c4-7 p32 was lower than control (6.1%). Again, despite higher number of $CD34^+$ cells, efficiency in generating $CD34^+/CD45^+$ cells was lower in mutant iPSCs.

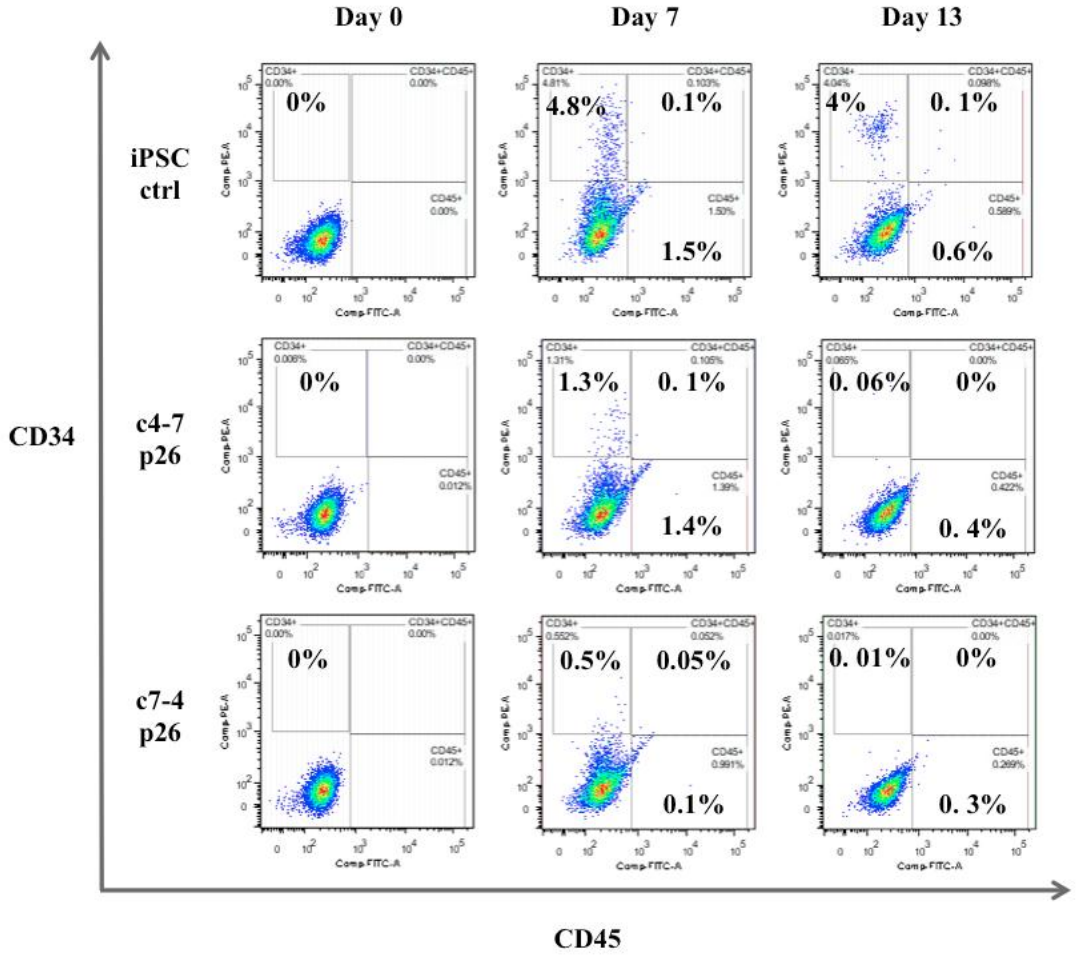

Figure A6 – FACS analysis of HSC differentiation of iPSCs control and *DKC1*[A353V] (c4-7 and c7-4) over time. Percentage of $CD34^+$ cells was increased in control iPSCs on day 7, reflecting in increased generation of $CD34^+/CD45^+$ hematopoietic progenitors when compared with mutants (day 13).

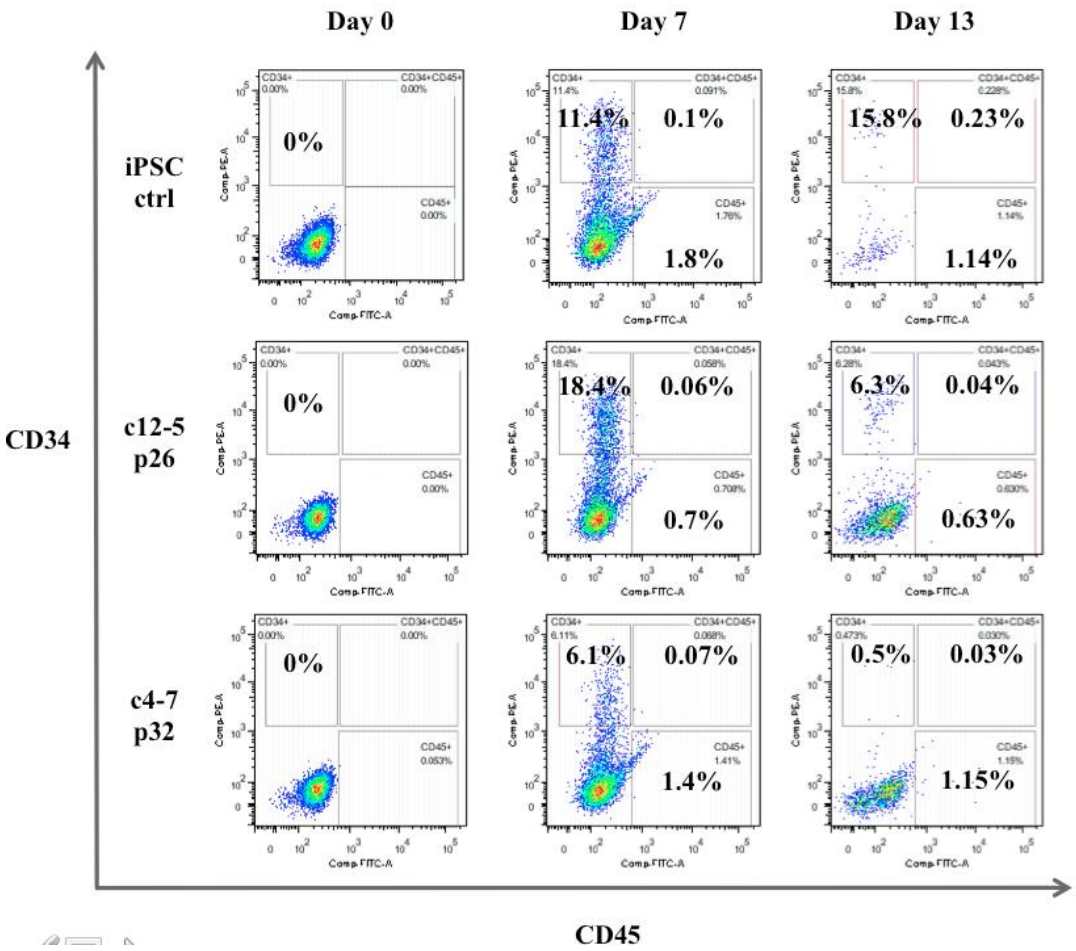

Figure A7 – FACS analysis of HSC differentiation of iPSCs control and *DKC1*[A353V] (c12-5 and c4-7) over time. Percentage of $CD34^+$ cells was increased in mutant iPSCs c12-5 on day 7, but was not efficient as iPSCs control to give rise to $CD34^+/CD45^+$ hematopoietic progenitors (day 13); c4-7 p32 presented decreased efficiency to differentiate and generate hematopoietic progenitors.

As demonstrated by the FACS analyzes (specifically the number of $CD34^+/CD45^+$ cells in the controls) the global efficiency of differentiation was low. The same control was previously differentiated, generating 7% double positive cells by the end of the differentiation (Winkler *et al*., 2013). Although the authors have applied a different protocol, and results from different methods are not directly comparable, the efficiency of the differentiation presented here was lower than expected. Additionally, CFC assay was performed with the cells collected on day 13 of differentiation. No colony was observed in CFC assay, even for the control, confirming the low efficiency of the differentiation method. Due to this issue, the method of HSC differentiation in adherent cells was replaced by the method of EBs formation prior to hematopoietic differentiation.

A.3.2. Hepatic differentiation

Hepatic differentiation of H1 ESCs as well as iPSCs control and *DKC1* mutant (clone 12) were performed in collaboration with Dr. T. Jake Liang (NIDDK, NIH). Previously, pluripotent cells were differentiated into DE and then guided towards hepatic specification, hepatoblasts maturation, and finally differentiated hepatocytes. DE differentiation of pluripotent cells was efficiently achieved, as demonstrated by immunostaining on day 3, in which cells were positive for the DE markers SOX17 and FOXA2 (Figure A8). However, hepatic specification was not achieved for *DKC1* iPSCs clone. The cells displayed impaired differentiation and proliferation (data not shown). Conversely, H1 ESCs and control iPSCs were able to differentiate towards hepatoblasts and hepatocytes. The efficiency of the differentiation in the control iPSCs was lower than H1 (Figure A9).

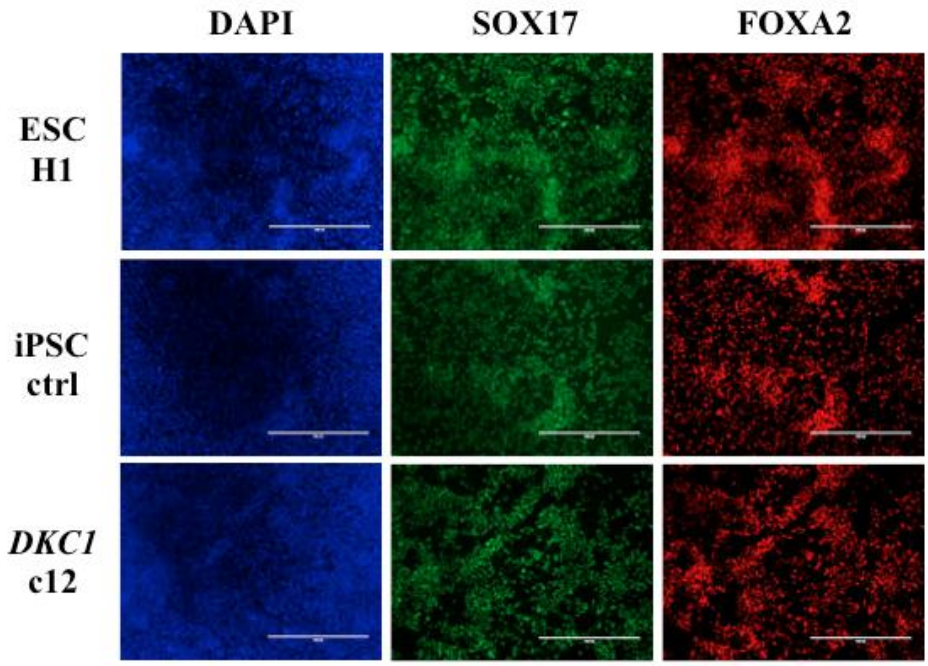

Figure A8 – Immunocytochemistry for DE markers. Staining performed on day 3; majority of cells were positive for markers, confirming efficiency of DE induction.

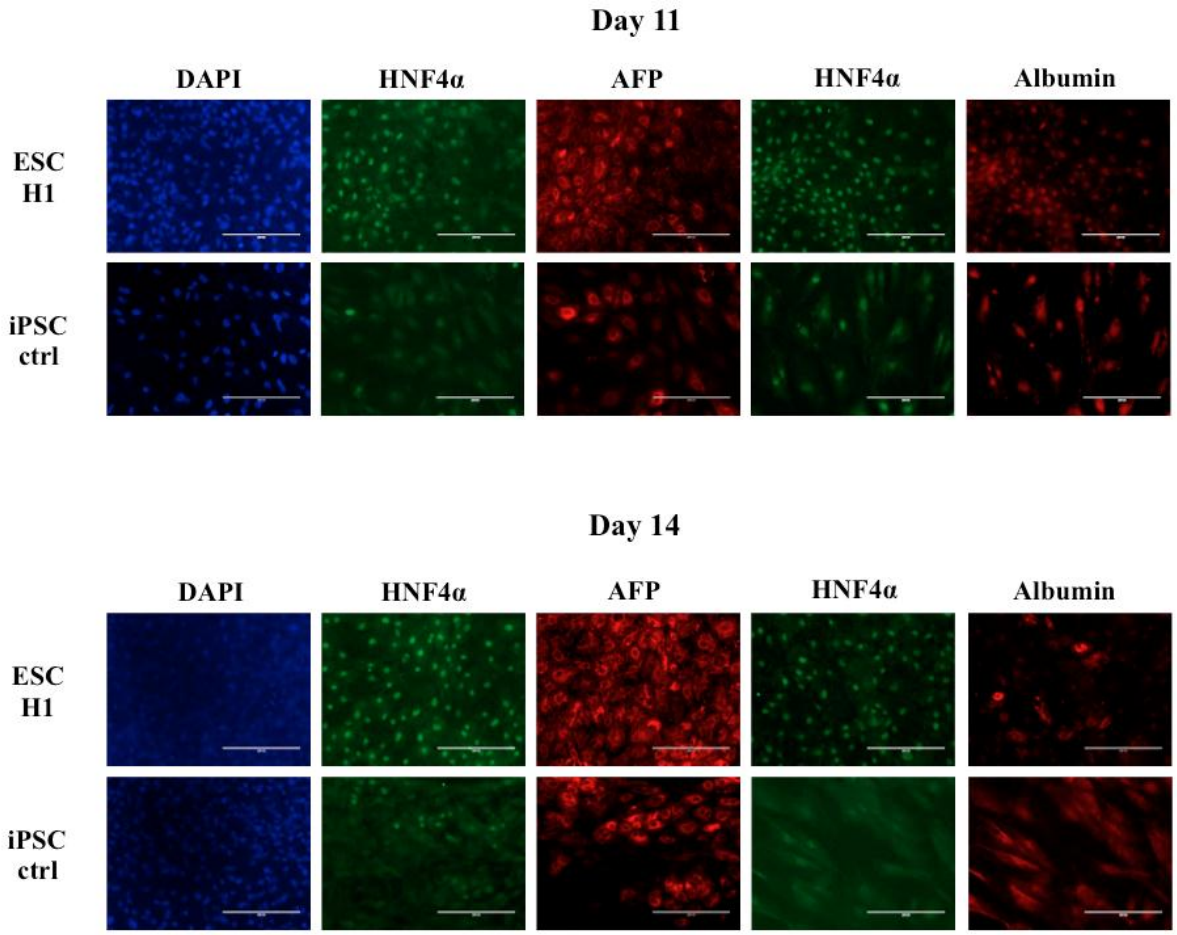

Figure A9 – Immunocytochemistry for hepatic markers. Staining performed on days 11 and 14; H1 ESCs and iPSCs control both stained positive for all markers.

A second approach of hepatic differentiation was tested on H1 hESCs. The first step for the procedure was the generation of DE, which was tested in two different initial confluences of colonies (85% and 60%). In both cases, cells started differentiating the day after exposure to Activin A and WNT3a cytokines, but could no longer be cultured due to cellular death in the last day of DE derivation, the day 2 (Figure A10.A and B).

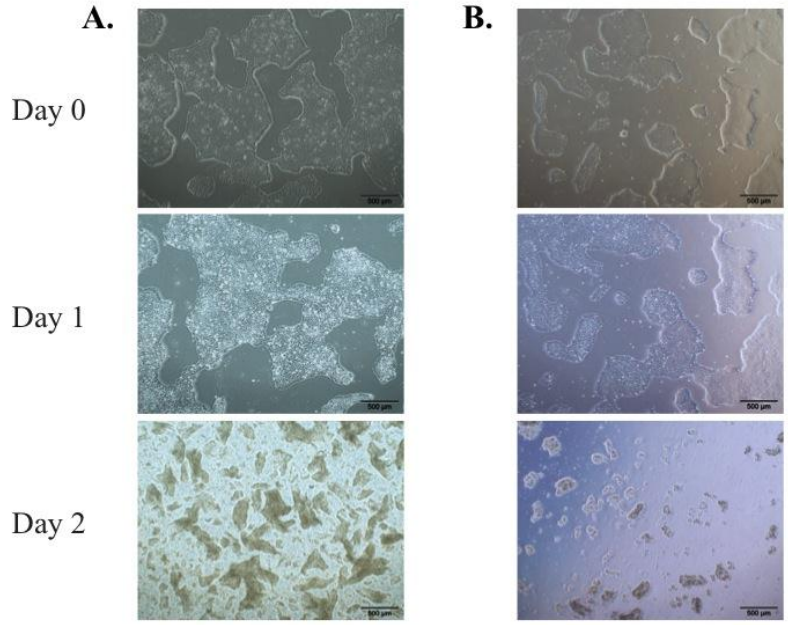

Figure A10 – Hepatic differentiation of H1 hESC. Days 0 to 2 of definitive endoderm generation prior to hepatoblasts differentiation; clumps of dead cells on day 2. (**A**) Initial confluence of 85%. (**B**) Initial confluence of 60%.

Then, an initial confluence of 30% was tested. As observed on Figure A11, the H1 ESCs at low confluence were guided until the last stage of differentiation. The morphological changes observed in the cells at the end of the differentiation were consistent with the morphology of hepatocyte-like cells (Figure A12). Currently, expression profiles of these cells are under investigation in order to check the efficiency of the hepatocytes' derivation.

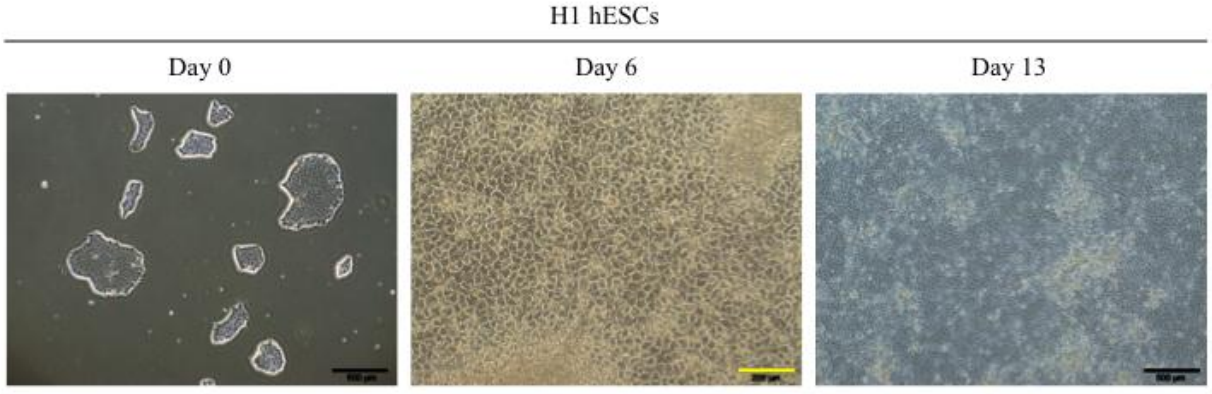

Figure A11 – Morphological changes during hepatic differentiation of H1 hESC. Initial confluence was 30% at day 0. After 6 days of derivation, polygonal cells resembling hepatoblasts were observed. On day 13, a good number of cells in the differentiated tissue displayed hepatocyte-like morphology. Scale bars: black = 500 µm, yellow = 200 µm.

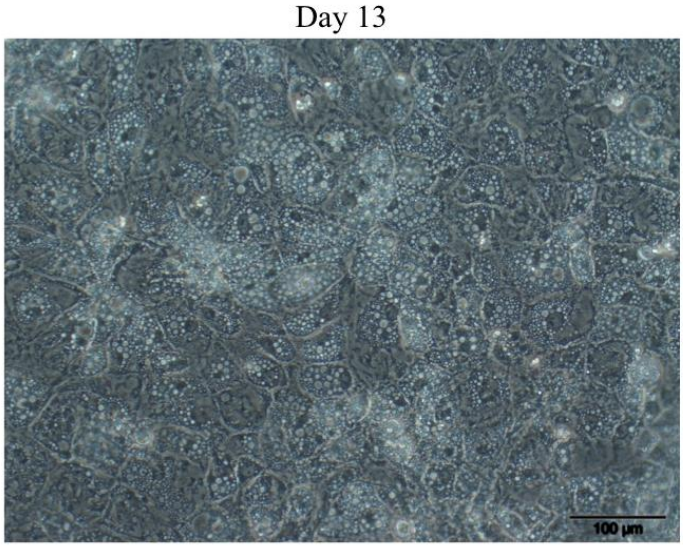

Figure A12 – Hepatocyte-like cells on day 13 of hepatic differentiation of H1 hESC. Cells in the differentiated tissue displayed large polygonal shape, and multiple nuclei, which resembled hepatocyte morphology. Scale bar = 100 µm.

The three tests performed on H1 highlighted the importance of the initial confluence of PSCs prior to differentiation. Thus, confluence represents a factor that influences the success of the differentiation process. Moreover, the growth rate of the cells is another important factor that should be considered before establishing an initial confluence. In conclusion, for each PSC line, the growth rate and initial confluence should be carefully defined in order to ensure a successful derivation of hepatocytes. New experiments are planned with the iPSCs, both control and *DKC1*[A353V] clones.

A.3.3. Intestinal tissue differentiation

In order to establish this differentiation method, two PSC lines were tested (H1 ESCs and one iPSCs control). The differentiation towards DE was achieved after three days of exposure to Activin A, as evidenced by immunostaining of SOX17 and FOXA2 performed on day 3 (Figure A13). Both pluripotent cells presented similar DE differentiation efficiency, but different confluence and morphological characteristics (Figure A14).

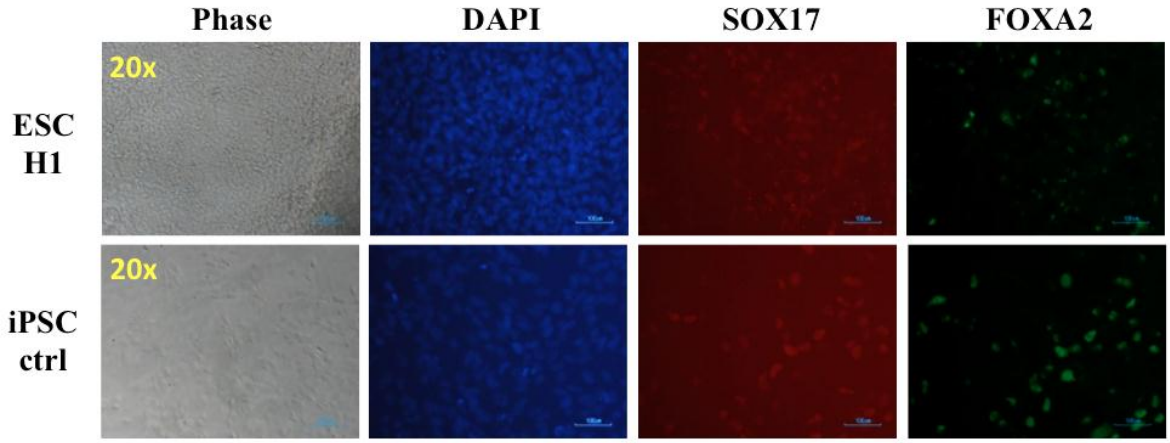

Figure A13 – Immunocytochemistry for DE markers. Staining performed on day 3; both pluripotent cells lines presented similar DE differentiation efficiency based on amount of positive cells for markers.

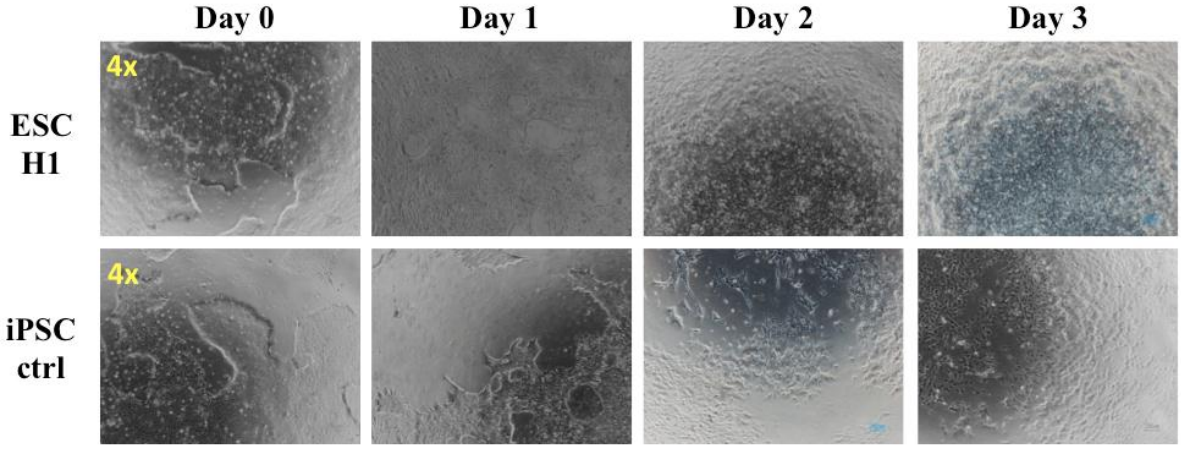

Figure A14 – Cell morphology changes during DE induction. On day 0, confluence of pluripotent cells immediately before Activin A exposure (~85%). The following days, amount of floating cells was increased on iPSC control and confluence of attached tissue was clearly higher in H1.

Following DE induction, cells were exposed to FGF4 and WNT3a to induce differentiation into mid- and hindgut. The next day of exposure (day 4), three-dimensional structures became visible on H1; hindgut spheroids bud from monolayer epithelium on days 5-7, which were collected daily and transferred to three-dimensional Matrigel culture. No spheroids were observed in iPSCs control (Figure A15). Staining for CDX2 was performed in the attached monolayer epithelium on day 7, and majority of cells were positive in both pluripotent cell lines. However, confluence was clearly higher in H1 than in iPSCs control (Figure A16). Although majority of cells was $CDX2^{+}$, no spheroid was observed for iPSCs control and differentiation could not be continued. Spheroids collected from H1 were grown

into intestinal organoids in the presence of RSpondin1, Noggin, and EGF (Figure A17). On day 14, organoids were transferred to new Matrigel and split on day 28. Organoids collected on day 15 resembled intestinal epithelium in early development, presenting a tube-like structure (Figure A18). Moreover, no morphological evidence of tissue from other germ layers was found. Thus, H1 was successfully differentiated into intestinal tissue, but the differentiation of the control iPSCs was impaired, and could not be continued beyond de DE.

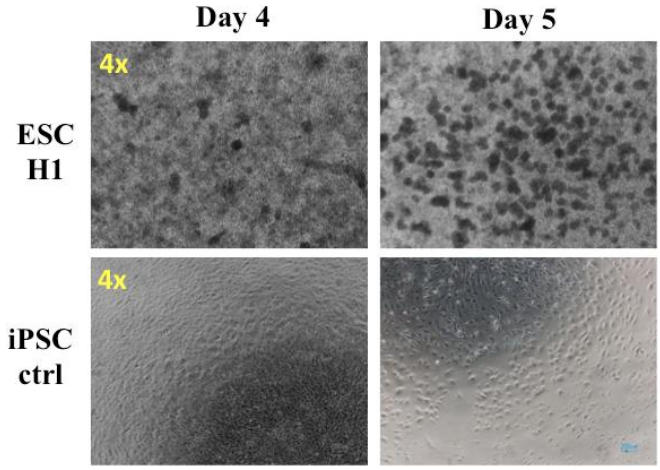

Figure A15 – Differentiation into mid- and hindgut. H1: 3D structures became visible on day 4; hindgut spheroids bud from the adherent layer of epithelium on days 5-7 and were collected daily. iPSCs control: no spheroid was observed and density of adherent tissue was clearly lower than H1.

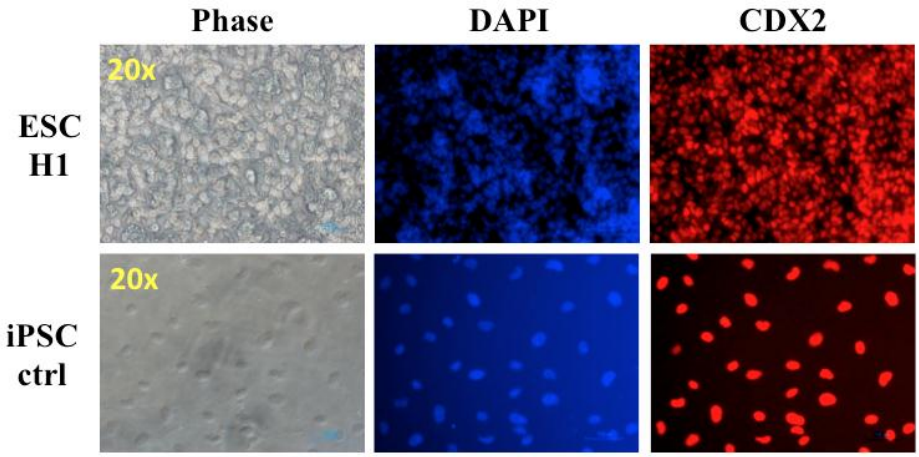

Figure A16 – Immunocytochemistry for CDX2. Majority of cells stained positive for CDX2, but density was clearly higher in H1 compared to control iPSCs.

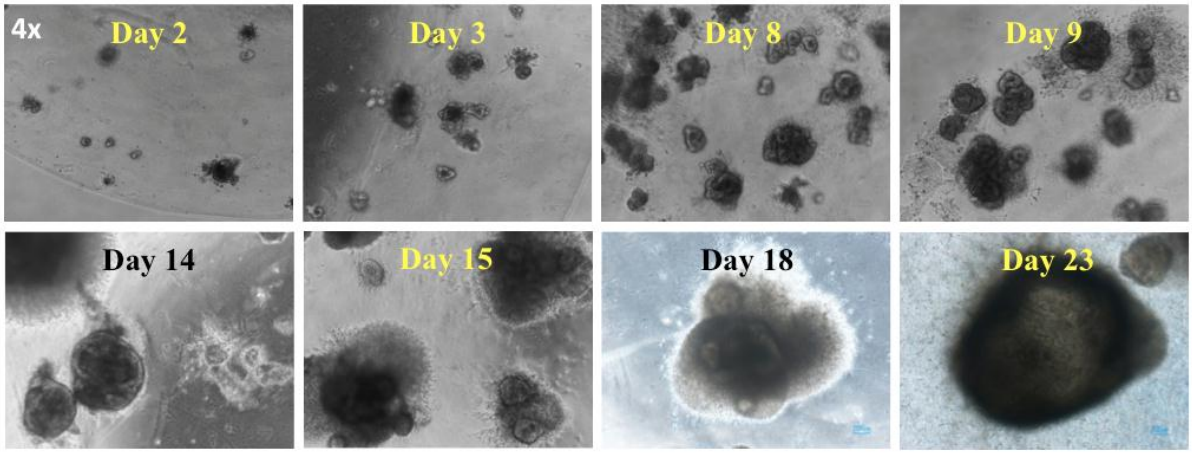

Figure A17 – Hindgut spheroids growing into intestinal organoids. Spheroids collected and transferred to 3D Matrigel culture were maturated into organoids and cultured for 28 days before passaging.

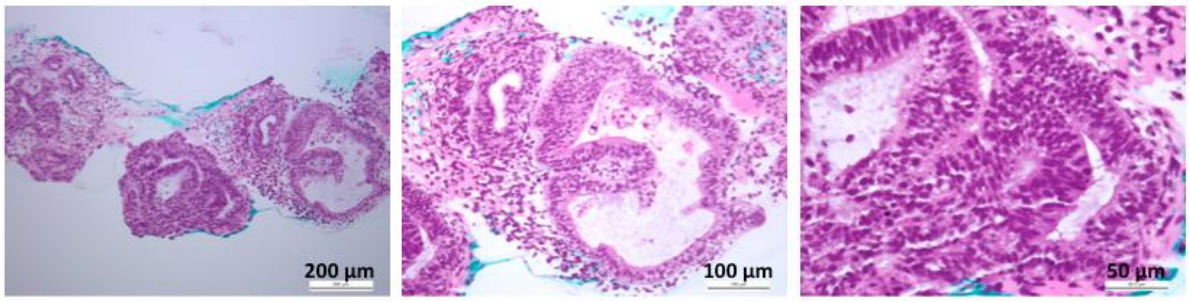

Figure A18 – Histological analysis of organoids on day 15. Organoids collected on day 15 presented tube-like structure and resembled intestinal epithelium at early development.

Since initial confluence of pluripotent cells is a limiting factor in intestinal differentiation, another test of differentiation was performed including control iPSCs in two different initial confluences, as well as *DKC1*[A353V] iPSCs c12-5 (p29). Again, cells were differentiated into DE (Figure A19). Increased cell death and morphological differences in control iPSCs at higher initial confluence were observed. Control iPSCs in lower confluence and *DKC1* c12-5 formed a dense adherent tissue, but density was lower than observed for H1 in the first test. Majority of cells stained positive for DE markers, but iPSCs control in higher initial confluence maintained regions of non-differentiated cells (Figure A20). After exposure to FGF4 and WNT3a to induce differentiation into mid- and hindgut, three-dimensional structures were visualized attached in the adherent epithelium of control iPSCs (lower initial confluence) and *DKC1* c12-5. However, no floating spheroid was observed; morphology of control iPSCs (higher initial confluence) was completely different of usually observed after mid- and hindgut induction (Figure A21). Monolayer epithelium of iPSCs control (lower

initial confluence) and *DKC1* c12-5 was stained for CDX2 on day 7 (Figure A22). Although cells stained positive for CDX2, no spheroid was derived and differentiation was discontinued from this step.

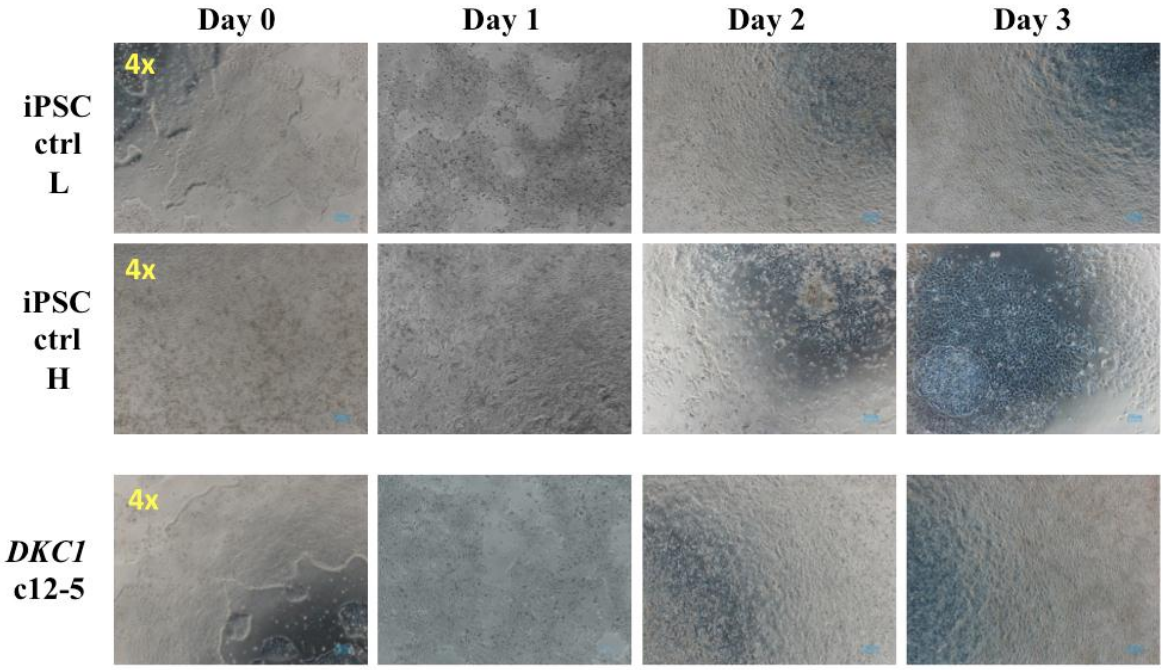

Figure A19 – Cell morphology changes during DE induction. Two initial confluences were tested for iPSCs control, lower (L, ~75%), and higher (H, ~100%). Confluence of *DKC1* c12-5 was ~85%.

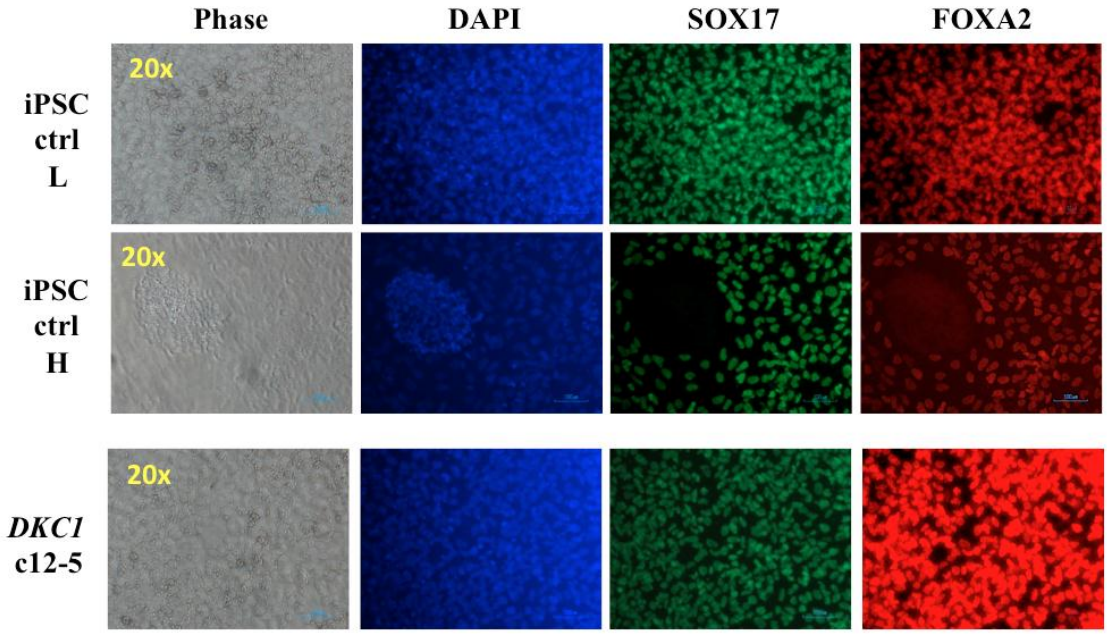

Figure A20 – Immunocytochemistry for DE markers. Cells stained on day 3; majority of differentiated cells from iPSCs control in lower initial confluence (L) and *DKC1* c12-5 stained positive for both SOX17 and FOXA2. DE differentiation of iPSCs control in higher initial confluence (H) was not completely achieved, as evidenced by absence of stained cells in some regions of attached tissue.

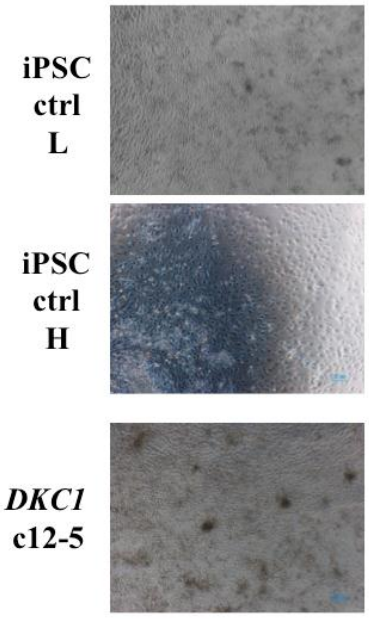

Figure A21 – Cell morphology changes on day 6. Formation of adherent 3D structures was observed on control iPSCs at lower initial confluence (L) and *DKC1* c12-5, but there was no spheroid formation; control iPSCs at higher initial confluence (H) displayed unusual morphology in this step.

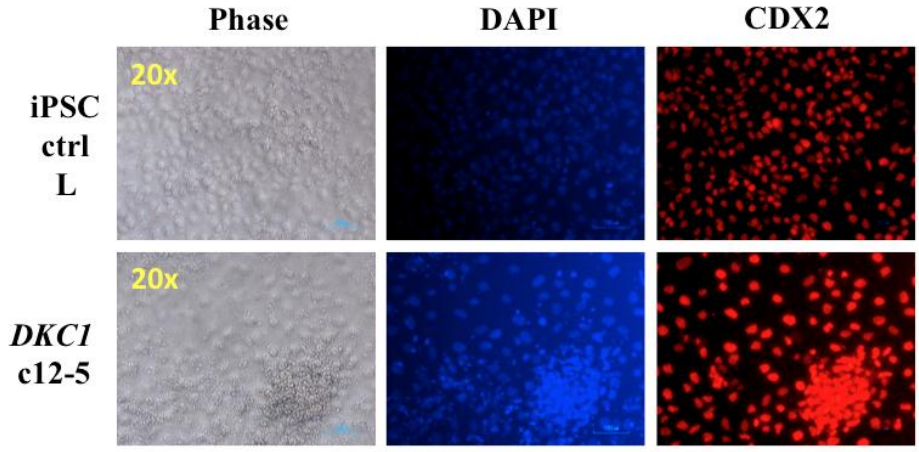

Figure A22 – Immunocytochemistry for CDX2. Cells stained on day 7; majority of differentiated cells from iPSCs control in lower initial confluence (L) and *DKC1* c12-5 stained positive for CDX2.

Next, intestinal differentiation was conducted on control iPSCs and *DKC1*[A353V] clone 4-7. Both iPSC lines were apparently guided to DE generation, as shown in Figure A23-A. However, spheroid-like structures were just visualized on *DKC1*-mutant clone in the end of day 7 (mid- and hindgut differentiation). These structures were collected and cultured for additional 26 days on three-dimensional Matrigel cultures supplemented with cytokines (Figure A23-B). The histological analysis of putative organoids collected on day 26 revealed the generation of a stromal tissue, not resembling the intestinal epithelium (Figure A23-C).

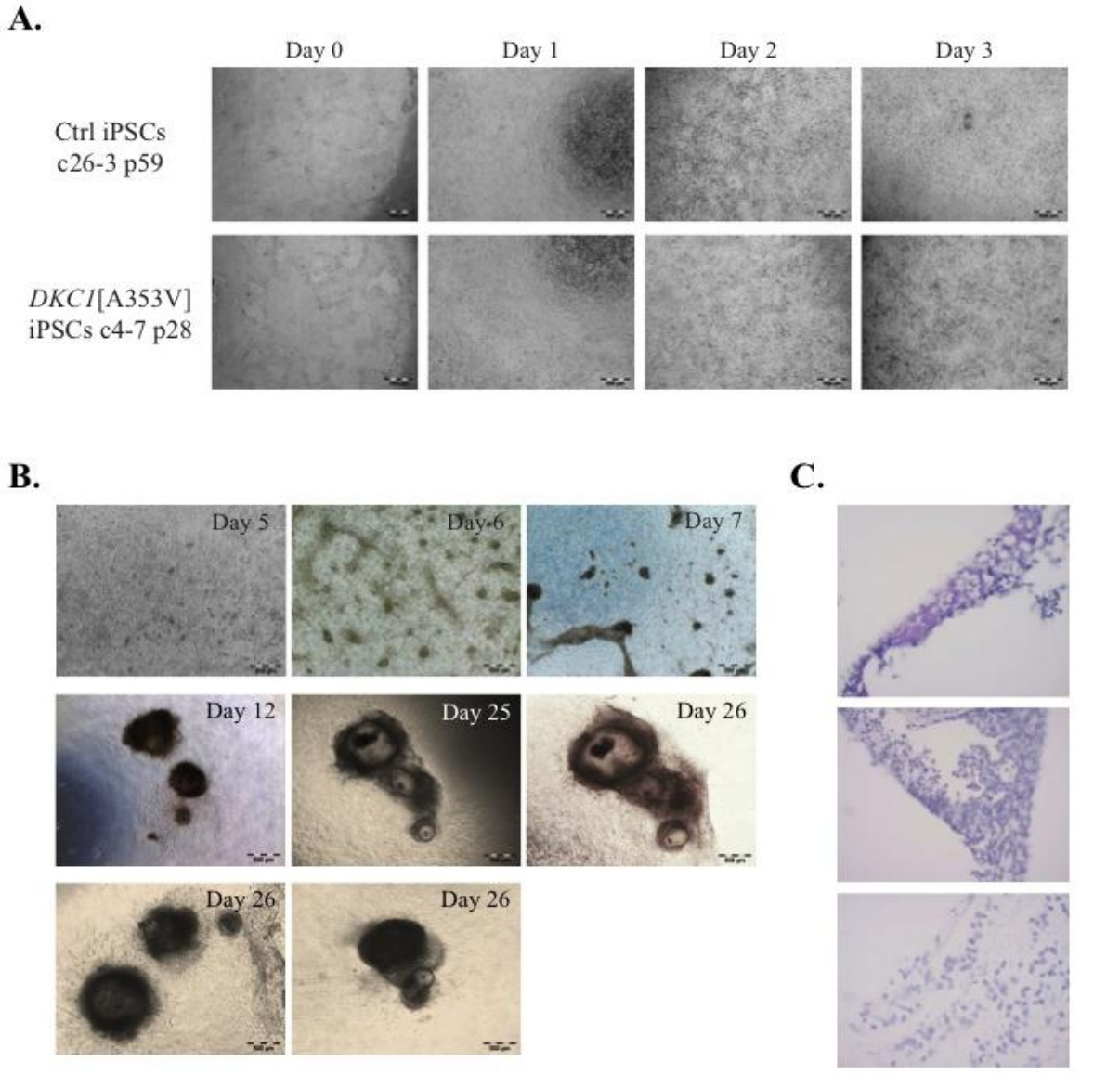

Figure A23 – Intestinal tissue differentiation of iPSCs control and *DKC1*[A353V] clone 4-7. (**A**) Definitive endoderm differentiation. (**B**) Formations of structures (spheroids) by day 5 to 7; collection and culture of spheroids into organoids in 3D matrigel culture for 26 days. (**C**) Histological analysis of putative organoids collected on day 26; hematoxylin and eosin staining.

As observed in the hepatic differentiation, the initial confluence is critical for the successful derivation of intestinal tissue from PSCs. Conversely to hepatic differentiation, the initial confluence of PSCs for the derivation of intestinal tissue must be 85% or higher, and PSCs must be fully undifferentiated (McCracken *et al*., 2011). Thus, the difficulty in this differentiation is to fulfill this prerequisite, since high confluences may accelerate spontaneous differentiation. One alternative for this issue is the adaptation of the PSCs in non-colony type monolayer culture (Chen *et al*., 2012). This type of culture allows the growth of the PSCs in a monolayer and homogenized cellular state at high confluences

(100%) without loss of pluripotent features. New tests of intestinal tissue differentiation are planned for control and *DKC1*[A353V] iPSCs, also establishing the culture of these cells in the non-colony type.

A.4. Conclusions

The differentiation of PSCs requires laborious tests in order to establish ideal conditions for the successful differentiation. For some differentiations, such as hematopoietic and hepatic, multiple methods are available, which requires testing of multiple protocols and, occasionally, some adaptation. Two protocols of hematopoietic differentiation were tested in the present study: starting with adherent PSCs or EBs prior to cytokines. The method that requires adherent PSCs was disregarded after several tests due to its variability and low efficiency. The tests of differentiations in hepatic and intestinal tissue demonstrated the need of careful establishment of initial confluence of the PSCs prior to differentiation. The experience acquired in the tests may provide useful insights for the next experiments.

A.5. References

Armanios, M. Y., Chen, J. J., Cogan, J. D., Alder, J. K., Ingersoll, R. G., Markin, C., Lawson, W. E., Xie, M., Vulto, I., Phillips, J. A., Lansdorp, P. M., Greider, C. W., and Loyd, J. E. (2007). Telomerase mutations in families with idiopathic pulmonary fibrosis. *N Engl J Med* 356, 1317-26.

Basma, H., Soto-Gutiérrez, A., Yannam, G. R., Liu, L., Ito, R., Yamamoto, T., Ellis, E., Carson, S. D., Sato, S., Chen, Y., Muirhead, D., Navarro-Alvarez, N., Wong, R. J., Roy-Chowdhury, J., Platt, J. L., Mercer, D. F., Miller, J. D., Strom, S. C., Kobayashi, N., and Fox, I. J. (2009). Differentiation and transplantation of human embryonic stem cell-derived hepatocytes. *Gastroenterology* 136, 990-9.

Calado, R. T. (2009). Telomeres and marrow failure. *Hematology Am Soc Hematol Educ Program*, 338-43.

Calado, R. T. (2011). Immunologic aspects of hypoplastic myelodysplastic syndrome. *Semin Oncol* 38, 667-72.

Calado, R. T., and Young, N. S. (2008). Telomere maintenance and human bone marrow failure. *Blood* 111, 4446-55.

Calado, R. T., and Young, N. S. (2009). Telomere diseases. *N Engl J Med* 361, 2353-65.

Chadwick, K., Wang, L., Li, L., Menendez, P., Murdoch, B., Rouleau, A., and Bhatia, M. (2003). Cytokines and BMP-4 promote hematopoietic differentiation of human embryonic stem cells. *Blood* 102, 906-15.

Chen, K. G., Mallon, B. S., Hamilton, R. S., Kozhich, O. A., Park, K., Hoeppner, D. J., Robey, P. G., and McKay, R. D. (2012). Non-colony type monolayer culture of human embryonic stem cells. *Stem Cell Res* 9, 237-48.

Hartmann, D., Srivastava, U., Thaler, M., Kleinhans, K. N., N'kontchou, G., Scheffold, A., Bauer, K., Kratzer, R. F., Kloos, N., Katz, S. F., Song, Z., Begus-Nahrmann, Y., Kleger, A., von Figura, G., Strnad, P., Lechel, A., Günes, C., Potthoff, A., Deterding, K., Wedemeyer, H., Ju, Z., Song, G., Xiao, F., Gillen, S., Schrezenmeier, H., Mertens, T., Ziol, M., Friess, H., Jarek, M., Manns, M. P., Beaugrand, M., and Rudolph, K. L. (2011). Telomerase gene mutations are associated with cirrhosis formation. *Hepatology* 53, 1608-17.

Jonassaint, N. L., Guo, N., Califano, J. A., Montgomery, E. A., and Armanios, M. (2013). The gastrointestinal manifestations of telomere-mediated disease. *Aging Cell* 12, 319-23.

Jung, M., Dunbar, C. E., and Winkler, T. (2015). Modeling Human Bone Marrow Failure Syndromes Using Pluripotent Stem Cells and Genome Engineering. *Mol Ther*.

McCracken, K. W., Howell, J. C., Wells, J. M., and Spence, J. R. (2011). Generating human intestinal tissue from pluripotent stem cells in vitro. *Nat Protoc* 6, 1920-8.

Medine, C. N., Lucendo-Villarin, B., Zhou, W., West, C. C., and Hay, D. C. (2011). Robust generation of hepatocyte-like cells from human embryonic stem cell populations. *J Vis Exp*, e2969.

Mushiroda, T., Wattanapokayakit, S., Takahashi, A., Nukiwa, T., Kudoh, S., Ogura, T., Taniguchi, H., Kubo, M., Kamatani, N., Nakamura, Y., and Group, P. C. S. (2008). A genome-wide association study identifies an association of a common variant in TERT with susceptibility to idiopathic pulmonary fibrosis. *J Med Genet* 45, 654-6.

Ng, E. S., Davis, R., Stanley, E. G., and Elefanty, A. G. (2008). A protocol describing the use of a recombinant protein-based, animal product-free medium (APEL) for human embryonic stem cell differentiation as spin embryoid bodies. *Nat Protoc* 3, 768-76.

Sullivan, G. J., Hay, D. C., Park, I. H., Fletcher, J., Hannoun, Z., Payne, C. M., Dalgetty, D., Black, J. R., Ross, J. A., Samuel, K., Wang, G., Daley, G. Q., Lee, J. H., Church, G. M., Forbes, S. J., Iredale, J. P., and Wilmut, I. (2010). Generation of functional human hepatic endoderm from human induced pluripotent stem cells. *Hepatology* 51, 329-35.

Tsakiri, K. D., Cronkhite, J. T., Kuan, P. J., Xing, C., Raghu, G., Weissler, J. C., Rosenblatt, R. L., Shay, J. W., and Garcia, C. K. (2007). Adult-onset pulmonary fibrosis caused by mutations in telomerase. *Proc Natl Acad Sci U S A* 104, 7552-7.

Yamaguchi, H., Baerlocher, G. M., Lansdorp, P. M., Chanock, S. J., Nunez, O., Sloand, E., and Young, N. S. (2003). Mutations of the human telomerase RNA gene (TERC) in aplastic anemia and myelodysplastic syndrome. *Blood* 102, 916-8.

Yamaguchi, H., Calado, R. T., Ly, H., Kajigaya, S., Baerlocher, G. M., Chanock, S. J., Lansdorp, P. M., and Young, N. S. (2005). Mutations in TERT, the gene for telomerase reverse transcriptase, in aplastic anemia. *N Engl J Med* 352, 1413-24.